To the Graduate Council:

I am submitting herewith a dissertation written by Yul Roh entitled "Electrochemical Remediation of Radionuclide- and Trichloroethene-Contaminated Groundwater Using Zero-valent Iron/Iron Oxides and Mineralogical Characterization of Iron Hydroxides Formed from Zero-valent Iron." I have examined the final copy of this dissertation for form and content and recommend that it be accepted in partial fulfillment of the requirements for the degree of Doctor of Philosophy, with a major in Plant and Soil Sciences.

John E. Foss, Major Professor

We have read this dissertation
and recommend its acceptance:

Accepted for the Council:

Associate Vice Chancellor
and Dean of The Graduate School

ELECTROCHEMICAL REMEDIATION OF RADIONUCLIDE- AND TRICHLOROETHENE-CONTAMINATED GROUNDWATER USING ZERO-VALENT IRON/IRON OXIDES AND MINERALOGICAL CHARACTERIZATION OF IRON HYDROXIDES FORMED FROM ZERO-VALENT IRON

A Dissertation

Presented for the

Doctor of Philosophy

Degree

The University of Tennessee, Knoxville

Yul Roh

December 1998

Ag-VetMed
Thesis
98b
.R65

DEDICATION

To my parents, Mr. and Mrs. Yeonsuk and Yunsoon Roh,

who have given me invaluable educational opportunities

and

To my wife, Munye Kang, with much love, admiration, and appreciation

항상 사랑과 헌신으로 보살펴 주신
부모님과 아내에게

ACKNOWLEDGMENT

I would like to express my gratitude to my major professor, Dr. S. Y (Sukyoung) Lee and John Foss for their guidance and encouragement throughout my graduate study at the University of Tennessee, Knoxville. I am also grateful to my committee members, Dr. John Ammons, Dr. Michael Essington, and Dr. Chris Cox for their assistance, input and encouragement through my research. I wish to express my sincere appreciation to Dr. Mark Elless, Dr. Hi-Soo Moon, and Ms. C. A. Stiles for their help, advice and fruitful discussions. In addition, I would like to thank Mr. I. L. Larsen and the people at the Environmental Sciences Division, Oak Ridge National Laboratory for their help, advice and fruitful discussions throughout my stay in the laboratory. I acknowledge the financial support received from the Oak Ridge National Laboratory, which is managed by Lockheed Martin Energy Research Corp. for the U. S. Department of Energy under contract number DE-AC05-96OR22464.

I would like to thank my family for their support and patience, without which my graduate study would not have been possible. I thank my parents for their constant and dedicated support. I am especially indebted to my wife, Munye Kang, for her sacrifice and moral support. I also thank my daughter, Esther, and my son, Brian, for the joy and inspiration they have brought to me. Lastly, but most sincerely, I thank God for his guidance and love.

ABSTRACT

Recently, metal-based degradation of chlorinated organic compounds and immobilization of radionuclides and heavy metals for groundwater remediation have become popular topics in environmental science and engineering research. Although the zero-valent iron (Fe^0)-based reactive barrier has been introduced as a cost-effective remediation technology for groundwaters contaminated by chlorinated organic compounds and reducible metals, the current approach of the technology has been criticized for its low process efficiency (reaction rate) and the effective life of the medium (longevity).

The objectives of this study are to (1) develop and evaluate electro-enhanced technology using Fe^0 for mobile radionuclides [e.g., TcO_4^- and $UO_2(CO)_3^{2-}$] and trichloroethene (TCE) in groundwater, (2) develop and evaluate an iron-oxide-based electroremediation for TCE-contaminated groundwater, (3) perform mineralogical characterization of the precipitates formed during contaminated groundwater treatment, and (4) understand the mechanisms of the chemical processes involved in Fe^0 oxidation and the effect of cations and anions on the initial precipitation and subsequent phase transformation of the precipitates.

Application of direct current on the Fe^0 medium column results in a significant enhancement of the dechlorination rate of TCE and the longevity of Fe^0 as a reductive medium for radionuclides. Several factors affect the removal of radionuclides and TCE, including (1) electrode configuration, (2) applied voltage and current, (3) distance between cathode and anode, (4) material used as electrodes, and (5) influent concentration

and water chemistry. Reduction of radionuclides and coprecipitation with eroded iron as an iron hydroxide mineral appears to be the preferred removal process. The dechlorination mechanism appears to be reductive using the electrons supplied by the iron oxidation and external power supply. Because the electro-enhanced process is a remediation technology based on chemical reduction and precipitation of radionuclides and degradation of chlorinated organic compounds through external current supply rather than the addition of chemicals, this Fe^0 barrier technology has the potential to simplify the decontamination process for treating groundwater contaminated with radionuclides, heavy metals, and chlorinated organic compounds.

Direct current applied to palladized multiphasic iron oxide minerals not only increases the efficiency and effective life of the medium by controlling iron oxidation but also increases the dechlorination rate of solvents by providing an external supply of electrons. The palladized multiphasic iron oxide medium has some advantages over the palladized Fe^0 medium. Because the palladized multiphasic oxide is less susceptible to passivation by iron hydroxide coating than palladized Fe^0, no significant reduction in flow rate or generation of ferrous iron (Fe^{2+}) in the effluent are anticipated during TCE-contaminated groundwater treatment.

The mineralogical characterization of the precipitates in reactive Fe^0 columns shows that the principal corrosion products are magnetite, intermediate products (green rusts), and hydrated forms of ferric oxides, such as akaganeite (β-FeOOH), goethite (α-FeOOH), or lepidocrocite (γ-FeOOH), depending on the degree of oxidation and the chemical environment. Other minerals, including calcite, aragonite, siderite, mackinawite,

and native metal sulfur, are also precipitated on the surface of reactive medium, depending on the groundwater chemistry. Factors affecting the mineralogy of the precipitates include (a) contaminant type and chemical composition of groundwater and (b) occurrence of sulfate-reducing bacteria. These amorphous and crystalline minerals formed on the reactive medium and reduced the effectiveness and porosity of the Fe^0 medium.

A pyroaurite-type mineral was synthesized as a host iron mineral for the radionuclides through anodic corrosion of iron from Fe^0 foam. The results showed that reduced uranium and technetium were incorporated in the trioctahedral layer of the pyroaurite structure by substitution of ferrous/ferric iron. The excess positive charges generated by the substitution were neutralized by the carbonate complex in the interlayer of the mineral. The electrochemical synthesis of a crystalline pyroaurite-type mineral could be an effective and economical approach to remediating groundwaters contaminated by uranium, technetium, and other reducible heavy metals. The formation of such a well-crystalline waste product is fortuitous because its solubility is expected to be much lower than that of an amorphous iron oxide phase, thereby immobilizing the entrapped contaminants more effectively.

TABLE OF CONTENTS

CHAPTER PAGE

Introduction 1

PART 1: Pertinent Literature Review 6

1. ENVIRONMENTAL BEHAVIOR OF URANIUM, TECHNETIUM, AND TRICHLOROETHENE 7

   1.1 Uranium (U) 7
   1.2 Technetium (Tc) 10
   1.3 Trichloroethene (TCE) 12

2. REMEDIATION OF RADIONUCLIDE- AND TCE-CONTAMINATED GROUNDWATER 15

   2.1 Conventional Process 15
   2.2 Immobilization of Heavy Metals and Radionuclides Using Fe^0 17
   2.3 Dechlorination of Trichloroethene Using Fe^0 19

3. IRON HYDROXIDE FORMATION FROM Fe^0 22

   3.1 Geochemical Processes in Reactive Fe^0 Barrier 22
   3.2 Iron Hydroxide, Iron Sulfide, and Calcium Carbonate Formation 23

REFERENCES 28

PART 2: Electroremediation of Radionuclide- and TCE-Contaminated Groundwater Using Zero-valent Iron (Fe^0) 36

1. ABSTRACT 37

2. INTRODUCTION 39

   2.1 Underlying Electrochemical Principles 41
   2.3 Description of the Electroremediation Process 44

3. MATERIALS AND METHODS 47

3.1 Simulation of Contaminated Waters 47
3.2 Materials Used as Fe^0 47
3.3 Sampling and Analyses 49
3.4 Experimental Setup 50
3.5 Mineralogical Characterization of Corroded Iron Materials 55

4. RESULTS AND DISCUSSION 57

4.1 Immobilization of ^{235}U and ^{99}Tc 57
4.2 Dechlorination of TCE 64
4.3 Water Chemistry 73
4.4 Mineralogical Characterization of the Corroded Iron Materials 75

5. CONCLUSIONS 79

REFERENCES 81

PART 3: Electrochemical Dechlorination of TCE By Palladized Iron Oxide Minerals 84

1. ABSTRACT 85

2. INTRODUCTION 87

3. MATERIALS AND METHODS 90

3.1 Materials 90
3.2 Methods 92
3.3 Sampling and Analyses 95

4. RESULTS 97

4.1 Dechlorination of TCE Using Multiphasic Iron Oxides 97
4.2 Dechlorination of TCE Using Palladized, Multiphasic Fe Oxides 100

5. DISCUSSION 104

6. CONCLUSIONS 106

REFERENCES 107

PART 4: Iron Hydroxide Formation from Zero-valent Iron (Fe^0) During Contaminated Groundwater Treatment and Its Effects on Reactive Wall Performance 109

1. ABSTRACT 110

2. INTRODUCTION 112

3. MATERIALS AND METHODS 115

   3.1 Materials Used as a Reactive Medium 115
   3.2 Geochemical Characterization 116
   3.3 Mineralogical Characterization of Precipitates 117

4. RESULTS AND DISCUSSION 118

   4.1 Geochemical Changes in Reactive Iron Barrier 118
   4.2 Mineralogical Characterization of the Precipitates 124
   4.3 Effect of Precipitates on Iron Wall Performance 138

5. CONCLUSIONS 143

REFERENCES 145

PART 5: Electrochemical Synthesis of Pyroaurite-type Minerals 149

1. ABSTRACT 150

2. INTRODUCTION 151

3. MATERIALS AND METHODS 154

   3.1 Material Synthesis 154
   3.2 Mineralogical Analysis 155

4. RESULTS 159

5. DISCUSSION 167

6. CONCLUSIONS 169

REFERENCES 170

VITA 173

LIST OF TABLES

TABLE PAGE

PART 1: Pertinent Literature Review

Table 1. Physical and chemical characteristics of trichloroethene 13

PART 2: Electroremediation of Radionuclide and TCE-Contaminated Groundwaters Using Zero-valent Iron (Fe^0)

Table 1. Chemical composition of simulated and contaminated waters 48

Table 2. Results of removal efficiency of ^{235}U and ^{95m}Tc from simulated contaminated water with different electrode arrangements 59

Table 3. Results of removal efficiency of ^{235}U and ^{95m}TC under varying flow rate (from 1 to 20 mL/min) using column type 2A 60

Table 4. Results of removal efficiency of ^{235}U and ^{95m}Tc under varying flow rate (from 1 to 20 mL/min) using column type 2B 61

Table 5. Results of removal efficiency of ^{235}U and ^{95m}Tc under varying voltages and initial concentrations 63

Table 6. Results of ^{235}U and ^{95m}Tc removal efficiency from contaminated water with two different distances between anode and cathode 64

PART 3: Electrochemical Dechlorination of TCE Using Palladized, Multi-phasic Iron Oxide Minerals

Table 1. Composition of Portsmouth X-701B water 94

Table 2. Summary of the TCE dechlorination experiments using multiphasic Fe oxides 99

PART 4: Iron Hydroxide Formation from Zero-valent Iron (Fe^0) During Contaminated Groundwater Treatment and Its Effects on Reactive Wall Performance

Table 1. Reactive Fe^0 medium used for treatment of contaminated waters 116

Table 2. Chemical composition in influent and effluent streams of the reactive barrier used in the field 119

Table 3. Chemical composition in influent and effluent streams of the reactive barrier used in laboratory 121

Table 4. Summary of the reactive iron barrier experiments in the field and laboratory 127

Table 5. Porosity analyses using point counting of pore, metallic iron, and iron hydroxide phases 140

PART 5: Electrochemical Synthesis of Pyroaurite-type Minerals

Table 1. X-ray diffraction data of the precipitates formed from four systems 163

LIST OF FIGURES

FIGURE PAGE

PART 1: Pertinent Literature Review

Figure 1. Schematic representation of formation and transformation pathways of common iron oxides together with the approximate transformation conditions 25

PART 2: Electroremediation of Radionuclide- and TCE-Contaminated Groundwaters Using Zero-valent Iron (Fe^0)

Figure 1. Photograph showing the electroremediation experimental setup 1 (26-cm-long by 2.54-cm-internal diameter glass column) with external DC power and water supply 52

Figure 2. Schematic diagram showing experimental setup 2 (35-cm-long by 2-cm-internal diameter glass column) of the electroremediation using Fe^0 filing 53

Figure 3. TCE degradation with different electrode arrangement and varying flow rate 66

Figure 4. Effect of direct current application on TCE dechlorination 67

Figure 5. Results of column tests for TCE dechlorination conducted at four different flow rates 70

Figure 6. (a) By-product distribution upon TCE dechlorination with cathodic arrangement and (b) by-product distribution upon TCE dechlorination without current 72

Figure 7. Comparison of uranyl fluorescence spectra of (a) uranyl nitrate, (b) uranyl carbonate, and (c) U precipitated or adsorbed on Fe^0 and in iron precipitates 76

Figure 8. Scanning electron micrograph of (a) spherical amorphous iron hydroxide, and (b) the precipitate displaying platy, hexagonal shaped pyroaurite-type mineral, green rust 78

PART 3: Electrochemical Dechlorination of TCE Using Palladized, Multiphasic Iron Oxide Minerals

Figure 1. Scanning electron migraph of the palladized multiphasic Fe oxide foam (a, b, c) consisted of magnetite (m), wüestite (w), hercynite (h), and palladium (p) and EDX spectra (d) 91

Figure 2. Schematic diagram showing experimental setup of the electroremediation using multiphasic Fe oxides 93

Figure 3. TCE dechlorination using (a) multiphasic Fe oxides without current; (b) multiphasic Fe oxides with current; and (c) palladized, multiphasic Fe oxides without current 98

Figure 4. Gas chromatographic analyses of the Portsmouth X-701B TCE-contaminated water: (a) before treatment and (b) after treatment with palladized, multiphasic Fe oxides with current 102

Figure 5. TCE dechlorination using palladized, multiphasic Fe oxides with current (30 V, 0.5 A) 103

PART 4: Iron Hydroxide Formation from Zero-valent Iron (Fe^0) During Contaminated Groundwater Treatment and Its Effect on Iron Wall Performance

Figure 1. Dissolved Fe^{2+} concentration in effluent of the reactive Fe^0 medium in the laboratory experiment 123

Figure 2. SEM and EDX spectra of the reactive Fe^0 barrier used at the Portsmouth site (a,b) and at the Y-12 site (c,d) 128

Figure 3. Scanning electron micrograph:(a) green rust formed from Peerless Fe^0 filing used at Portsmouth site, (b) green rust formed from Peerless Fe^0 filing during electrochemical dechlorination of TCE, (c) green rust formed from Master Builder Fe^0 filing used at the Y-12 site, and (d) green rust formed from Cercona Fe^0 foam during electrochemical immobilization of radionuclides 129

Figure 4. Scanning electron micrograph of (a) iron hydroxide formation from dome-shaped iron (hydr)oxides, (b) goethite formation with micropore, and (c) XRD analysis of lepidocrocite (l) and goethite (g) formed from Fe^0 filing used at the Portsmouth site. 132

Figure 5. Scanning electron micrograph of (a) calcite and (b) aragonite formed on Fe^0 filing used at the Y-12 site, and (c) XRD analysis of siderite (s) and magnetite (m) formed from Fe^0 filing used at the Y-12 site 134

Figure 6. Scanning electron micrograph of (a) mackinawite and (b) sulfur formed from Fe^0 filing used at the Portsmouth site, and (c) XRD analysis of mackinawite (m) formed from Fe^0 filing used at the Portsmouth site 137

Figure 7. Scanning electron micrograph of polished cross section:(a,b) Peerless Fe^0 filing and (c,d) Master Builder Fe^0 filing used at the Portsmouth site 139

PART 5: Electrochemical Synthesis of Pyroaurite-type Minerals

Figure 1. Photograph showing an electrochemical synthesis system with external DC power and contaminated water supply 156

Figure 2. X-ray diffaction analyses of the crystalline precipitates: (a) U-Tc-Fe carbonates, (b) Mg-Fe carbonates, (c) Co-Fe-carbonates, and (d) Na-Fe-carbonates . 160

Figure 3. (a) Scanning electron micrograph of the coprecipitates displaying barrel- or keg-shaped morphology and (b) energy dispersive X-ray spectra showing the chemical composition of the precipitate is mainly iron and uranium 161

Figure 4. Fourier transformed infrared spectra of pyroaurite-type iron mineral (a) Co-Fe-carbonates, and (b) U-Tc-Fe carbonates 165

Figure 5. Comparison of fluorescence spectra of (a) uranyl nitrate, (b) uranyl carbonate, and (c) crystalline mineral 166

INTRODUCTION

Many Department of Energy (DOE) sites have problems associated with plumes of radionuclides (e.g., ^{99}Tc, $^{235,238}U$, ^{90}Sr, ^{60}Co) and chlorinated organic compounds, such as trichloroethene (TCE), trichloroethane (TCA), and dichloroethene (DCE) isomers. The chlorinated organic compounds as well as heavy metals are also common contaminants at Department of Defense (DoD) and Environmental Protection Agency (EPA) Superfund sites. Some of these contaminants have been transported to surface waters through seepage discharge and others to groundwater through matrix diffusion and fracture flow processes. Groundwater contamination has been a major environmental concern because of its widespread occurrence and because of difficulties in treatment as a result of the depths of the water-bearing layers. Most conventional separation technologies for contaminated waters are developed on the basis of ion exchange, adsorption, or coprecipitation processes; however, these technologies use chemicals or adsorbents that create secondary-contaminated wastes. The most common method of groundwater remediation, pump-and-treat, has proven to be remarkably ineffective. As a consequence, a great incentive exists for research on alternative remediation technology development.

Previous studies have tested the use of granular iron for the passive in situ remediation (permeable reactive subsurface barrier) of groundwater containing chlorinated organic compounds and reducible heavy metals and radionuclides. A permeable reactive subsurface barrier is defined as an emplacement of reactive materials in the subsurface designed to intercept a contaminant plume, provide a preferential flow path through the reactive medium, and transform the contaminants into environmentally acceptable forms.

A variety of materials are used as reactive barriers, including activated carbon,

zeolite, limestone, peat, microorganisms, or sawdust; however zero-valent iron (Fe^0) is being evaluated by a number of laboratories for its potential as a reactive material that will minimize the subsurface migration of chlorinated organic compounds and certain reducible metals and radionuclides. Mixing palladium with iron particles catalyzes the reactive barrier to treat contaminants that iron alone cannot effectively treat and also decreases the reaction time required to eliminate volatile organic compounds. There is a broad consensus that the remediation process is an abiotic redox reaction involving reduction of the organic compounds and reducible metals and oxidation of the metal. Many researchers proposed possible mechanisms for the degradation process of chlorinated organic compounds. The reaction appears to be pseudo-first order with respect to the organic and inorganic concentration.

The products of the reaction were chloride (Cl^-), ferrous iron (Fe^{2+}), reduced metals, and non-chlorinated (or less chlorinated) hydrocarbons. In a reactive barrier, Fe^0 is oxidized through the reduction of water, releasing additional Fe^{2+} to solution as well as H_2 and OH^-. These geochemical changes can result in precipitation on the reactant surfaces, potentially reducing the reactivity and permeability of the reactive zone over time. Waters high in carbonates might result in a significant buildup of calcite ($CaCO_3$) or siderite ($FeCO_3$). In addition, iron hydroxides and iron sulfide can also be expected to precipitate as a result of geochemical changes and the occurrence of sulfate-reducing bacteria (SRB) in an iron-water system. Although the Fe^0-based reactive barrier has been demonstrated to be a cost-effective method for chlorinated organic compounds and reducible metal contaminated groundwater remediation, the current approach is limited by

its low process efficiency and the effective life of the reactive medium.

Therefore, a electro-enhanced treatment system with an Fe^0 filing and a palladium-coated multiphasic iron oxide medium was developed to solve the problems associated with in situ and ex situ Fe^0 applications. The effect of direct current application on the performance of a reactive Fe^0/iron oxide barrier is discussed in Parts 2 and 3. Precipitates formed in response to geochemical changes in the reactive Fe^0 columns were mineralogically characterized to examine the effect of precipitates on the performance of the reactive Fe^0 and transformation of the iron oxides from Fe^0 (Part 4). A pyroaurite-type mineral as an intermediate product formed during the hydrolytic oxidation of Fe^{2+} to FeOOH was electrochemically synthesized as a host mineral for uranium and technetium. The mechanisms involved in iron oxidation and the effect of cations and anions on the initial precipitation and subsequent phase transformation during the contaminated groundwater treatment were investigated (Part 5).

This dissertation has five parts which are related to each other, but each part has a specific objective:

- Part 1: To review the previous studies related to dissertation subject, electrochemical remediation of radionuclide- and trichloroethene-contaminated groundwater using zero-valent iron/iron oxides and mineralogical characterization of iron hydroxides formed from zero-valent iron,

- Part 2: To develop and evaluate the electro-enhanced remediation technology using an Fe^0 medium for mobile radionuclides [e.g., TcO_4^- and $UO_2(CO)_3^{2-}$] and

TCE in groundwater,

- Part 3: To develop and evaluate the electrochemical processes in an iron-oxide-based flow-through electro-column under direct current for dechlorination of TCE-contaminated groundwater,

- Part 4: To perform mineralogical characterization of the precipitates formed during contaminated groundwater treatment using Fe^0 under varying conditions, such as groundwater chemistry and contaminant concentrations, and

- Part 5: To understand the chemical processes involved and the effect of cations and anions on the initial precipitation and subsequent phase transformation during the electrochemical synthesis of pyroaurite-type minerals (green rust).

PART 1

PERTINENT LITERATURE REVIEW

1. ENVIRONMENTAL BEHAVIOR OF URANIUM, TECHNETIUM, AND TRICHLOROETHENE

1. 1 Uranium

Uranium (U) is the most common radioactive contaminant in soils and waters and is found chiefly at former nuclear weapons processing facilities (Riley et al., 1992). It occurs naturally and is comprised of three main isotopes. By weight, natural U consists of 99.283% ^{238}U, 0.71% ^{235}U, and 0.0054% ^{234}U with half-lives of 4.5×10^9 y, 7.1×10^8 y, and 2.47×10^5 y, respectively. Depleted and enriched U have lower and higher isotopic ratios of $^{234,235}U$ to ^{238}U, respectively, to that found for natural U. In nature, U occurs mainly in ore deposits of uraninite (UO_2) or coffinite ($USiO_4$), which are mined for weapon and reactor-fuel production. Mine-tailing-process and spent fuel treatment wastes are the major sources of U contamination of soils and groundwaters.

Uranium may exist in aqueous solutions in three oxidation states: U(IV), U(V), and U(VI), with U(VI) predominating in oxidizing environments when groundwater pH is >5 (Langmuir, 1978). Two forms of U, U(IV) and U(VI), contrast sharply in their behavior in the natural environment. Uranium(VI) is quite mobile because uranyl cations readily form soluble complexes with common groundwater anions or neutral species such as carbonates $[UO_2(CO_3)_2]^{2-}$ or $[UO_2(CO_3)_3]^{4-}$, phosphates $[UO_2(HPO_4)_2]^{2-}$, or sulfates $[UO_2SO_4]$. The thermodynamic data not only show that U(IV) is less stable relative to U(VI), but that U(V) as UO_2^+ has a large stability field in reduced waters below pH 7 (Langmuir, 1978). As a large monovalent ion, UO_2^+ is apparently a weaker complex than

UO_2^{2+} (Ahrland et al., 1973). Complexes of UO_2^{+} are less stable than those of UO_2^{2+} or U^{4+} formed with the same ligand (Langmuir, 1978).

In near-surface groundwater systems, chemical interactions such as ion exchange and adsorption with variable-charge sites on mineral surfaces act as mobility-retarding agents. The higher stability of U(VI) relative to U(IV) species and the existence of soluble U(V) greatly increases the mobility of U for a wide range of natural conditions (Langmuir, 1978). The presence of reductants in the soil environment alters the oxidation state from the mobile U(VI) form to the readily precipitated U(IV) form. Dissolved U(VI) can be removed from groundwater by chemical reduction to U(IV) which precipitates as UO_2 or by rapid sorption to geologic media (Olsen et al., 1986). The U(IV) species tend to precipitate as insoluble uraninite (UO_2) or coffinite ($USiO_4$), having solubilities < 30 μg/L, under reducing conditions (Langmuir, 1978).

At typical concentrations of chloride, fluoride, phosphate, and sulfate in groundwater, uranous (U^{4+}) fluoride complexes are dominant species in anoxic water below pH 3 – 4. Uranyl (UO_2^{2+}) cation is chemically more dynamic in the environment than its reduced cationic analogue, U^{4+}, because of the tendency of U^{4+} to precipitate as a hydroxide or oxide. Immobilization of U in contaminated soil is expedited by the presence of iron and manganese oxides, and by lowering Eh values for reducing the U(VI) form to a U(IV) form (Lisitian and Kuznetsova, 1967). At typical ligand concentrations in groundwater, the most important uranyl complexes are formed with fluoride, phosphates, and carbonate under acid, near neutral, and alkaline conditions, respectively (Langmuir, 1978). Reduction of mobile uranyl species to U(IV) with precipitation of highly insoluble

uraninite (or coffinite) must often reflect the concurrent oxidation of proportionate amounts of more abundant oxidizable species of, for example, iron, sulfur, and/or carbon (Langmuir, 1978). For example, U reduction and precipitation at pH 8 might involve HS^- oxidation to SO_4^{2-},

$$4[UO_2(CO_3)_3^{4-}] + HS^- + 15H^+ = 4UO_2(s) + SO_4^{2-} + 12CO_2(g) + 8H_2O \qquad (1)$$

or Fe^{2+} oxidation to relatively amorphous $Fe(OH)_3$ ($K_{sp} = 10^{-38.5}$),

$$UO_2(CO_3)_3^{4-} + 2Fe^{2+} + 3H_2O = UO_2(s) + 2Fe(OH)_3 + 3CO_2(g) \qquad (2)$$

Other oxidation reactions, including oxidation of pyrite (FeS_2) to Fe^{2+} and SO_4^{2-}, CH_4 to CO_2, and H_2 to H_2O (Lisitian and Kuznetsova, 1967) are also capable of reducing U(VI) to U(IV) and precipitating $UO_2(s)$.

The sorption of UO_2^{2+} to solid substances has been studied as a mobility-limiting process, particularly with respect to adsorption by Fe oxides (Payne and Waite, 1991; Hsi and Langmuir, 1985; Ho and Miller, 1985; Maya, 1982) and phyllosilicate minerals (Borovec, 1981; Tsunashima et al., 1981; Liser et al., 1991). Even though sorption reaction has been thought to constrain the mobility of naturally occurring dissolved U (Tsunashima et al., 1981) and of U associated with mill tailings (Thompson et al., 1986; Bonotto, 1989), quantitative modeling of uranyl adsorption to natural substrates has been limited to oxides and oxyhydroxides (Hsi and Langmuir, 1985; Payne and Waite, 1991).

Iron oxyhydroxides in particular have been studied (Hsi and Langmuir, 1985) because they have a high adsorption capacity and are common accessory minerals or coatings in sediments and soils where uranyl adsorption reactions are significant.

1.2 Technetium

Technetium (Tc) is produced by spontaneous fission of ^{235}U in nature; however, its major claim to fame is being the world's first artificially created element, mainly from neutron activation of ^{99}Mo and by slow neutron fission of ^{235}U or ^{239}Pu in nuclear reactors (Wildung et al., 1977). The major radioisotope of Tc of concern in contaminated soils and waters is ^{99}Tc, a beta-emitter having a half-life of 2.1×10^5 y, which was deposited into soils and waters following fallout from worldwide nuclear testing and during reprocessing activities of spent fuel waste.

Compounds of Tc in the multiple oxidation states from +7 to -1 are well known; the more stable states are those of Tc(+7) and Tc(+4) (Schwochau, 1983). Generally, Tc compounds having an oxidation number <+4 are easily oxidized to tetravalent and subsequently hexavalent states, whereas Tc (+5) and Tc (+6) frequently disproportionate into Tc (+4) and Tc (+7) (Schwochau, 1983). The predominant form of Tc under oxic conditions is the pertechnetate anion (TcO_4^-) (Pourbaix, 1966), which is highly soluble in water and is of particular environmental concern because of its persistence and mobility (Wildung et al.,1979). Under reducing conditions, TcO_2 and its hydrolysis products may be the stable forms (Wildung et al., 1979). The pertechnetate ion is highly stable over a broad pH range and at concentrations of 1.1×10^{-5} to 0.18 *M* (Wildung et al., 1979). It is

likely the most stable chemical species in aqueous solutions, including perhaps natural waters. However, pertechnetate is known to be reduced by Zn, hydrazine, hydroxylamine, ascorbic acid, $SnCl_2$, HCl, and dilute H_2SO_4 to form the hydrated dioxide $TcO_2 \cdot 2H_2O$ in aqueous solutions, although complete reduction to Tc(IV) may be slow (Anders, 1960).

Heptavalent Tc exists as the heptaoxide (Tc_2O_7), pertechnetate (TcO_4^-), potassium pertechnetate ($KTcO_4$), ammonium pertechnetate (NH_4TcO_4), and as pertechnyl chloride, $TcO_3 \cdot Cl$ (Emsley, 1991) with pertechnetate being the most common form. Heptavalent Tc was easily reduced in ferrous iron solution and coprecipitated as amorphous $(FeTc)(OH)_3$ (Lee and Bondietti, 1983a). The amorphous hydroxide was transformed into Tc-bearing maghemite and goethite during one-month aging (Lee and Bondietti, 1983a). By electrolysis, reduction of Tc(VII) can occur on the platinum electrode via adsorbed hydrogen atoms (Mazzocchin et al., 1974). The overall scheme for the reduction of Tc(VII) to Tc(IV) should be :

$$TcO_4^- + 4H^+ + 3e^- = TcO_2 + 2H_2O \qquad (3)$$

Technetium(IV) is a stable form with the particular species being dependent on the media and pH. Technetium(IV) exists as TcO_2 at pH 3 and precipitates from a chloride media above pH 2 (Grassi, 1979). It is possible that other species, such as TcO^{2+}, $TcO(OH)^+$, and Tc^{4+}, occur in highly acid media (pH < 1.51) (Grassi, 1979). Walton et al. (1986) reported that Tc(IV) was rapidly removed by Fe (III) oxyhydroxides by chemisorption and also incorporated within the Fe_2O_3 lattice during a short time period.

The sequential-extraction results indicated that Tc is primarily associated with the oxides (Sheppard and Thibault, 1988,1992). Studies by Bondietti and Francis (1979) indicate that the pertechnetate anion (TcO_4^-) can be reduced to Tc(IV), forming rather insoluble TcO_2 in anoxic waters or soils that contain an appreciable amount of organic matter. Therefore, it is possible that Tc may be accumulating in highly reducing zones in soils.

The removal of Tc from contaminated groundwater can be accomplished by inorganic sorbents (iron fillings or powder and Fe_3S_4) and ion-exchange resins (Dowex SRB-OH and Reillex resins) (Del Cul et al., 1993, 1995). A reducing environment in the absence of organic complexing agents converts TcO_4^- to insoluble, hydrated TcO_2. When TcO_4^- enters a soil or bedrock environment and encounters reducing species (such as Fe^{2+}), it is converted to insoluble TcO_2, resulting in a substantial reduction in its migration potential. Studies under conditions of deep geologic media have lead to the conclusion that the potential hazard to man posed by Tc has been overestimated because of the reducing environment found in groundwater and deep geologic formations (Bondietti and Francis, 1979).

1.3 Trichloroethene

Trichloroethene (TCE) is an unsaturated aliphatic chlorinated hydrocarbon that is known as a toxic material with maximum contamination levels (MCL) of 0.005 mg/L in drinking water (Cotruvo and Vogt, 1990). Trichloroethene is introduced as a solvent from various industrial applications. Several important physical and chemical characteristics of TCE are presented in the Table 1. Typically, short-chain aliphatic

compounds like TCE cannot be removed from groundwater using conventional water treatment techniques such as coagulation, sedimentation, or filtration (Wood and Demarco, 1980). Instead, they are generally removed by air stripping and adsorption (Love and Eiler, 1982). Unfortunately, these methods of removal do not destroy the potentially unsafe compounds, but have only maneuvered them from one phase to another.

Table. 1. Physical and chemical characteristics of trichloroethene

Trichloroethene		Trichloroethene	
Formula	CCl_2=CHCl	Specific gravity	1.46 at 20 °C
Color	Colorless	Odor	Chlorinated solvent
Melting Point	-87 °C	Viscosity	Less than water
Boiling Point	86.7 °C	Solubility in water	1100 mg/L at 20 °C
Vapor pressure	95 mm at 30 °C	USEPA MCL	0.005 mg/L

Source: Verschueren (1983); Cheremisinoff (1990); Cotruvo and Vogt (1990)

Trichloroethene, once discharged onto the ground surface, will percolate very quickly into the unsaturated vadose zone because rainwater and moisture in the soil facilitate rapid transportation of the chemicals to the groundwater. The chemical reaches the groundwater and sinks through groundwater until it reaches a less permeable layer. There, it will spread out under the influence of gravity or sink through holes in the confining aquifer. Once dense chlorinated solvents such as perchlorethene (PCE) and TCE have entered the environment, restoring the chemical quality of the soil or groundwater can be difficult, costly, and take a long time. Trichloroethene will transform

into dichloroethene (DCE) isomers, vinyl chloride (VC), and ethene through biotic and abiotic processes (natural attenuation) in soil and waters. Drinking water limits for halogenated organic compounds, as established by the U.S. EPA, are as follows (Cotruvo and Vogt, 1990; Fetter, 1992): TCE, 0.005 mg/L; 1,1-DCE 0.007 mg/L; cis-1,2 DCE, 0.07 mg/L; trans-1,2- DCE, 0.1 mg/L; and VC, 0.002 mg/L.

The possible application of zero-valent iron (Fe^0) to clean a groundwater contaminated with volatile organic compounds (VOCs) has also been studied (Gillham and O'Hannesin, 1994; Matheson and Tratnyek, 1994; Burris et al., 1995; Orth and Gillham, 1996; Roberts et al., 1996; Schlimn and Heitz, 1996; Liang et al, 1997a,b). In large part, this was initiated by the suggestion of Gillham and coworkers that Fe^0 could be utilized as a dechlorination medium in a passive approach to groundwater remediation (Gillham and O'Hannesin, 1992). On the basis of thermodynamic considerations (Roberts et al., 1996), Fe^0 should be able to reductively dechlorinate VOCs to nontoxic, benign products such as ethene and ethane.

2. REMEDIATION OF RADIONUCLIDE- AND TCE-CONTAMINATED GROUNDWATER

2.1 Conventional Process

Radionuclides in water are usually removed by ion exchange, reverse osmosis, microfiltration, precipitation, and/or flocculation (Sorg, 1990). These methods can be expensive for large water volumes, low metal concentrations, high salt content, and low discharge limits. Conventional coagulation/filtration treatment showed that the U removal efficiency was dependent on the coagulant dosage and the final pH of the test solutions (Sorg, 1990). The pH dependency of U removal was related to the stability and charge characteristics of the uranyl species and the metal hydroxides precipitates at the adjusted pH of the solutions (Lee and Bondietti, 1983b). Removal of U by Na- and Ca-form resins on pond water (pH > 8.3) was low because the U was in the carbonate (anionic species) form (Lee et al., 1982; Lee and Bondietti, 1983b). Recently, there has been some research into the use of living and nonliving microbial biomass for the bioremediation and recovery of heavy metals from aqueous streams (Summers, 1992). Commercial applications of this research are still limited by the high cost of growing pure cultures of cells and microorganisms and by the need for their immobilization or separation from the aqueous stream. Rhizofiltration (Salt et al., 1995; Cunningham and Ow, 1996), an emerging new technology implanting the use of terrestrial plant roots in the remediation of aqueous streams, may provide a cost-effective method to treat pollutants at concentrations that are too low for efficient removal by conventional treatment, but still too high to allow

discharge to the environment. However, even the rhizofiltration system has its limitations because a desirable low concentration of U in the effluent was not achieved in the experiment with high influent U concentration (> 1000 μg/L) (Dushenkov et al., 1997).

A common approach for remediating contaminated groundwater with semi-volatile organic compounds is the pump-and-treat technology (i.e., pumps water from the ground and treats it ex situ). The ex situ treatment involves air stripping (Gross and Termath, 1985) and granular activated carbon adsorption (Yun et al., 1998). However, these technologies do not destroy VOCs but simply transfer them to another medium. Trichloroethene and PCE can be destroyed by advanced methods like oxidation using ozone with ultraviolet light, and hydrogen peroxide (Glaze and Kang, 1988). These alternatives are cost-intensive and difficult to use in situ. Collectively, pump-and-treat technologies involve high capital and energy costs. Moreover, they are less efficient as a substantial amount of uncontaminated groundwater is removed along with contaminated water. Biodegradation (Wilson and Wilson, 1985) of VOCs under aerobic (Nelson et al., 1987) and anaerobic (Freedom and Gosset, 1989) conditions has also been reported. These fortuitous metabolisms, however, need xenobiotics like toluene or phenol (Hopkins, 1993) for the induction of the required enzymes in certain methanogenic microorganisms, and these biological processes are very slow. As a result, the priority of treatment is now shifting to in situ treatment. One such emerging technology is reductive dehalogenation of VOCs and reductive adsorption and coprecipitation of metals and radionuclides using a nontoxic zero-valent metal (such as Fe^0).

2.2 Immobilization of Heavy Metals and Radionuclides Using Fe^0

Immobilization of heavy metals and radionuclides by Fe^0 is a heterogenous physicochemical process that involves reduction, sorption, and precipitation. Previous work has shown that CrO_4^{2-} is rapidly reduced by Fe^0 to Cr^{3+} (Gould, 1982; Blowes et al., 1997; Powell et al., 1995). Subsequent precipitation of $Cr(OH)_3$ or $Cr_xFe_{1-x}(OH)_3$ causes dramatic reductions in dissolved Cr concentrations (Eary and Rai, 1988; Pratt et al., 1997). Zero-valent iron is also known to be capable of reducing Ag^+, Cu^{2+}, Hg^+, Mo^{6+}, Tc^{7+}, and U^{6+} by oxidation (Cantrell et al., 1995; Bostick and Fellows, 1998). The reduced species can be adsorbed or coprecipitated with oxidized iron, thereby eliminating or greatly reducing contaminant migration (Cantrell et al., 1995; Del Cul and Bostick, 1995; Powell et al., 1995; Smith, 1996).

Thermodynamic calculations suggest that Fe^0 should be able to reduce mobile oxyanions CrO_4^{2-}, $UO_2(CO_3)_2^{2-}$, TcO_4^-, and MoO_4^{2-} species to their immobile reduced species. Zero-valent iron is a reducing agent because of its ease of oxidation under ambient environmental conditions (Pourbaix, 1973). For example, the redox couple formed by Fe^0 and dissolved aqueous Fe^{2+},

$$Fe^0 = Fe^{2+} + 2e^- \qquad (4)$$

has a standard electrode potential (E^0) of +0.44V (Siegel, 1974). The positive E^0 indicates that this reaction can occur spontaneously as written and suggests that Fe^0 can be a reducing agent for many redox-labile contaminants that have a redox pair at higher

electrode potentials (e.g., U, Tc, TCE). Dissolved oxygen (DO), when present, is the preferred oxidant (eq. 5) and, when combined with eq. 4, results in rapid corrosion (eq. 6):

$$O_2 + 2H_2O + 4e^- = 4OH^- \quad (5)$$

$$2Fe^0 + O_2 + 2H_2O = 2Fe^{2+} + 4OH^- \quad (6)$$

Further oxidation of Fe^{2+} by O_2 leads to the formation of ferric hydroxides (Matheson and Tratnyek, 1994). Water can also serve as the oxidant (eq. 7), and thus, corrosion can occur under anaerobic conditions (eq. 8):

$$2H_2O + 2e^- = H_2 + 2OH^- \quad (7)$$

$$Fe^0 + 2H_2O = Fe^{2+} + H_2 + 2OH^- \quad (8)$$

Both Fe oxidation reactions (eqs. 6 and 8) increase the pH, thus favoring the formation of Fe hydroxide precipitates. Because of their redox chemistry, U and Tc are easily susceptible to reduction and coprecipitation through oxidation of Fe^0. Zero-valent iron is the strong reductant that, when oxidized at the anode, will induce the reduction of U and Tc, as shown in the following half-cell reactions:

$$2Fe^0 = 2Fe^{3+} + 6e^- \quad E^0 = +0.037V \quad (9)$$

$$1.5UO_2^{2+} + 6H^+ + 3e^- = 1.5U^{4+} + 3H_2O \quad E^0 = +0.327V \quad (10)$$

$$TcO_4^- + 4H^+ + 3e^- = TcO_2 + 2H_2O \quad E^0 = +0.74V \quad (11)$$

Overall reaction will be:

$$2Fe^0 + 1.5UO_2^{2+} + 10H^+ + TcO_4^- = 2Fe^{3+} + 1.5U^{4+} + TcO_2 + 5H_2O \quad E^0 = +1.104V \qquad (12)$$

The Fe^{3+}, U^{4+}, and Tc^{4+} ions would be readily complexed by the hydroxyls produced at the cathode and would coprecipitate out of solution as U/Tc-bearing Fe hydroxide minerals.

Experiments with ferrous or mixed-valence Fe minerals, such as magnetite and ferrous sulfide, suggest that Tc precipitation and sorption is possible under aerobic and anaerobic conditions (Lee and Bondietti, 1983a; Liang et al., 1996). Upon reduction, Tc may be immobilized as $(Tc_xFe_{1-x})(OH)_3$ or $(Fe_{3-x}Tc_x)O_4$ (Lee and Bondietti, 1983a). The Fe^0 provides the substrate for precipitation of reduced U species and produces only a minimal amount of waste that is in the form of pyroaurite-type mineral (Roh et al., 1996).

Although the Fe^0-based reactive barrier has been demonstrated to be a cost-effective method for heavy metal- and radionuclide-contaminated plume remediation, further research is required to assess remaining questions such as the long-term integrity and effectiveness of the metal in a range of hydrogeochemical environments, the reaction mechanisms, clogging as a result of iron hydroxide precipitation, and water quality degradation by corroded iron.

2.3 Dechlorination of Trichloroethene Using Fe^0

Reductive dechlorination of chlorinated solvents by fine-grained Fe^0 was studied in

well-mixed anaerobic batch systems (Matheson and Tratnyek, 1994). In the presence of a proton donor like water, alkylhalides (RX) typically undergo reductive dehalogenation:

$$RX + 2e^- + H^+ = RH + X^- \qquad (13)$$

The estimated standard reduction potential of the above half reaction for various alkyl halides range from +0.5 to +1.5 V at pH 7 (Vogel et al., 1987). The net reductive dehalogenation reaction by iron is equivalent to iron corrosion with the alkyl halides serving as the oxidizing agents (Matheson and Tratnyek, 1994). They showed that the reductive dechlorination rate of TCE could be increased by the amalgamation of iron with other metals and the increase in surface area of the iron. It is proposed that the degradation process of TCE is a consequence of the directive, oxidative corrosion of the iron (Matheson and Tratnyek, 1994). The end products of TCE degradation could be ethene and ethane. Assuming the ethene to be the end product, the redox couple can be written as

$$3Fe^0 = 3Fe^{2+} + 6e^- \qquad (14)$$

$$C_2HCl_3 + 3H^+ + 6e^- = C_2H_4 + 3Cl^- \qquad (15)$$

Thus, the complete degradation of 1 mol of TCE would add 1 mol of ethene and 3 mol each of Cl^- and Fe^{2+} to the solution phase. Some of the by-products, such as cis-1,2-dichloroethene (DCE), 1,1-DCE, and vinyl chloride (VC), are themselves of concern as

drinking water contaminants. Dechlorination rates of intermediates products to end products are relatively slow.

The natural degradation rate of TCE to ethene in an abiotic system was reported as 1.1×10^{10} h (Jeffers et al., 1989). Orth and Gillham (1996) reported that the mean half-life degradation of TCE using Fe^0 was 3.25 hours. For palladized Fe^0, the TCE half-life was 35 minutes and had the lesser amounts of by-products (Liang et al., 1997a). The reductive dehalogenation reaction is generally divided into two categories (Campbell et al., 1997): (1) hydrogenolysis (a reduction in which a carbon-halogen bond is broken and hydrogen replaces the halogen substituent) and (2) reductive elimination (a reaction in which two groups, such as hydrogen and chlorine, are lost from adjacent carbon atoms so that a double bond is formed). Matheson and Tratnyek (1994) have also studied the reductive mechanism and stated that iron participates in the reductive dechlorination reaction primarily as a direct, electrolytic reduction. Reduction by hydrogen produced during the corrosion process is not believed to be a major contributor. Zero-valent iron is an inexpensive and common material.

To date, the precise pathways through which metals reduce chloroethylenes have not been fully elucidated, nor have reaction products or intermediate been completely characterized (Roberts et al., 1996). Although the Fe^0-based reactive barrier has been demonstrated to be a cost-effective method for TCE-contaminated plume remediation, the current approach is limited in maximization of process efficiency and effective life of media. Therefore, the volume of material in the barrier is the only parameter that determines its effective life for given site-specific hydrologic and geochemical conditions.

3. IRON HYDROXIDE FORMATION FROM Fe^0

3.1 Geochemical Processes in Reactive Fe^0 Barrier

Zero-valent iron is inherently unstable under ambient geochemical conditions so that spontaneous oxidation will generate both electrons and dissolved iron in aqueous environments (Pourbaix, 1973). The oxidation results in the reduction of coexisting aqueous species, consumption of DO, and precipitation of Fe hydroxide minerals. Metal corrosion is an electrochemical process in which oxidation of Fe^0 to Fe^{2+} is the anodic half reaction. The associated cathodic reaction may vary with the reactivity of available electron acceptors. In anoxic pure aqueous media, the acceptors include H^+ and H_2O, the reduction of which yields OH^- and H_2. Thus, the overall process of corrosion in anaerobic Fe^0-H_2O systems is described by the following reactions:

$$Fe + 2H_2O = Fe^{2+} + H_2 + 2OH^- \qquad (16)$$

Therefore, effluent pH increase and Eh decrease are the result of electrolysis of water by the iron-water reaction, which also produces large quantities of hydroxyl ions and hydrogen gas. When pH increases and Eh decreases significantly, precipitates of iron hydroxide form.

Important geochemical processes in reactive iron medium include dissolution, precipitation kinetics, sorption to Fe^0 surfaces, and chemical behavior of contaminants (i.e., radionuclides, heavy metals, and chlorinated organic carbons). Because of the redox

potential of several radionuclides, heavy metals, and chlorinated organic compounds, they are easily susceptible to reduction and coprecipitation through oxidation of Fe^0 as shown in the following reactions (Roh et al., 1996; Powell et al., 1995; Matheson and Tratnyek, 1994):

$$2Fe^0 + 1.5UO_2^{2+} + 10H^+ + TcO_4^- = 2Fe^{3+} + 1.5U^{4+} + TcO_2 + 5H_2O \quad (17)$$

$$Fe^0 + CrO_4^{2-} + 4H_2O = Fe(OH)_3 + Cr(OH)_3 + 3OH^- \quad (18)$$

$$3Fe^0 + C_2HCl_3 + 3H^+ = 3Fe^{2+} + C_2H_4 + 3Cl^- \quad (19)$$

At the same time, when contaminated water is passed through a reactive barrier of Fe^0 system, it undergoes geochemical changes, such as Eh/pH, carbonate alkalinity, DO, sulfate, and Fe^{2+} concentration in effluent.

3.2 Iron Hydroxide, Iron Sulfide, and Calcium Carbonate Formation

The geochemical changes in a reactive iron barrier can result in precipitation on the reactant surfaces, potentially reducing reactivity and permeability of the reactive zone over time. Waters high in carbonates might result in a significant buildup of aragonite ($CaCO_3$), calcite ($CaCO_3$), or siderite ($FeCO_3$) (Blengino et al., 1995). In addition, iron hydroxides and iron sulfide can also be expected to precipitate as a result of geochemical changes and the occurrence of sulfate-reducing bacteria (SRB) in the iron-water system (Blengino et

al., 1995; Badan et al., 1991; Hao et al., 1996). Green rusts form as corrosion products of steel, especially microbially induced corrosion, and as a mineral in poorly drained soils (Trolard et al., 1997; Genin et al., 1998).

Oxidation of iron can proceed along several reaction pathways (Schwertmann and Cornell, 1991) (Figure 1). Continued corrosion of iron leads to saturation and precipitation of $Fe(OH)_2$. The Eh-pH diagram indicated that the iron metal will be passivated by a green rust, such as $[Fe_4(OH)_8Cl \bullet nH_2O]$, $[Fe_6(OH)_{12}][CO_3 \bullet nH_2O]$, and $[Fe_7(OH)_{18}SO_4 \bullet nH_2O]$, in a moderately neutral solution ($6.5 < pH < 8.0$) and passivated by iron hydroxide (FeOOH) in the presence of an alkaline solution ($pH > 8.0$) (Olowe and Genin, 1991; Drissi et al., 1995; Genin et al., 1996; Refait et al., 1997; Simon et al., 1997). In the absence of oxygen and at low temperature, $Fe(OH)_2$ is stable but is predicted thermodynamically to convert to magnetite, intermediate products (green rusts), and hydrated forms of iron ferric oxides. Green rusts often form as an intermediate product during the hydrolytic oxidation of Fe^{2+} solutions to FeOOH (Schwertmann and Cornell, 1991). Green rusts convert to goethite (α-FeOOH), lepidocrocite (γ-FeOOH), maghemite (Fe_2O_3), or magnetite (Fe_3O_4), depending on the rate of oxidation and dehydration (Hansen et al., 1994). The freshly precipitated ferrihydrite reacts with excess Fe^{2+} in the system and induces the hydrolysis of Fe^{2+}, which leads to the formation of green rusts (Schwertmann and Cornell, 1991). Green rust is a reductant capable of dechlorination of TCE and reduction of heavy metals and radionuclides (Roh et al., 1996; Myneni et al., 1997). A synthetic and natural material of similar crystal structure is likely to reduce nitrate and heavy metals under abiotic conditions, although these reactions are

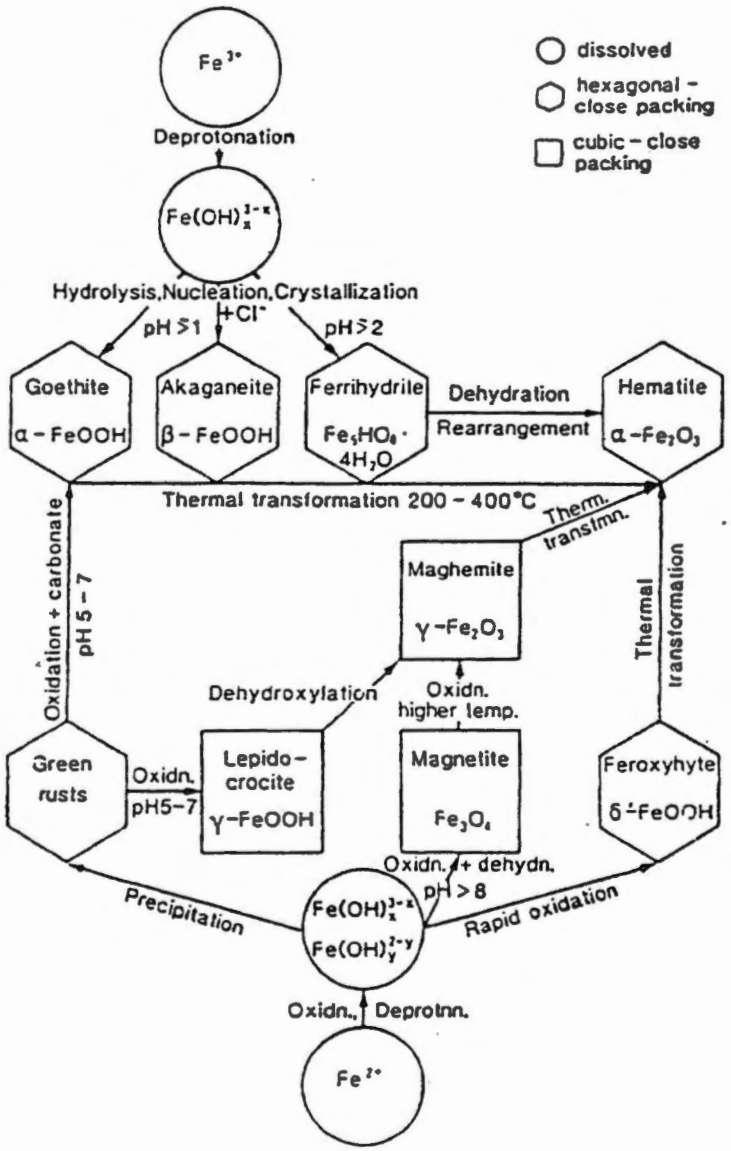


Figure 1. Schematic representation of formation and transformation pathways of common iron oxides together with the approximate transformation conditions (Schwertmann and Cornell, 1991)

generally quite slow (Hansen et al., 1996).

Hydroxyl ions produced by corrosion increase pH and react with dissolved carbonate species in the groundwater to produce carbonate ions:

$$H_2CO_3^0 + 2OH^- = CO_3^{2-} + 2H_2O(l) \quad (20)$$

$$HCO_3^- + OH^- = CO_3^{2-} + H_2O(l) \quad (21)$$

Buildup of carbonate ions eventually will result in precipitation of carbonate solid species.

$$Ca^{2+}(aq) + CO_3^{2-} = CaCO_3(s) \quad (22)$$

$$Ca^{2+}(aq) + HCO_3^-(aq) = CaCO_3(s) + H^+ \quad (23)$$

$$Fe^{2+}(aq) + CO_3^{2-} = FeCO_3(s) \quad (24)$$

$$Fe^{2+}(aq) + HCO_3^-(aq) = FeCO_3(s) + H^+ \quad (25)$$

Therefore, waters high in carbonates might result in a significant buildup of calcite ($CaCO_3$) and siderite ($FeCO_3$), depending on the chemical composition of the groundwater.

Anaerobic bacteria are commonly associated with the corrosion of metals (Hamilton, 1985). The sulfate-reducing bacteria (SRB) normally influence the corrosion of metals are:

$$SO_4^{2-} + 8H^+ + 8\ e^- = S^{2-} + 4H_2O \text{ (cathodic depolarization reaction by SRB)} \quad (26)$$

$$4Fe^0 + SO_4^{2-} + 4H_2O = FeS + 3Fe(OH)_2 + 2OH^- \text{ (iron sulfide precipitation)} \quad (27)$$

For abiotic systems, the simultaneous presence of oxygen and hydrogen sulfide further accelerates the corrosion process of metallic iron with the prominent corrosion product being ferrous sulfide, FeS (Lewandowski et al., 1997). Oxidation of iron sulfides results in generation of a highly corrosive product, elemental sulfur, according to the reaction (Lewandowski et al., 1997):

$$2H_2O + 4FeS + 3O_2 = 4S^0 + 4FeO(OH) \quad (28)$$

Microbial, Fe^0 treatment systems may offer advantages over abiotic Fe^0 schemes because reductive dechlorination was apparently supported using cathodic hydrogen produced by anaerobic corrosion of the added Fe^0 (Weathers et al., 1997). A potential negative consequence of bacteria is biofouling (Weathers et al., 1997), because the proliferation in an improperly designed reactive barrier could reduce the hydraulic conductivity of the barrier, thereby hindering the flow of groundwater through it.

REFERENCES

Ahrland, S., J. O. Liljenzin, and J. Rydberg, J. 1973. Solution chemistry. *In* Comprehensive inorganic chemistry, Vol. 5. Actinides, pp. 465-635. Pergamon Press

Anders, E. 1960. Radiochemistry of technetium. USAEC Rep., NAS-NS-3021. Natl. Tech. Inf. Serv., Springfield, Verginia.

Badan, B., M. Magrini, and E. Ramous. 1991. A study of the microbiological-corrosion products of steel and cast iron pipes in fresh water. J. Material Sci. 26:1951-1954

Blengono, J, M., M. Keddam, J. P. Labbe, and L. Lobbiola. 1995. Physico-chemical characterization of corrosion layers formed on iron in a sodium carbonate-bicarbonate containing environments. Corrosion Sci. 37(4):621-643

Blowes, D. W., C. J. Ptacek, and J. L. Jambor. 1997. In-situ remediation of Cr(VI)-contaminated groundwater using permeable walls:Laboratory studies. Environ. Sci. Technol. 31(12):3348-3357

Bondietti, E. A., and C. W. Francis. 1979. Geologic migration potential of technetium-99 and neptunium-237. Science. 203:1337-1340

Bonotto, D. M. 1989. The behavior of dissolved uranium in groundwater of the Morro do Ferro torium deposit, Brazil. J. Hydro. 107:155-168

Borovec, Z. 1981. The adsorption of uranyl species by fine clay. Chem. Geol. 32:45-58

Bostick, W. D., and R. L. Fellows. 1998. Use of sodium hypochlorite and steel wool to remove and recover mercury from mixed waste. K/TSO-58, The East Tennessee Technology Park, Oak Ridge, Tennessee

Burris, D. R., T. J. Campbell, and V. S. Manoranjan. 1995. Sorption of trichloroethene and tetrachloroethene in a batch reactive metallic iron-water system. Environ. Sci. Technol. 29(11):2850-2855

Campbell, T. J., D. R. Burris, A. L. Roberts, and T. R. Wells. 1997. Trichloroethene and tetrachloroethylene reduction in a metallic iron-water-vapor batch system. Environ. Sci. Technol. 16(4):625-630

Cantrell, K. J., D. I. Kaplan, and T. W. Wietsma. 1995. Zero-valent iron for the in situ remediation of selected metals in groundwater. J. Hazard. Mat. 42:201-212

Cheremisinoff, P. N. 1990. Calculating and reporting toxic chemical releases for pollution control. Matewan, New Jersey, USA. Scitech Publishers.

Cotruvo, J. A., and C. D. Vogt. 1990. Water quality standards and goals. *In* Water quality and treatment: A hand book of community water supplies. 4th ed., McGraw-Hill, New York.

Cunningham, S. D., and D. W. Ow. 1996. Promises and prospects of phytotoremediation. Plant Physiol. 110:715-719

Del Cul, G. D., W. D. Bobstick, D. R. Trotter, and P. E. Osborne. 1993. Tc-99 removal process of solutions and contaminated groundwater. Sep. Sci. Technol. 28(1-3):551-564

Del Cul, G. D., and W. D. Bostick. 1995. Simple method for technetium removal from aqueous solutions. Nucl. Technol. 109:161-162

Drissi, S. H., Ph. Refait, M. Abdelmoula, and J. M. R. Genin. 1995. The preparation and thermodynamic properties of Fe(II)-Fe(III) hydroxide-carbonate (Green Rust 1); Pourbaix diagram of iron in carbonate-containing aqueous media. Corrosion Sci. 37(12):2025-2041

Dushenkov, S., D. Vasudev, Y. Kapulink, D. Gleba, D. Fleisher, K. C. Ting, and B. Ensley. 1997. Removal of uranium from water using terrestrial plants. Environ. Sci. Technol. 31:3468-3474

Eary, L. E., and D. Rai. 1988. Chromate removal from aqueous wastes by reduction with ferrous iron. Environ. Sci. Technol. 22:972-977

Emsley, J. 1991. The elements. 2nd ed. Clarendon Press, Oxford.

Fetter, C. W. 1992. Contaminant hydrology. Macmillan Publishing Company, New York.

Freedom, D. L., and J. M. Gosset. 1989. Biological reductive dechlorination of tetrachloroethelene and trichloroethene to ethylene under methanogenic conditions. Appl. Environ. Micro. 55:2144-2151

Genin, J. M. R., A. A. Olowe, and Ph. Refait. 1996. On the stoichiometry and Pourbaix diagram of Fe(II)-Fe(III) hydroxy-sulfate or sulfate containing green rust 2:an electrochemical and Mössbauer spectroscopy study. Corrosion Sci. 38:1751-1762

Genin, J. R., G. Bourrie, F. Trolard, M. Abdelmoula, A. Jaffrezic, P. Refait, V. Maitre, B. Humbert, and A. Herbillon. 1998. Thermodynamic equilibria in aqueous suspensions of synthetic and natural Fe(II)-Fe(III) green rusts: Occurrences of the mineral in hydromorphic soils. Environ. Sci. Technol. 32:1058-1068

Gillham, R. W., and S. F. O'Hannesin. 1992. Metal-catalyzed abiotic degradation of halogenated organic compounds. Paper presented at the 1992 IAH Conference Modern Trends in Hydrogeology, May 10-13, 1992, Hamilton, Ontario, Canada.

Gillham, R. W., and S. F. O'Hannesin. 1994. Enhanced degradation of halogenated aliphatics by zero-valent iron. Ground Water 32(6): 958-967

Glaze, W. H., and J. W. Kang. 1988. Advanced oxidation processes for treating groundwater contaminated with TCE and PCE: Laboratory studies. J. Am. Water Work Assoc. May:57-63

Gould, J.P. 1982. The kinetics of hexavalent chromium reduction by metallic iron. Water Research. 16: 871-877

Grassi, J., J. Dvynck, and B. Tremillon. 1979. Electrochemical studies of technetium at a mercury electrode. Anal. Chim Acta 107:47-58

Gross, R.L., and S.G. Termath. 1985. Packed tower aeration strips TCE from groundwater. Environ. Prog. 4:119-124

Hamilton, W. A. 1985. Sulfate-reducing bacteria and anaerobic corrosion. Ann. Rev. Microbiol. 39:195-217

Hansen, H. C. B., O. K. Borggaard, and J. Sorensen. 1994. Evaluation of the free energy of formation of Fe(II)-Fe(III) hydroxide-sulfate (green rust) and its reduction of nitrite. Geochim. Cosmochim. Acta. 58:2599-2608

Hansen H. C. B., C. B. Koch, H. Nancke-Krogh, O. K. Borggaard, and J. Sorensen. 1996. Abiotic nitrate reduction to ammonium:Key role of green rust. Environ. Sci. Technol. 30:2053-2056

Hao, O. J., J. M. Chen, and L. Huang. 1996. Sulfate reducing bacteria. Critical Reviews in Environ. Sci. and Technol. 26(2):155-187

Ho, C. H., and N. H. Miller. 1985. Effect of humic acid on uranium uptake by hematite particles. J. Colloid Interface Sci. 106:281-288

Hopkins, G. L., L. Semperini, and P. L. McCarthy. 1993. Microcosm and in situ field studies of biotransformation of trichloroethene by phenol utilizing microorganisms. Appl. Environ. Micro. 59(7):2277-2285

Hsi, C. K. D., and D. Langmuir. 1985. Adsorption of uranyl onto ferric oxyhydroxides: Application of the surface complexation site-binding model. Geochim. Cosmochim. Acta

49:1931-1941

Jeffers, D. M., L. M. Ward, L. M. Waytowitc, and N. L. Wolfe. 1989. Homogeneous hydrolysis rate constants for selected chlorinated metanes, ethanes, ethenes, and propanes. Environ. Sci. Technol. 23(8):965-969

Langmuir, D. 1978. Uranium solution-mineral equilibria at low temperatures with applications to sedimentary ore deposits. Geochim. Cosmochim. Acta. 42:547-569

Lee, S. Y., S. K. Hall, and E. A. Bondietti. 1982. Methods of removing uranium from drinking water:II. Present municipal water treatment and potential removal methods. Office of Drinking Water, U. S. EPA 570/9-82/003

Lee, S. Y., and E. A. Bondietti. 1983a. Technetium behavior in sulfide and ferrous iron solutions. Mat. Res. Soc. Symp. Proc. 15:315-322

Lee, S. Y., and E. A. Bondietti. 1983b. Removing uranium from drinking water by metal hydroxide and anion exchange resin. J. Am Water Work Assoc. 75:537-540

Lewandowski, Z., W. Dickinson, and W. Lee. 1997. Electrochemical interactions of biofilms with metal surfaces. Wat. Sci. Tech. 36(1):295-302

Liang, L., B. Gu, and X. Yin. 1996. Removal of technetium-99 from contaminated water with sorbents and reductive materials. Sep. Sci. Technol. (6):111-122

Liang, L., N. Korte, J. D. Goodlaxson, J. Clausen, Q. Fernando, and R. Muftikian, 1997a. By product formation during the reduction of TCE by zero-valent iron and palatist iron. Ground Water Monitoring and Remediation. Winter:122-127

Liang, L., O. R. West, N. E. Korte, J. D. Goodlaxson, D. A. Pickering, J. L. Zutman, F.J. Anderson, C. A. Welch, M. J. Pelfery, M. J. Dickery. 1997b. The X-625 groundwater treatment facility. A field-scale test of trichloroethylene dechlorination using iron filing for the X-120/X-749 groundwater flume. ORNL/TM-13217. Oak Ridge National Laboratory, Oak Ridge, Tennessee.

Liser, K. H., S. Quandt-Klenk, and B. Thybusch. 1991. Sorption of uranyl ions on hydrous silicon dioxide. Radiochim. Acta 57:45-50

Lisitian, A. K., and E. C. Kuznetsova. 1967. Role of microorganisms in development of geochemical reduction barriers where limonitization bedded zones wedge out. Intern. Geol. Review. 9:1180-1191

Love, T., and R. G. Eiler. 1982. Treatment of drinking water containing trichloroethylene

and related industrial solvents. J. Am. Water Works Assoc. 74:413-425

Matheson, L. J., and P. G. Tratyek. 1994. Reductive dehalogenation of chlorinated methanes by iron metal. Environ. Sci Technol. 28:2045-2053

Maya. L. 1982. Sorbed uranium(VI) species on hydrous titania, zirconia, and silica gel. Radiochim. Acta. 31:147-151

Mazzocchin, G. A., F. Magno, U. Mazzi, and R. Portanova. 1974. Voltametric behavior of aqueous technetate(VII) ion. Inorganic Chim. Acta 9:263-268

Myneni, S. C. B., T. K. Tokunaga, and G. E. Brown. 1997. Abiotic selenium redox transformation in the presence of Fe(II,III) oxides. Science. 278(5340):1106-1109

Nelson, M. J. K., S. O. Montgomery, W. R. Mahaffey, and P. H. Prichard. 1987. Biodegradation of trichloroethene and involvement of an aromatic biodegradative pathway. Appl. Environ. Micro. 53(5):949-954

Olowe, A. A., and J. M. R. Genin. 1991. The mechanism of oxidation of ferrous hydroxide in sulfated aqueous media:Importance of the initial ratio of the reactants. Corrosion Sci. 32(9):965-984

Olsen C. R., P. D. Lowry, S. Y. Lee, I. L. Larsen, and N. H. Cutshall. 1986. Geochemical and environmental process affecting radionuclide migration from a formerly used seepage trench. Geochim. Cosmochim. Acta. 50:593-607

Orth, W. S., and R. W. Gillham. 1996. Dechlorination of trichloroethene in aqueous solution using Fe(0). Environ. Sci. Technol. 30(1):66-71

Payne, T. E., and T. D. Waite. 1991. Surface complexation modeling of uranium sorption data obtained by isotope exchange techniques. Radiochim. Acta 52:497-493

Pourbaix, M. 1966. Atlas of electrochemical equilibria, Pergamon Press, Oxford.

Pourbaix, M. 1973. Lectures on electrochemical corrosion. Plenum Press, New York.

Powell, R. M., R. W. Puls, S. K. Hightower, and D. A. Sabatini. 1995. Coupled iron corrosion and chromate reduction: Mechanisms for subsurface remediation. Environ. Sci. Technol.29(8):1913-1922

Pratt, A. R., D. W. Blowes, and C. J. Ptacek. 1997. Products of chromate reduction on proposed surface remediation material. Environ. Sci. Technol. 31(9):2492-2498

Refait, Ph., S. H. Drissi, and J. Pytkiewicz. 1997. The anionic species competition in iron aqueous corrosion:Role of various green rust compounds. Corrosion Sci. 39:1699-1710

Riley, R. G., J. M. Zachara, and F. J. Wobber. 1992. Chemical contaminants on DOE lands and selection of contaminant mixtures for subsurface science research. Battelle Pacific Northwest Labs., Rich land, Washington. DOE/ER-0547-T

Roberts, A. L., L. A. Totten, W. A. Arnold, D. R. Burris, and T. J. Campbell. 1996. Reductive elimination of chlorinated ethelenes by zero-valent metals. Environ. Sci. Technol.30(8):2654-2659

Roh, Y., S. Y. Lee, and M. P. Elless. 1996. Electroremediation of uranium and technetium cotaminated waters. Extended Abstract. Annual Meeting of the Chemical Society, I&EC Division, Emerging Technologies in Hazardous Waste Management VIII, Sept., 9-12, 1996. Birmingham, Alabama. pp. 582-585.

Salt, D. E., M. Blaylock, N. P. B. A. Kumar, V. Dushenkov, B. D. Ensley, I. Chet, and I. Raskin. 1995. Phytoremediation: a novel strategy for the removal of toxic elements from the environment using plants. Biotechnology 13:468-474

Schlimn, C., and E. Heitz. 1996. Development of a wastewater treatment progress: Reductive dehalogenation of chlorinated hydrocarbons by metals. Environ. Prog. 15(1):38-47

Schwertmann, U., and R. M. Cornell. 1991. Iron oxides in the laboratory. VCH Publishers, Inc., New York.

Schwochau, K. 1983. The present status of technetium chemistry. Radiochim. Acta. 32:139-152

Sheppard, M. I., and D. H. Thibault. 1992. Desorption and extraction of selected heavy metals from soils. Soil Sci. Soc. Am. J. 56:415-423

Siegel, F. R. 1974. Applied Geochemistry. John Wiley and Sons, Inc., New York, 353p

Simon, L., J. M. R. Genin, and Ph. Refait. 1997. Stand free enthalpy of formation of Fe(II)-Fe(III) hydroxysulphite green rust one and its oxidation into hydroxysulfate green rust two. Corrosion Sci. 39:1673-1685

Smith, E. H. 1996. Uptake of heavy metals in batch systems by a recycled iron-bearing material. Water Res. 30(10):2424-2434

Sorg, T. J. 1990. Removal of uranium from drinking water by conventional treatment

methods. *In* Cothern, C. R., and P. A. Revers (eds.). Radon, radium and uranium in drinking water Lewis Publishers, Inc. Chelsea, Michigan

Summers, A. O. 1992. The hard stuff: Metals in bioremediation. Curr. Opin. Biotechnol. 3(3):271-276.

Thompson, B. M., P. A. Longmire, and D. G. Brookins. 1986. Geochemical constraints on underground disposal of uranium mill tailings. Applied Geochem. 1:335-343

Trolard. F., J. M. R. Genin, M. Abdelmoula, G. Bourrie, B. Humbert, and A. Herbillon. 1997. Identification of a green rust mineral in a reductomorphic soil by Mossbaur and Raman spectroscopies. Geochim. Cosmochim. Acta. 61:1107-1111

Tsunashima, A., G. W. Brindley, and M. Bastovanov. 1981. Adsorption of uranium from solutions by montmorillonite: Composition and properties of uranyl montmorillonites. Clays Clay Min. 29:10-16

Verschueren, K. 1983. Handbook of environmental data on organic chemicals. New York. Van Nostrand Reinhold.

Vogel, T. M., C. S. Criddle, and P. L. McCarty. 1987. Transformation of halogenated aliphatic compounds. Environ. Sci. Technol. 21(8):722-736

Walton, F. B., J. Paquette, J. P. M. Ross, and W. E. Lawrence. 1986. Tc(IV) and Tc (VII) interactions with iron oxyhydroxides. Nucl. Chem. Waste Manag. 6:121-126

Weathers, L. J, G. F. Parkin, and P. J. Alvarez. 1997. Utilization of cathodic hydrogen as electron donor for chloroform cometabolism by a mixed methanogenic culture. Environ. Sci.Technol. 31:880-885

Wildung, R. E., T. R. Garland, and D. A. Cataldo. 1977. Accumulation of technetium by plants. Health Physics. 32:314-317

Wildung, R. E., K. M. McFadden, and T. R. Garland. 1979. Technetium sources and behavior in the environment. J. Environ. Qual. 8(2):156-161

Wilson, J. T., and B. H. Wilson. 1985. Biotransformation of trichloroethene in soil. 1985. Appl. Environ. Micro. 49(1):242-243

Wood, P. R., and J. DeMarco. 1980. Effectiveness of various adsorbents in removing organic compounds for water. Part I. Removing purgeable halogenated organics by activated carbon adsorption of organics from aqueous phase. Ann Arber Science Publishers, Inc., Ann Arber, Michigan.

Yun, J. H., D. K. Choi, and S. H. Kim. 1998. Adsorption equilibria of chlorinated organic-solvents onto activated carbon. Ind. Engr. Chem. Res. 37:1422-1427

PART 2

ELECTROREMEDIATION OF RADIONUCLIDE- AND TCE-CONTAMINATED GROUNDWATER USING ZERO-VALENT IRON (Fe^0)

1. ABSTRACT

Reactive medium including zero-valent metals such as zero-valent iron (Fe^0) adsorbs, degrades, and precipitates radionuclides and chlorinated solvents as a contaminant plume flows through the treatment medium. Although the Fe^0 based reactive barrier has been demonstrated to be a cost-effective method for trichloroethene (TCE) and reducible metal- and radionuclide-contaminated plume remediation, the current approach is limited by low process efficiency and uncertain, effective life of the medium. The passive in situ system cannot control the spontaneous oxidation of Fe^0 because the volume and types of material in the barrier are the only parameters that determine its effective life for a given site-specific hydrologic and geochemical condition. The objective of this study is to develop and evaluate electrochemically enhanced dechlorination of TCE and immobilization of radionuclides, uranium (U) and technetium (Tc), in groundwater using Fe^0. The bench-scale flow-through Fe^0 reactor column with direct current (DC) application was introduced to increase the efficiency and effective life of Fe^0 medium by controlling the rate of iron oxidation and to enhance the dechlorination rate of TCE and immobilization of radionuclides by providing an external supply of electrons. The removal mechanism appears to be reductive coprecipitation of radionuclides by iron oxidation and providing an eroded iron substrate as well as reductive dechlorination by creating a reducible environment in the reactive iron barrier. Several factors influence the removal of radionuclides and dechlorination of TCE including (1) electrode configuration, (2) applied voltage, (3) distance between cathode and anode, (4) material used as electrodes, and (5)

influent concentration and water chemistry. Reduction of U^{6+} to U^{4+} and Tc^{7+} to Tc^{4+} and coprecipitation of radionuclides as iron hydroxide appear to be the preferred removal mechanism by supplying electrons and corroded iron substrates. The dechlorination mechanism appears to be reductive, with the electrons supplied by the iron oxidation and external power supply serving as the additional source of the electrons.

2. INTRODUCTION

Many U.S. Department of Energy (DOE) sites have problems associated with wastewater and groundwater plumes containing unacceptable levels of radionuclides (e.g., ^{99}Tc, $^{235,238}U$) and chlorinated organic compounds (COCs) such as TCE, trichloroethane (TCA), and dichloroethene (DCE) isomers. Conventional separation technologies for removing uranyl carbonate complexes and pertechnetate anion include anion exchange resins or coprecipitation by ferrous sulfate and sodium hydroxide treatment (Lee and Bondietti, 1983a,b). However, such chemical treatment not only generates secondary wastes but also leaves chemicals (Na^+, SO_4^{2-}) in the treated waters. Likewise, elution of the exchange materials for regeneration requires chemicals that will also remain in the secondary wastes.

A commonly-used method for remediating groundwater contaminated with COCs is called "the pump-and-treat technology", which pumps water from the ground and treats it by absorbents. Alternative remediation technologies to pump-and-treat are in situ and ex situ reactive barrier using zero-valent metals. Permeable walls containing treatment medium can be installed in the path of flowing groundwater to passively remove dissolved constituents (Matheson and Tratnyek, 1994; Cantrell et al., 1995; Del Cul and Bostick, 1995). Zero-valent iron is an effective medium for the dechlorination of a wide range of COCs (Matheson and Tratnyek, 1994; Gotpagar et al., 1997) and reductive sorption and coprecipitation of toxic metals and radionuclides (Powell et al, 1996; Roh et al., 1996). Types and volume of the reactive medium in the barrier are the only parameters that

determine its effective life for a given site-specific hydrologic and geochemical condition. A practical requirement for using Fe^0 as a permeable barrier material is that the kinetics of the reaction should be reasonably fast because a slow reaction rate would require a prohibitively thick barrier to extend the contaminant's residence time within the barrier.

Several types of reactions can occur in this reactive permeable wall. Reducible heavy metals and radionuclides in groundwater can be removed by reductive sorption and precipitation on iron hydroxides or as an iron hydroxide form (Cantrell et al., 1995; Roh et al., 1996). This reaction occurs through a reduction of the metals and radionuclides, and is generally not reversible under the natural conditions in groundwater as long as the contaminants remain in the iron hydroxide phase (Powell et al., 1995; Roh et al., 1996). Cantrell et al. (1995) proposed that UO_2^{2+} may be removed from solution by any of three mechanisms: (1) reduction of U^{6+} by Fe^0 to form less soluble U^{4+} (i.e., $UO_2 \cdot xH_2O$) phase; (2) sorption onto iron oxide corrosion products by ion exchange at hydroxyl sites; or (3) a combination of reduction/precipitation and adsorption to newly precipitated iron hydroxides occurring concurrently. Liang et al.(1996) proposed that removal of Tc by Fe^0 filing may be attributed to a combination of: (1) reductive conversion of the aqueous mobile Tc^{7+} to a lower oxidation state species such as Tc^{4+}, which is relatively immobile; (2) sorption of the reduced species onto iron hydroxide surfaces; and (3) coprecipitation of Tc with iron hydroxides on surfaces. The mechanism of the enhanced degradation of TCE may be an abiotic reductive dechlorination (Matheson and Tratnyek, 1994), with iron serving as the source of electrons, but the mechanism is uncertain. Matheson and Tratnyek (1994) suggest three general pathways that may be available to dehalogenate

alkylhalides. The first pathway involves the metal directly and implies that reduction occurs by electron transfer from the Fe^0 surface to the adsorbed alkylhalide. The second pathway involves Fe^{2+} that is an immediate product of corrosion in aqueous systems. Finally, the third pathway for reductive dehalogenation by iron involves hydrogen produced as a product of corrosion with water. These reaction kinetics are controlled by mass transport to Fe^0 surface, adsorption on Fe^0 surface, chemical reaction at Fe^0 surface, and mass transport of reaction products.

The objectives of this study were (1) to develop and evaluate electroremediation technology using Fe^0 for radionuclides, including TcO_4^-, and $UO_2(CO_3)_2^{2-}$, and TCE in contaminated seepage and groundwater and (2) to gain a better understanding of the removal mechanism of TCE degradation and radionuclide immobilization from groundwater using Fe^0.

2.1 Underlying Electrochemical Principles

Many contaminants of concern under oxidizing conditions are relatively mobile in soils and groundwaters, and represent a significant risk to human health and the environment. However, these contaminants under reducing conditions tend to be much more immobile in soils and groundwaters as they are chemically reduced to lower valence states that are chemically less soluble in water than the oxidized forms. Therefore, reducing agents are desirable for effective containment or precipitation of such contaminants in soils and waters. In principle, these reducing agents are themselves oxidized when their electrons are transferred to the contaminant. Zero-valent iron is such a reducing agent because of

its ease of oxidation under ambient environmental conditions. For example, the redox couple formed by Fe^0 and dissolved aqueous Fe^{2+},

$$Fe^0 = Fe^{2+} + 2e^- \qquad (1),$$

has a standard electrode potential (E^0) of +0.44V (Siegel, 1974). The positive E^0 indicates that this reaction can occur spontaneously as written and suggests that iron metal can be a reducing agent for many redox-labile contaminants that have a redox pair at higher electrode potentials (e.g., U, Tc). Dissolved oxygen (DO), when present, is the preferred oxidant (eq. 2) and, when combined with eq. 1, results in rapid corrosion (eq. 3):

$$O_2 + 2H_2O + 4e^- = 4OH^- \qquad (2)$$

$$2Fe^0 + O_2 + 2H_2O = 2Fe^{2+} + 4OH^- \qquad (3)$$

Further oxidation of Fe^{2+} by O_2 leads to the formation of ferric hydroxides (Matheson and Tratnyek, 1994). Water can also serve as the oxidant (eq. 4), and thus, corrosion can occur under anaerobic conditions (eq. 5):

$$2H_2O + 2e^- = H_2 + 2OH^- \qquad (4)$$

$$Fe^0 + 2H_2O = Fe^{2+} + H_2 + 2OH^- \qquad (5)$$

Both iron oxidation reactions (eqs. 3 and 5) increase the pH, thus favoring the formation

of iron hydroxide precipitates.

Because of their redox chemistry, U and Tc are easily susceptible to reduction and coprecipitation through oxidation of Fe^0. For example, U(VI) is quite mobile in soil environments because uranyl cations readily form soluble complexes with common groundwater anions or neutral species; in contrast, U(IV) is sparingly soluble and tends to precipitate as uraninite and coffinite (Langmuir, 1978). Reduction of mobile uranyl species to U(IV) with precipitation of sparingly soluble uraninite or coffinite can occur naturally in soils, provided a strong reductant such as iron is present. Similarly, Tc is also more mobile in oxidizing conditions than in reducing conditions. The predominant form of Tc under oxic conditions is the pertechnetate anion, TcO_4^- (Pourbaix, 1966). Upon reduction, Tc may be immobilized as $(Tc_xFe_{1-x})(OH)_3$ or $(Fe_{3-x}Tc_x)O_4$ (Lee and Bondietti, 1983a).

Electrochemical treatment can mimic this natural process, but at significantly greater rates. In our system, Fe^0 is the strong reductant that, when oxidized at the anode, will induce the reduction of U and Tc, as shown in the following half-cell reactions:

$$2Fe^0 = 2Fe^{3+} + 6e^- \qquad E^0 = +0.037V \qquad (6)$$

$$1.5UO_2^{2+} + 6H^+ + 3e^- = 1.5U^{4+} + 3H_2O \qquad E^0 = +0.327V \qquad (7)$$

$$TcO_4^- + 4H^+ + 3e^- = TcO_2 + 2H_2O \qquad E^0 = +0.74V \qquad (8)$$

This gives a final spontaneous reaction of

$$2Fe^0 + 1.5UO_2^{2+} + 10H^+ + TcO_4^- = 2Fe^{3+} + 1.5U^{4+} + TcO_2 + 5H_2O \quad E^0 = +1.14V \quad (9)$$

The Fe^{3+}, U^{4+}, and Tc^{4+} ions would be readily complexed by the hydroxyls produced at the cathode and would coprecipitate out of solution as U/Tc-bearing iron hydroxide mineral.

Reductive dehalogenation of organic compounds, such as TCE, is also possible through oxidation of Fe^0. In the presence of a proton donor like water, chlorinated organic compounds (R-Cl) typically undergo reductive dechlorination (Matheson & Tratnyek, 1994):

$$R\text{-}Cl + 2e^- + H^+ = R\text{-}H + Cl^- \quad (10)$$

The estimated standard reduction potential of the above half reaction for various chlorinated organic compounds range from +0.5 to +1.5 V at pH 7 (Vogel et al., 1987). The net reductive dehalogenation reaction by iron (eq. 11) is equivalent to iron corrosion with the alkyl halides serving as the oxidizing agents (Matheson and Tratnyek, 1994).

$$Fe^0 + R\text{-}Cl + H^+ = Fe^{2+} + R\text{-}H + Cl^- \quad (11)$$

2.2 Description of the Electroremediation Process

The electroremediation of water contaminated with radionuclides and TCE is based on

electrolysis, a process producing chemical changes by passing DC through electrodes. The expected chemical reactions in the reaction vessel are as follows:

Anode (Fe^0): 1. $Fe^0 = Fe^{2+} + 2e^-$ (Dissolved Fe^{2+} production by electrode erosion)

2. $TcO_4^- + 1.5Fe^0 + 4H^+ = TcO_2 + 1.5Fe^{2+} + 2H_2O$

3. $UO_2(CO_3)_2^{2-} + Fe^0 + 4H^+ = UO_2 + Fe^{2+} + 2CO_2 + 2H_2O$

4. $Fe^0 + R\text{-}Cl + H^+ = Fe^{2+} + R\text{-}H + Cl^-$

5. $2H_2O = 4H^+ + O_2 + 4e^-$

Buffer Area: 1. $TcO_4^- + 3Fe^{2+} + 4H^+ = TcO_2 + 3Fe^{3+} + 2H_2O$

2. $UO_2(CO_3)_2^{2-} + 2Fe^{2+} + 4H^+ = UO_2 + 2Fe^{3+} + 2CO_2 + 2H_2O$

3. $R\text{-}Cl + Fe^{2+} + H^+ = R\text{-}H + Fe^{3+} + Cl^-$

Cathode (Fe^0): 1. $2H_2O + 2e^- = 2OH^- + H_2$

2. $Fe^0 + R\text{-}Cl + H^+ = Fe^{2+} + R\text{-}H + Cl^-$

3. $R\text{-}Cl + H_2 = R\text{-}H + H^+ + Cl^-$

4. $Fe^{2+/3+} + TcO_2 + UO_2 + OH^- \Rightarrow Fe(Tc,U)OOH$ precipitate

Water is oxidized at a iridium-coated titanium anode releasing molecular oxygen, electrons, and protons. Electrons transverse an external circuit to a Fe^0 cathode, where they engage in reductive dechlorination reactions. The hydrogen ions generated at the anode move from anode to cathode, and are consumed as a reductant simultaneously with the Fe^0 oxidation. The rate at which hydrogen is produced is fixed by the current, this, in turn, is dependent on the applied voltage and the conductivity of the medium. The

generation rate of hydroxyl ions is dependent on the applied voltages and iron oxidation. Therefore, an electrochemically-enhanced, iron-based barrier can accelerate the natural process at significantly greater rates. The DC applied on the iron-based reactive wall will control the oxidation rate of the iron and the dechlorination rate of the chlorinated solvents because transfer of electrons and protons to the iron-based reactive medium will enhance the reductive dechlorination of TCE (Criddle and McCarthy, 1991). Reductive dehalogenation is a two-electron, one proton process that takes places at the electrode surfaces (Roberts et al., 1996). Matheson and Tratnyek (1994) proposed that it should be possible to rapidly dehalogenate chloroorganics with hydrogen gas if a suitable dechlorination catalyst is used. The contaminants of concern are easily dechlorinated from the contaminated water by means of iron oxidation, and electron and proton transfer.

3. MATERIALS AND METHODS

3.1 Simulation of Contaminated Waters

Uranyl carbonate [$^{235}UO_2(CO_3)_2^{2-}$] solution was prepared by adding 5 mL of uranyl nitrate [$UO_2(NO_3)_2^{2-}$] solution into a 0.5 *M* sodium carbonate solution. For the pertechnetate anion, sodium pertechnetate ($^{95m}TcO_4^-$, half life = 61 days) purchased from Du Pont Nen Products was used in this experiment because the fission product ^{99}Tc constitutes a potential long-term environmental hazard due to its long half-life (2.13×10^5 yr). The uranyl carbonate and pertechnetate solutions were diluted with 200-mL tap water to simulate contaminated water. Table 1 shows the chemical composition of the simulated contaminated water. Uranium-contaminated groundwater collected at the Bear Creek Valley, Y-12 Plant, Oak Ridge, Tennessee was also used for immobilization of U using Fe^0 filing. Bear Creek groundwater is dominated by Ca, Na, and bicarbonate which reflects inputs from the underlying carbonate geology and contaminated site (S-3 pond) (Table 1). Water for dechlorination experiments was obtained from a zone of contaminated groundwater at the Portsmouth Gaseous Diffusion Plant (Piketon, Ohio) (Table 1). Organic contaminants of this water include TCE (500 – 780 µg/L).

3.2 Materials Used as Fe^0

A sponge-like Fe^0 foam and two Fe^0 filings were used as the electrode material. The Fe^0 foam (Cercona of America, Inc., Dayton, Ohio) has the following characteristics: (a) 92% Fe^0, balanced with aluminosilicate; (b) 0.9 g/cc bulk density; and (c) 0.5-1 m^2/g

Table 1. Chemical composition of simulated and contaminated waters

Constituents	Simulated water[1]	X-625 Water, Portsmouth Gaseous Diffusion Plant, Piketon, Ohio[2]
pH	7.1	6.1 – 6.2
Eh (mV)	+400	+ 420
DO‡ (mg/L)	0.2 – 5	4 – 5
Alkalinity as $CaCO_3$ (mg/L)	ND†	83 – 85
Chloride (mg/L)	ND	38
Sulfate (mg/L)	ND	400
Nitrate as Nitrogen (mg/L)	ND	ND
Calcium (mg/L)	33.97	21.3
Iron (mg/L)	< 0.01	0.3
Magnesium (mg/L)	9.3	13.3
Manganese (mg/L)	ND	ND
Potassium (mg/L)	1.58	1.7
Sodium (mg/L)	5.35	18.7
^{235}U (mg/L)	7 – 2590	ND
TCE (µg/L)	ND	500 – 780

[1] Radionuclide (^{235}U and ^{95m}Tc)-contaminated water simulated using tap water
[2] TCE-contaminated water (Annual Report for 1997 Groundwater Monitoring Quarterly Sampling Results from Portsmouth Gaseous Diffusion Plant, Ohio)
† Not determined
‡ Dissolved oxygen

estimated specific surface area. Mineralogy of the Fe^0 foam is Fe^o, fayalite (Fe_2SiO_4), and hercynite ($FeAl_2O_4$). The Fe^0 filings are (1) fine grade Fe^0 filings purchased from Master Builders, Inc. (Streetsbros, Ohio) and (2) stock Fe^0 filing purchased from Peerless Metal Powders and Abrasives (Detriot, Michigan). The Master Builder Fe^0 filing has the following characteristics: (1) mesh size, 40 mesh (i.e., 0.24 mm), (2) ~95% Fe^0, and (3) 5% other metals and silicon. The Peerless Fe^0 filing has following characteristics: (1) mesh size between 8 and 50 (i.e., 2.38 to 0.30 mm); (2) 86% Fe^0, 3-4 % carbon, ~3% silicon and other trace metals; and (3) mostly Fe^0 with magnetite.

3.3 Sampling and Analyses

Samples for ^{235}U and ^{95m}Tc in solution were collected from the influent and effluent. Gamma activity of the ^{235}U and ^{95m}Tc isotopes in the solutions were determined using a high purity intrinsic germanium gamma-ray detector equipped with a Nuclear Data Model 6700 microprocessor programmed in 4096 channels (Cutshall and Larsen, 1980). The counting error (2δ) was kept at <2% for all solutions.

Samples for TCE and byproducts were collected from the influent and effluent lines using a 5.0-mL glass syringe. The aqueous samples were injected into a purge-and-trap concentrator (Teker 3000, Tekmar, Cincinnati, Ohio). The samples from the concentrator were then analyzed for reaction by-products by gas chromatographer (GC) (HP-5890 Series II, Hewlett Packard, Wilmington, Delaware) equipped with a flame ionization detector (FID) and a 0.53-mm capillary column (DB624, J&W Scientific, Folsom, California). The following GC retention times were measured: TCE, 9.654 minutes; cis-

1,2-DCE, 6.476 minutes; trans-DCE, 4.782 minutes; 1,1-DCE, 3.657 minutes; vinyl chloride (VC), 2.156 minutes; and ethene/ethane, 1.668 minutes. It was not possible to distinguish ethene from ethane with the instrument used. The method detection limits (MDL) for chlorinated organic compound, as determined by the U.S. EPA method (EPA, 1988), were 0.005 mg/L for TCE; 0.005 mg/L for 1,1-DCE; 0.02 mg/L for cis-1,2-DCE; and 0.005 mg/L for VC.

Redox potential measurements were made immediately after sample collection using a ORION EA™ 920 Expandable Ion analyzer (Orion Research, Beverly, Massachusetts) with a platinum micro-electrode (Microelectrodes, Inc., Londonerry, New Hampshire). The pH measurements were conducted using a combination of pH electrode and a ORION EA™ 920 expandable ion analyzer, standardized with pH buffer 7 and an appropriate buffer of either pH 4 or pH 10. Dissolved ferrous iron (Fe^{2+}) was measured by colorimetric techniques using test kits from Hach (Loveland, Colorado). Dissolved oxygen was measured by using self-filling ampoules for calorimetric analysis from CHEMets® (CHEMetrics, Inc., Calverton, Verginia).

3.4 Experimental Setup

Column experiments for radionuclide immobilization: Two experimental setups were used (1) with Cercona Fe^0 foam and (2) with Fe^0 filing. The first experimental setup was a glass column, 26-cm-long by 2.54-cm-internal diameter, containing an iridium-coated titanium oxide electrode in DC contact with Fe^0 foam. The electrode was connected to an external power supply (Fig. 1). Simulated, radionuclide-contaminated water (Table 1)

was metered to the column at a constant flow rate. The electrolytic cell (column) consisted of one or two anodes (i.e., upper anode and lower anode) and a cathode. The upper anode, an iridium-coated titanium oxide electrode, in contact with the influent contaminated solution was used to lower the solution pH via hydrolysis before reaching the lower anode. The lower anode, Fe^0 foam (8 g) in contact with an iridium-coated titanium oxide electrode, was used to oxidize Fe^0 to Fe^{2+}, which in turn was used to reduce the radionuclides. The solution then passed through the buffer region towards the cathode. The cathode, Fe^0 foam (19 g) in contact with an iridium-coated titanium oxide electrode, was used to increase the solution pH by forming OH^- from the electrolytic breakdown of water. The excess OH^- in the solution would accelerate the formation of radionuclide–iron hydroxide precipitates. Effects of electrode arrangement on performance were also investigated prior to selecting a particular arrangement (Table 2).

The second experimental setup consisted of a plexiglass column, 35-cm-long by 2-cm-internal diameter, containing an iridium-coated titanium oxide electrode in contact with Master Builder Fe^0 filing with the electrode connected to an external power supply (Fig. 2). Simulated, radionuclide-contaminated water (Table 1) was metered to the column at a constant flow rate. Two types of columns, anodic (2A) and cathodic (2B) electrode arrangements, have been studied for the electrochemical precipitation and adsorption of U and Tc. Two columns were packed with 12.5 cm Ottawa sand, 13.5 cm Master Builder Fe^0 filing (35 g), and 9 cm Ottawa sand from the influent end. Both columns have twoports for electrode insertion (lower and upper port from influent end) that werelocated at a distance of 10 and 23.5 cm from the influent end (Fig. 2). Electrode ports of the two

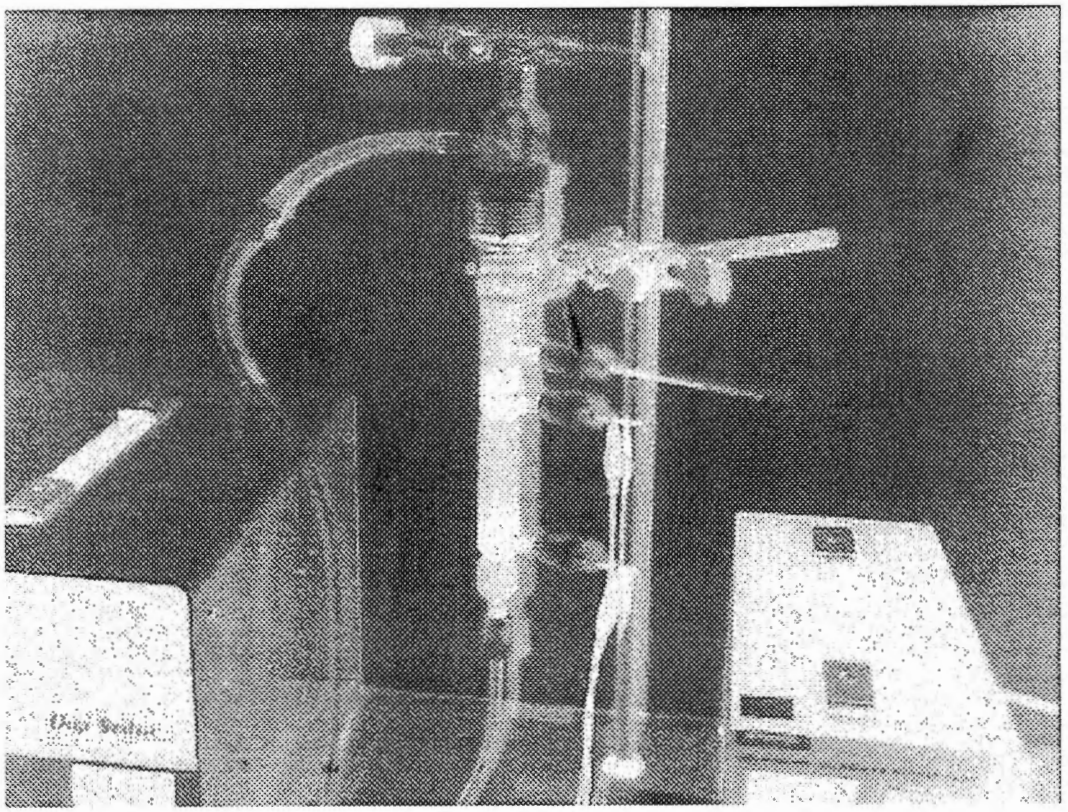


Figure 1. Photograph showing the electroremediation experimental setup 1 (26-cm-long by 2.54-cm-internal diameter glass column) with external DC power and water supply

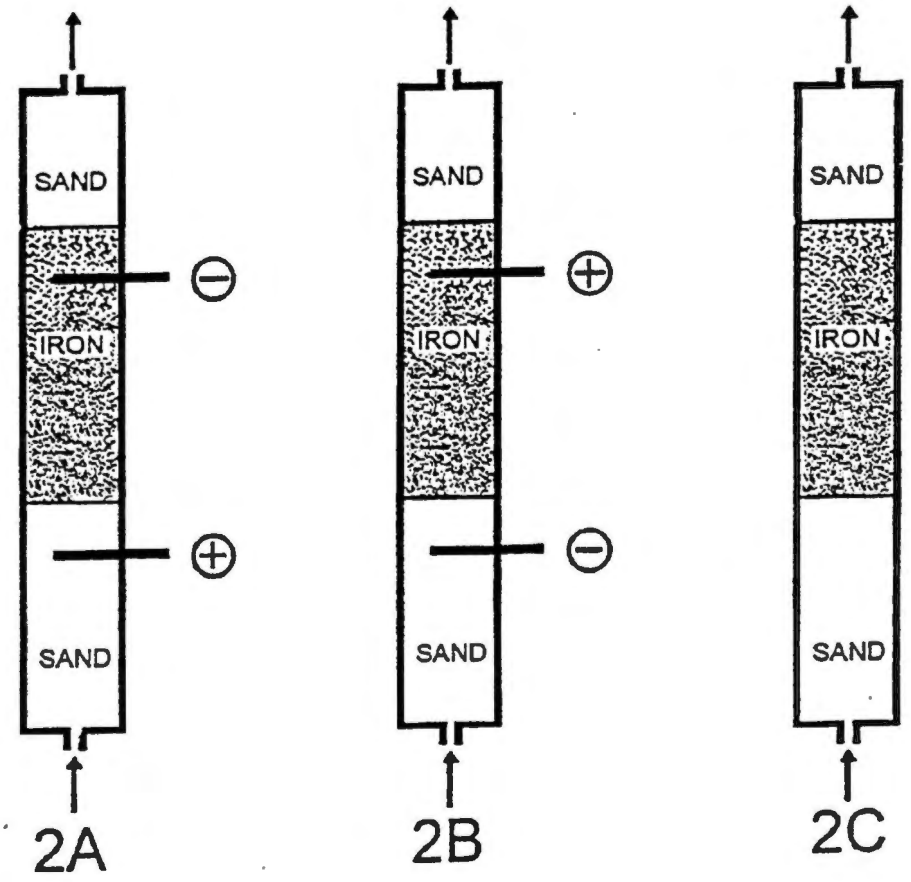


Figure 2. Schematic diagram showing experimental setup 2 (35-cm-long by 2-cm-internal diameter glass column) of the electroremediation using Fe^0 filing

columns were constructed using Teflon fitting with a titanium electrode. In column 2A, a titanium anode in the lower port is contacted with Ottawa sand and a titanium cathode in the upper port is electrically connected with Fe^0 for cathodic iron protection. In column 2B, a titanium cathode in the lower port is contacted with Ottawa sand and a titanium anode in the upper port is electrically connected to Fe^0 for anodic iron corrosion.

Column experiments for TCE dechlorination: Glass columns used for the experiment had a 2-cm-diameter and 35-cm-long and two side ports for electrodes at 8 and 29 cm from the inlet. Both ends were tightly sealed using polypropylene end fittings with O-rings. Three arrangements were used for dechlorination of TCE-contaminated waters (Table 1). In type 2A, an iridium-coated titanium cathode was contacted with iron filing (18 cm, 40 g) and the iridium-coated titanium anode was contacted with carbon pad (0.5 cm, 0.3 g) (Fig. 2). In type 2B, the anode was contacted with Fe^0 filing (18 cm, 40 g) and the cathode was contacted with carbon pad (0.5 cm, 0.3 g). In type 2C, the Fe^0 filing (18 cm, 40 g) was packed without electrodes. The remaining column space was packed with Ottawa sand.

The contaminated X-625 groundwater (Table 1) was held in a 10-L collapsible Tedlar sample bag to minimize losses due to volatilization during the column experiments. The groundwater was pumped from the collapsible bag to the column using a MasterFlex Digi-Staltic pump (Cole-Parmer, Vernon Hills, Illinois) at varying flow rates. Viton tubing was used for the portion of the pump roller assembly and all other portion of the delivery and collection system was Teflon tubing. One control column using sand was used to examine

any loss as a result of volatilization of TCE during the column experiments. The column containing only sand gave a TCE breakthrough curve typical of a nonreactive solute (i.e., the reactive concentration in the effluent was approximately 0.5 after one pore volume had passed through the column, and by two pore volumes, the influent and effluent concentration were approximately equal).

3.5 Mineralogical Characterization of the Corroded Iron Materials

The precipitates of radionuclide-bearing iron oxides were collected by filtration immediately after electrochemical treatments and after aging of the iron hydroxide in the treated solutions for 15 days at room temperature. The precipitates were examined by X-ray diffraction (XRD), scanning electron microscopy (SEM) with energy dispersive X-ray (EDX) analysis. All XRD analyses were performed on a Scintag XDS 2000 diffractometer (45 kV, 40 mA) equipped with CoKα radiation (Sunnyvale, CA). A JEOL JSM-35CF (Tokyo, Japan) SEM with EDX spectrometry was used for the analysis of morphology and chemical composition of the precipitates. The filtrates before and after aging and Fe^0 after column studies were characterized to understand the mechanism of reductive precipitation of U. A fluorescence spectroscopy was also used to identify the presence of oxidized U^{6+} species in the sample (Dai et al., 1996). Steady-state luminescence spectra were measured by means of a fiber-optic probe directly inserted in the crystalline mineral in the treated water (i.e., uranyl carbonate solution and uranyl nitrate solution) (Dai et al., 1994). The 337-nm line of a pulsed nitrogen laser (pulse = 5 ns) was used as the excitation source in this study. A fiber-optic superhead probe (Dillor)

was used for both the excitation and collection of the signal from the samples. The emission was collected at 180° with respect to the excitation direction and dispersed with a Spex 500M monochromator with a 150-nm groove/mm grating blaze at 655 nm. The dispersed radiation was detected using a charge coupled device (CCD) detector (Spex System One) with an entrance slit width of less than 0.8 nm and a resolution of 0.2 nm. The first major peak of the fluorescence spectrum was expected at 499.6-nm for the uranyl nitrate complex (Dai et al., 1996b). No fluorescence signal is expected for the reduced U(IV) species (Dai et al., 1997)

4. RESULTS AND DISCUSSION

4.1 Immobilization of ^{235}U and ^{99}Tc

There are several major factors which affect the electrochemical removal rate of Tc and U from contaminated water. These factors are (1) electrode configuration, (2) potential and current, (3) distance between anode and cathode, (4) materials used as electrodes, and (5) concentration and chemistry of the contaminated water. Through bench-scale column testing, the process control parameters were examined. Other possible variables may influence the process, but it is impossible to investigate all the variables and combination of the variables in the flow through system. Therefore, in this bench-scale column study, the following process parameters in the experimental conditions were examined: (1) effect of electrode arrangement; (2) effect of applied voltage and contaminant concentration; and (3) effect of distance between anode and cathode.

Effect of electrode arrangement using Fe^0 foam: Three types of anode and cathode arrangements with Fe^0 foam were tested for ^{235}U and ^{95m}Tc containing simulated waters using tap water (Table 1). These are (A) iridium anode at the top, iron foam anode in the middle, and iridium cathode at the bottom, (B) iridium anode at the top, iron foam anode in the middle, and iron foam cathode at the bottom, (C) iron foam anode at the top and iron foam cathode at the bottom, and (D) same as (C), but without current. The type A arrangement was intended to acidify the incoming solution by proton generation at the iridium anode, generate ferrous iron from the iron foam anode, and then hydroxylate and

precipitate the iron and radionuclides in the cathode region of the column. In this experiment, a 200-mL solution containing about 2600 mg/L ^{235}U and 1.2E-6 mg/L ^{95m}Tc was treated at a constant current of 0.2 A, voltage of 40 V, and a flow rate of 6.2 mL/min (Table 2). During the course of electrolysis, the pH of the solution at the upper and lower anodes decreased from 5.8 to 5.0, whereas, pH at the cathode increased to 7.5. The results of this electrode arrangement showed that the removal rates were about 70% for ^{235}U and about 50% for ^{95m}Tc (Table 2).

In the type B arrangement, the iridium cathode in the first arrangement was replaced by iron foam to increase the surface area for greater reducing capacity and hydroxyl generation. With a flow rate of 6.2 mL/ min, a 200-mL solution containing 1920 mg/L ^{235}U and 2.61E-06 mg/L ^{95m}Tc was treated with a constant current of 0.2 A and voltage of 40 V. The results of the second type electrode arrangement showed that the removal efficiency was about 93% for ^{235}U and about 70% for ^{95m}Tc. Therefore, the type B arrangement had a better efficiency than the type A arrangement (Table 2).

For the type C electrode arrangement, the iridium anode used in the type B arrangement was removed to evaluate the effectiveness of pre-acidification at the iridium anode on the overall removal process. Again, a 200-mL solution containing 2287 mg/L ^{235}U and 6.98E-06 mg/L ^{95m}Tc was passed through with a flow rate of 6.2 mL/min. The test results of the type C arrangement showed that about 99% of ^{235}U and 87% of ^{95m}Tc was removed by coprecipitation and adsorption with iron hydroxide (Table 2). The better performance of the type C arrangement indicated that pre-acidification used by the type B arrangement did not help the overall process efficiency.

Type D (without current) was used to evaluate the effect of DC on radionuclide immobilization. Type D showed that about 50% of ^{235}U and 32% of ^{95m}Tc was removed (Table 2).

Table 2. Results of removal efficiency of ^{235}U and ^{95m}Tc from simulated contaminated water with different electrode arrangements

Types of	^{235}U			^{95m}Tc		
electrode	C_o	C	C/C_o	C_o	C	C/C_o
arrangement	------ mg/L ------			------- mg/L ----------		
A	2593	780	0.30	1.19E-6	5.90E-7	0.49
B	1920	126	0.07	2.61E-4	7.70E-5	0.29
C	2287	25	0.01	6.98E-6	9.62E-7	0.13
D	2453	1250	0.51	5.24E-6	3.56E-6	0.68

Conditions: Current =0.2 A, Voltage = 40 V, Flow rate = 6.2 mL/min
Type A: Iridium anode on the top, Fe^0 foam anode in the middle, and iridium cathode at the bottom
Type B: Iridium anode on the top, Fe^0 foam anode at the middle, and iron form cathode at the bottom
Type C: Fe^0 foam anode at the top and Fe^0 foam cathode at the bottom
Type D: Fe^0 foam anode at the top and Fe^0 foam cathode at the bottom without current

The DC application to the Fe^0 foam did help the overall removal efficiency of radionuclides. From the reaction scheme shown earlier, three possible reductants are (a) Fe^0, (b) dissolved Fe^{2+}, and (c) electrons released by water hydrolysis at electrodes for radionuclide immobilization. The observed best results of radionuclide removal from the arrangement of Fe^0 foam indicated that coprecipitation and adsorption on iron (hydr)oxide precipitates could be the main removal mechanisms. Anodic arrangement of the Fe^0 foam promotes more iron dissolution from the foam than cathodic arrangements.

Effect of electrode arrangement using Fe^0 filing: Two types of anode and cathode arrangements in the columns were tested for U and Tc containing simulated waters with tap water: (1) an Fe^0 filing as the cathode at the top and an iridium anode at the bottom (type 2A); and (2) an Fe^0 filing anode at the top and an iridium cathode at the bottom (type 2B). In these column tests, simulated contaminated water was introduced from the

Table 3. Results of removal efficiency of ^{235}U and ^{95m}Tc under varying flow rate (from 1 to 20 mL/min) using column type 2A

Tests	Flow rate	Pore Volume Treated	^{235}U			^{95m}Tc		
			C_o	C	C/C_o	C_o	C	C/C_o
	mL/min		---- mg/L -----			------ mg/L -----		
2A-1	1	6.3	7.35	BD†	-‡	2.72E-9	BD	-
2A-2	2	18.9	7.35	BD	-	2.72E-9	BD	-
2A-3	3	28.4	7.35	BD	-	2.72E-9	BD	-
2A-4	4	41.6	7.35	0.10	0.01	2.72E-9	BD	-
2A-5	5	56.8	7.35	0.07	0.01	2.72E-9	BD	-
2A-10	10	72.6	7.35	0.18	0.03	2.72E-9	BD	-
2A-20	20	104.2	7.35	0.19	0.03	2.72E-9	5.8E-11	0.02

† Below detection limit, ‡ non calculable
Length between anode and cathode = 13.5 cm, Voltage = 30 V, Current = 0.05 A
Pore Volume = 18 mL, Porosity = 55%, and Master Builder Fe^0 filing = 35 g

bottom to the top of the column. When the Fe^0 filing was used as an anode, dissolution of the Fe^0 was enhanced by the DC application. Dissolved Fe^{2+} could reduce U and Tc while oxidizing to ferric iron (Fe^{3+}) in solution. When the Fe^0 filings were used as a cathode, U and Tc could be reduced on the surface of the Fe^0 by the applied current.

The experimental results showed that the anodic iron corrosion process had a faster removal rate than the cathodic iron protection process (Table 3 and 4). As flow rate of the columns was increased from 1 mL/min to 20 mL/min, about 1% or more U was detected at the flow rate 4 mL/min or higher in the cathodic iron column (2A), but U was

Table 4. Results of removal efficiency of ^{235}U and ^{95m}Tc under varying flow rate (from 1 to 20 mL/min) using column type 2B

Tests	Flow rate	Pore Volume Treated	^{235}U			^{95m}Tc		
			C_o	C	C/C_o	C_o	C	C/C_o
	mL/min		----- mg/L -----			------ mg/L ------		
2B-1	1	6.3	7.35	BD†	-‡	2.72E-9	BD	-
2B-2	2	18.9	7.35	BD	-	2.72E-9	BD	-
2B-3	3	28.4	7.35	BD	-	2.72E-9	BD	-
2B-4	4	41.6	7.35	BD	-	2.72E-9	BD	-
2B-5	5	56.8	7.35	BD	-	2.72E-9	BD	-
2B-10	10	72.6	7.35	BD	-	2.72E-9	BD	-
2B-20	20	104.2	7.35	0.51	0.08	2.72E-9	BD	-

†Below detection limit, ‡ non calculable
Length between anode and cathode = 13.5 cm, Voltage = 30 V, Current = 0.05 A
Pore Volume = 18 mL, Porosity = 55%, and Master Builder Fe^0 filing = 35 g

not detectable until the flow rate was 20 mL/min in the anodic iron column (2B). The anodic process was also more effective than the cathodic process for Tc (Table 3 and 4). The faster removal rate of the radionuclides indicated that the kinetics of electron transfer is slower from the cathodic surface to the dissolved metals than from an anodic surface to the dissolved metals. The applied current and iron oxidation could be a main source of

electron at the cathodic surface, but iron oxidation from Fe^0 to Fe^{2+} could be a main source for the reduction of radionuclides at the anodic area.

Effect of voltage and influent concentration using Fe^0 foam (Type 1C): To observe the effects of applied voltage and contaminant concentration, four different voltages (10, 20, 30, and 40 V) were applied to the solutions having two different initial concentrations: (a) about 100 mg/L of ^{235}U and 2E-7 mg/L of ^{95m}Tc; and (b) 800 mg/L of ^{235}U and 8E-7 mg/L of ^{95m}Tc. The results showed that the removal rates were greatest under the higher voltage at the higher influent concentration for both radionuclides (Table 5). The removal rates increased gradually with increasing applied voltage. The removal rate was always higher when the solution had a higher radionuclide concentration; however, the remaining concentration in these effluents was also higher than the concentration from the effluent solution started with a lower initial concentration. For example, the remaining U concentration was 80 mg/L when the initial concentration was 800 mg/L, but the remaining concentration was only 25 mg/L when the initial concentration was 120 mg/L under the same experimental conditions. Similar results were obtained from the ^{95m}Tc removal experiments. These results suggest that electrochemical reduction and coprecipitation of the radionuclides depend on electrolyte concentration and iron dissolution of the Fe^0 foam.

Table 5. Results of removal efficiency of ^{235}U and ^{95m}Tc under varying voltages and initial concentrations†

Tests	Conditions	^{235}U			^{95m}Tc		
		C_o	C	C/C_o	C_o	C	C/C_o
		------ mg/L -----			------ mg/L -----		
L-4	40 V	119.77	28.07	0.234	2.26E-7	6.73E-8	0.298
L-3	30 V	127.77	24.74	0.194	2.41E-7	1.21E-7	0.502
L-2	20 V	106.59	21.76	0.204	2.01E-7	1.16E-7	0.577
L-1	10 V	140.43	31.59	0.224	2.65E-7	1.76E-7	0.664
H-4	40 V	752.69	87.95	0.116	7.76E-7	1.72E-7	0.222
H-3	30 V	841.81	97.93	0.116	8.68E-7	2.09E-7	0.241
H-2	20 V	813.11	258.85	0.318	8.38E-7	3.77E-7	0.449
H-1	10 V	876.78	483.38	0.551	9.04E-7	4.87E-7	0.538

† Length between anode and cathode = 8.5 cm

Effect of distance from anode to cathode using Fe^0 foam (Type 1C): Two different distances, 11.5 and 8.5 cm, between the anode and cathode were investigated to determine the effect of anode/cathode distance on the removal efficiency of U and Tc. The results showed that the longer distance between the two electrodes was more effective than the shorter distance for removing U from the solution at a fixed applied voltage (Table 6). This may be attributed to the ferrous iron oxidation in the increased buffer area of the longer distance column. However, the experiments of Tc showed mixed results. The difference of initial Tc concentrations used for the two different anode/cathode distances could cause such inconsistent results observed from the experiments.

Table 6. Results of ^{235}U and ^{95m}Tc removal efficiency from contaminated water with two different distances between anode and cathode

Distance	^{235}U			^{95m}Tc		
	C_o	C	C/C_o	C_o	C	C/C_o
cm	---- mg/L ------			------ mg/L-------		
11.5	190.4	8.62	0.05	2.56E-5	1.16E-5	0.45
11.5	183.3	BD†	-‡	2.76E-5	4.30E-6	0.15
8.5	127.8	24.7	0.194	2.40E-7	1.20E-7	0.50
8.5	841.8	97.9	0.116	8.70E-7	2.10E-7	0.24

Conditions: Flow rate = 2.8 mL/min; Voltage = 30 V
†Below detection limit; ‡Non calculable

4.2 Dechlorination of TCE

There are several major factors which affect the electrochemical dechlorination rate of TCE from contaminated water: (a) voltage and current; (b) flow rate; (c) background electrolyte; (d) distance between anode and cathode; (e) surface area of electrode; and (f) electrode configuration. Other possible variables may influence the process, but it is impossible to investigate all the variables and combination of the variables at this time. Therefore, in this bench-scale study, the following process parameters in the experimental conditions were examined: (1) effect of electrode configuration; and (2) effect of flow rate on performance.

Effect of electrode arrangement using Fe^0 filing: The effectiveness of dechlorination depends on the electrode arrangements and flow rate. The effect of flow rate was

examined with different electrode arrangements. Cathodic arrangement (type 2A) was intended to protect iron from corrosion; whereas, anodic arrangement (type 2B) was intended to corrode more iron for ferrous iron generation, and a control column (type 2C) was used without a DC power supply (Fig. 2).

The results showed that TCE effluent concentration increased with increasing flow rate (Fig. 3). The cathodic arrangement performed the best among the three arrangements, whereas the anodic arrangement was less effective for dechlorination than the control column, which did not have external power. To confirm the advantage of the cathodic arrangement, its long term performance for dechlorination was compared with the performance of the control column. A small amount (< 2%) of TCE appeared in the effluent from both columns after passing through more than 60 pore volumes (Fig. 4). The TCE effluent concentration from the control column was much higher than the effluent from the cathodic column as the treatment continued. The pH of the effluent solutions increased from 7 to 8.5 at the beginning, but remained between 7.5 and 8 during both column experiments.

Because of the heterogeneous nature of the reactions, little information is known on the mechanisms by which metals enhance the dechlorination process of chlorinated organic compounds (Gillham and O'Hannesin, 1994; Gotpager et al., 1997). Though an examination of the degradation process and pathways was not the purpose of this study, several observations of relevance to the process can be made. From the reaction scheme shown earlier, three possible reductants are (a) Fe^0, (b) Fe^{2+}, and (c) hydrogen gas released during iron oxidation and dissociation of water (Matheson and Tratnyek, 1994).

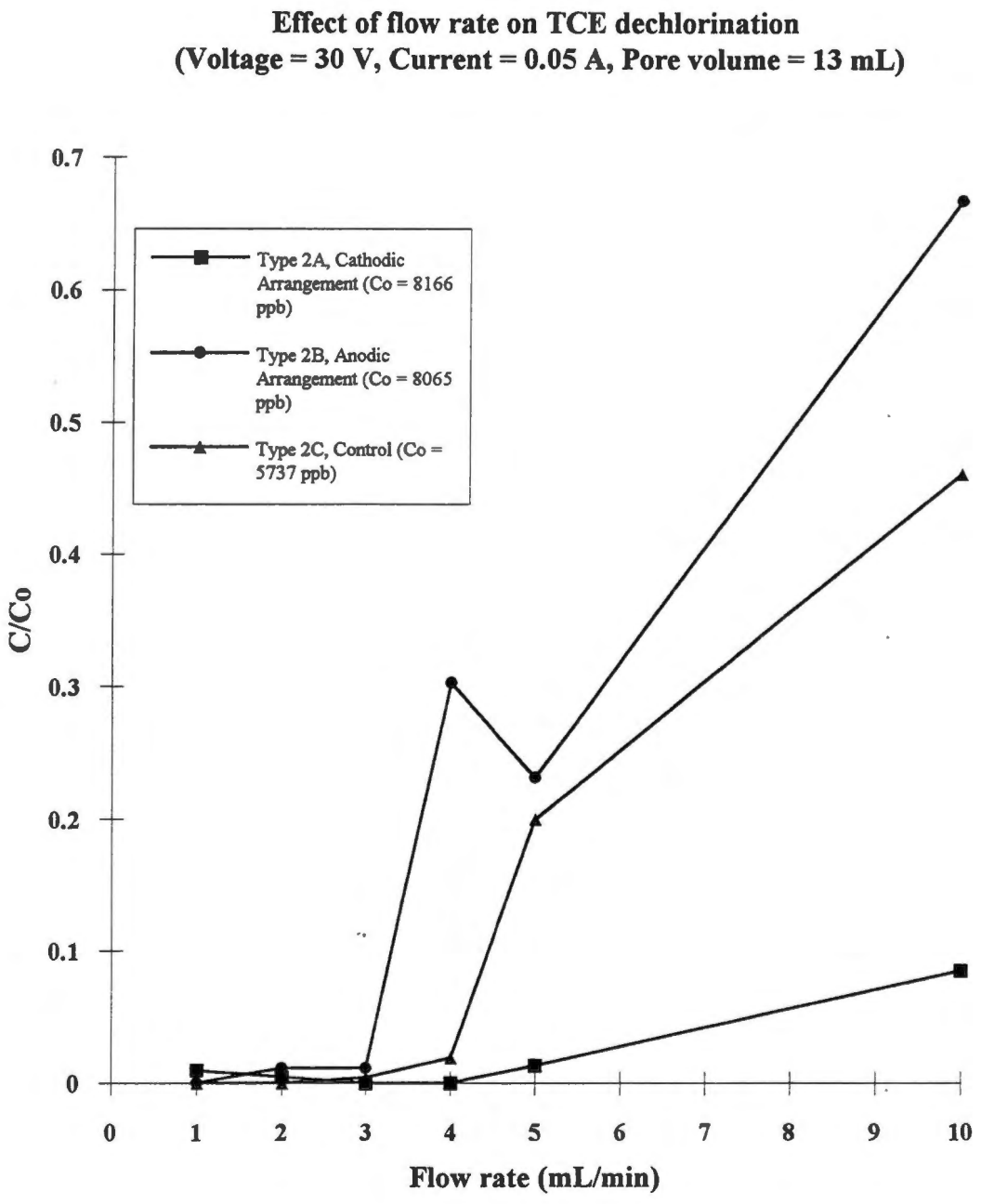


Figure 3. TCE degradation with different electrode arrangements and varying flow rate

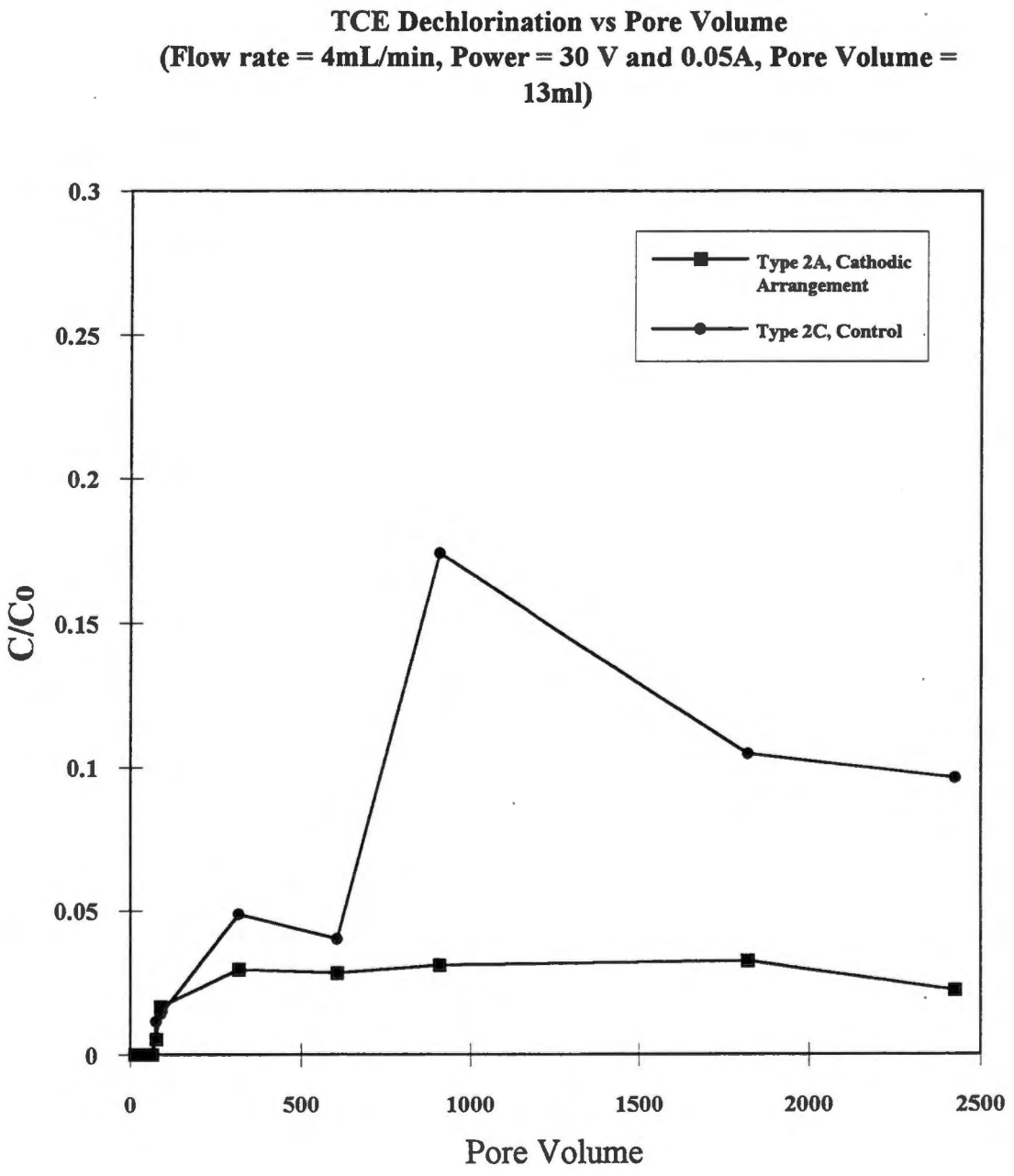


Figure 4. Effect of direct current application on TCE dechlorination

Thus, the reductive dechlorination observed in the process can occur by the following three processes (Chung et al., 1995): (a) direct electrolytic reduction at the Fe^0 surface; (b) dechlorination by oxidation of dissolved Fe^{2+} that is also produced by the corrosion; and (c) reduction by hydrogen produced during the iron corrosion and electrolysis of water process. Based on the observed results from the electrode arrangement testing, it appears that the first and second mechanisms may be prevalent in the cathodic arrangement. Because the cathodic arrangement promotes TCE dechlorination, a more reducing condition is generated than in the anodic arrangement (Pourbaix, 1976). The first and third mechanisms may be prevalent in the anodic arrangement, due to iron oxidation and hydrogen gas generation caused by iron corrosion and water electrolysis from the reaction scheme shown earlier (Reardon, 1995).

***Reaction Kinetics using Fe^0 filing*:** Tests were conducted on two columns, one contained Peerless Fe^0 filing and applying DC; the other had Peerless Fe^0 filing without current. Four different flow rates ranged from 1.7 mL/min to 4.2 mL/min with pore volume (27.5 mL) were used for TCE dechlorination. If the reaction is pseudo-first-order, a graph of $\ln[TCE] - \ln[TCE]_0$ versus residence time should be straight line. After 35 pore volumes of TCE-contaminated waters had passed through the column, the concentration profile appears to be stationary. The results of the column tests are plotted as $\ln[TCE] - \ln[TCE]_0$ versus residence time in Figure 5. The high r^2 value ($r^2 = 0.966$) from the results in the TCE dechlorination without current suggest that the degradation process within the column is indeed pseudo-first-order. However, the high degree of scatter ($r^2 = 0.667$) in

the data for TCE dechlorination with current suggests that the degradation process in the column with current is not pseudo-first-order. In the column with current, Fe^0 oxidation is not only the TCE degradation process but also an impressing external current is attributed to TCE dechlorination. Although this study is designed to develop and evaluate an electroremediation technology, modeling of the electro-enhanced treatment barrier is required to design a scaled-up reactive treatment barrier. The parameters to be determined for the optimization and modeling include residence time, dechlorination kinetics, iron dissolution rate, reactive surface area, impressed current, and anode-cathode configuration under simulated field conditions, including flow rate and TCE concentration.

The reaction half-lives over the period of operation were calculated on the basis of a pseudo-first-order reaction, which is described as follows:

$$dC/dt = -k'C \qquad (12)$$

where C is the concentration of TCE and k' is the pseudo-first-order reaction constant. The half-life is defined as the reaction time at which 50% removal is achieved (i.e., C/C_0 = 50%):

$$t_{1/2} = \ln(C/C_0)/k' = -\ln(0.5)/k' \qquad (13)$$

The $t_{1/2}$ for the TCE dechlorination without current was 10.3 hours and the $t_{1/2}$ for the

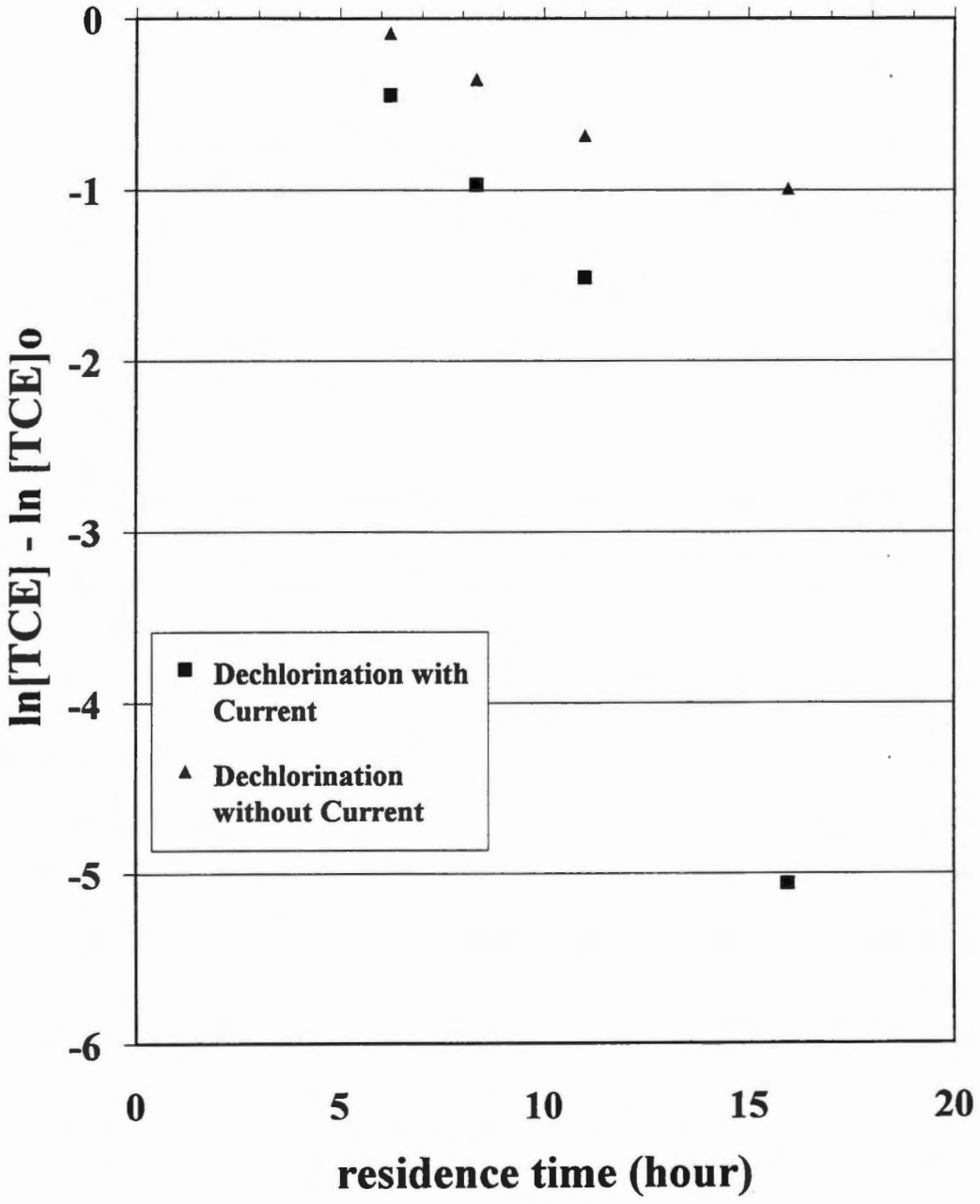


Figure 5. Results of column tests for TCE dechlorination conducted at four different flow rates

TCE dechlorination with current was about 1 hour. These results clearly show the cathodic arrangement to be more effective on TCE dechlorination than without current. Both reaction rates are faster than the other reported values ($t_{1/2}$ = 13.6 hr.) using column study (Gillham and O'Hannesin, 1994). There are many possible reasons for the different dechlorination since the reaction rates are sensitive to redox-related parameters, including (a) pH, (b) DO, (c) dissolved organics, and (d) anionic species, in the groundwater. It must be emphasized that the observed half-life is applicable only in the early stages of the reductive dechlorination process under the conditions provided to the column experiments. The reaction rates do not represent a life-time of the treatment system because the reaction kinetics could be effected by Fe-oxide formation and inorganic species precipitation which could affect surface reactivity and porosity of Fe^0 barrier, and, in some cases, surface complexation of the dissolved species on Fe-oxides. A reduction of dechlorination rate is expected because the Fe^0 filings could form protective hydroxide layers. At the Portsmouth and Y-12 site, long-term column testing demonstrated that the precipitation of iron corrosion products did reduce the hydraulic conductivity of the column, thus limiting the column's life time for effective operation of TCE removal from the contaminated waters (Liang et al., 1977; SAIC, 1998).

Dechlorination by-products of TCE: During the dechlorination of TCE, dichlorethene isomers (cis-1,2-DCE), vinyl chlorinate (VC), and completely dechlorinated hydrocarbons (ethane and ethene) were produced as volatile organic by-products (Fig. 6). Trans-1,2-DCE and 1,1-DCE were not detected from the effluents of all three columns in

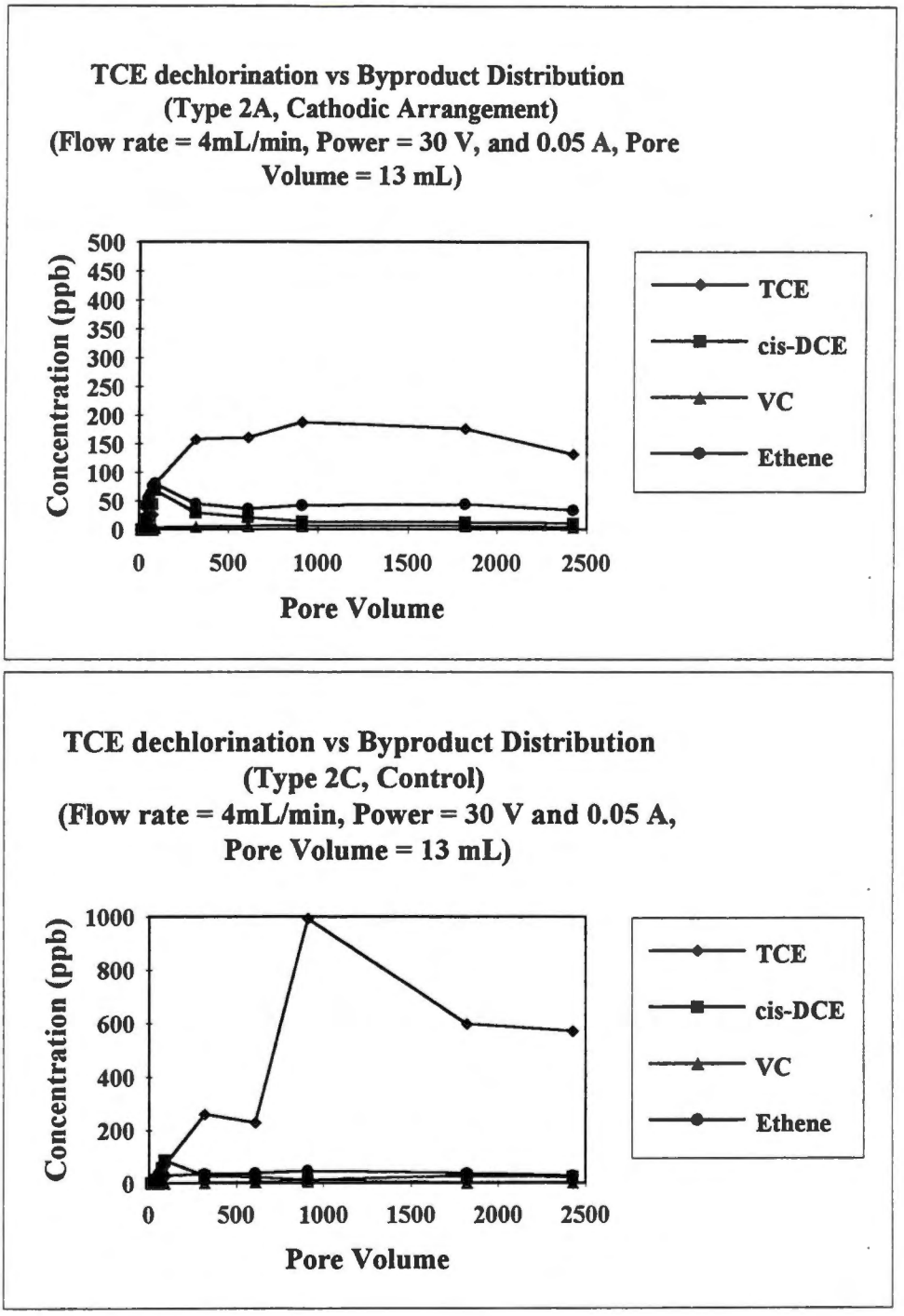


Figure 6. (a) By-product distribution upon TCE dechlorination with cathodic arrangement, and (b) by-product distribution upon TCE dechlorination without current

experimental setup 2. Figure 6 shows the distribution of TCE and byproduct vs pore volume for the cathodic arrangement and a column without current. Trichloroethene was the only chlorinated compound present in the initial solution. Cathodic arrangement is more effective than the control for TCE dechlorination. The TCE disappeared, rapidly accompanied by the appearance of cis-DEC, VC, and ethene/ethane. The amount of byproducts in the effluent was not different between the cathodic arrangement and the control columns (Fig. 6). The degradation of TCE is a step-wise dechlorination, as indicated by the detection and persistence of less chlorinated byproducts in the effluent solutions. Further investigation of breakdown by-products is required because the degradation products such as VC may be a critical compound in the design of the treatment system.

4.3 Water chemistry

Both the anodic and cathodic processes for immobilization of radionuclides showed a pH increase in the effluent solutions when the flow rate was slower than 4 mL/min (less than 41 pore volume passed). The increase of pH was more pronounced when the Fe^0 filing was used as a cathode. The solution pH increased from 5.8 (influent) to 8.5 (effluent) with an applied a flow rate of 3 mL/min (28.4 pore volume passed). When the Fe^0 column was used as an anode, the pH increase was about one pH unit at a flow rate of 1 mL/min (6.3 pore volume passed). In both applications, such pH increases were minimal or insignificant when the flow rates were higher than 4 mL/min (more than 41 pore volume passed). The high effluent pH in the cathodic column at a lower flow rate

and at the startup period indicates that electrolysis of water by Fe^0 filings was initially more extensive, thus producing larger quantities of hydroxyl ion and hydrogen gas.

The pH during the dechlorination of TCE was also increased as the contaminated water flowed through the column. A higher pH value of 8 to 9 was observed during the startup period of the both columns; however, the effluent pH decreased to 6.8 with time. Because the same TCE-simulated and contaminated water is flowing through the three columns, the buffering capacity of the simulated water should be identical. Thus, the difference in the effluent pH is most likely influenced by the medium and electrolysis of water via the DC application. The high effluent pH indicates that electrolysis of water by Fe^0 filings was initially more extensive, thus producing larger quantities of hydroxyl ions and hydrogen gas. Redox potential declined from an initial value of almost 2 mV to -80 mV at the low flow rate (< 3 mL/min) and startup period, then reached steady-state as pore volume increased. Dissolved oxygen decreased from 5 mg/L in the influent to 10 – 100 μg/L in the effluent in the cathodic arrangement and control column. Low DO in the effluent is attributed to the consumption of DO by redox reactions, meaning highly reducing conditions have been created. Concentration of the dissolved Fe^{2+} in effluent was generally within the range of 5 to 10 mg/L with an occasional value as high as 20 mg/L at the startup of the column study. Zero-valent iron was oxidized both by water and by the chlorinated organic compounds (Matheson and Tratnyek, 1994). Under the increased pH and decreased Eh conditions and dissolution of the Fe^0 in the reactive barrier, precipitation of ferrous hydroxide [$Fe(OH)_2$] and iron carbonate ($FeCO_3$) can be expected.

4.4 Mineralogical Characterization of the Corroded Iron Materials

The SEM with EDX spectra showed that both Fe^0 foam and filings revealed U-removal from the aqueous solution. The precipitates from both Fe^0 also showed that U in solution precipitated with corroded material from Fe^0 because similar EDX spectra were obtained. Technetium is also believed to be incorporated in the mineral, but could not be detected by the energy-dispersive X-ray analysis because of its low mass concentration. We employed the fluorescence spectroscopic technique in an attempt to identify the oxidation state of U on Fe^0 surfaces and precipitates generated from Fe^0. It is known that only oxidized U^{6+} gives strong fluorescence; whereas, the reduced U^{4+} does not (Dai et al., 1997). The fluorescence spectra were plotted for (a) uranyl nitrate, (b) uranyl carbonate, strong intensity in fluorescence (Fig. 7), but no fluorescence spectrum was observed for U on Fe^0 and in the precipitates, as a result of its reduced oxidation state. The results demonstrated that, in the presence of Fe^0, uranyl was primarily reduced to U^{4+}, which is precipitated on the Fe^0 surface and with the iron precipitates. Reduction of U^{6+} to U^{4+} is the preferred removal mechanism since the resulting U^{4+} species is less soluble and thus less mobile in groundwater (Langmuir, 1978), assuming that the U^{4+} species is not colloidal. Reductive precipitation of U and Tc is thermodynamically favorable according to the reaction (9). The reduced U(IV) coprecipitated with eroded iron to readily form iron hydroxide in solution (Baes and Mesmer, 1976; Dai et al., 1996a).

and (c) U on Fe^0 filing and in the precipitates. The uranyl nitrate and carbonate showed

The stability field of Fe^0 lies below the water redox line, indicating that Fe^0 should oxidize in the presence of water and will dissolve with evolution of hydrogen gas in acid,

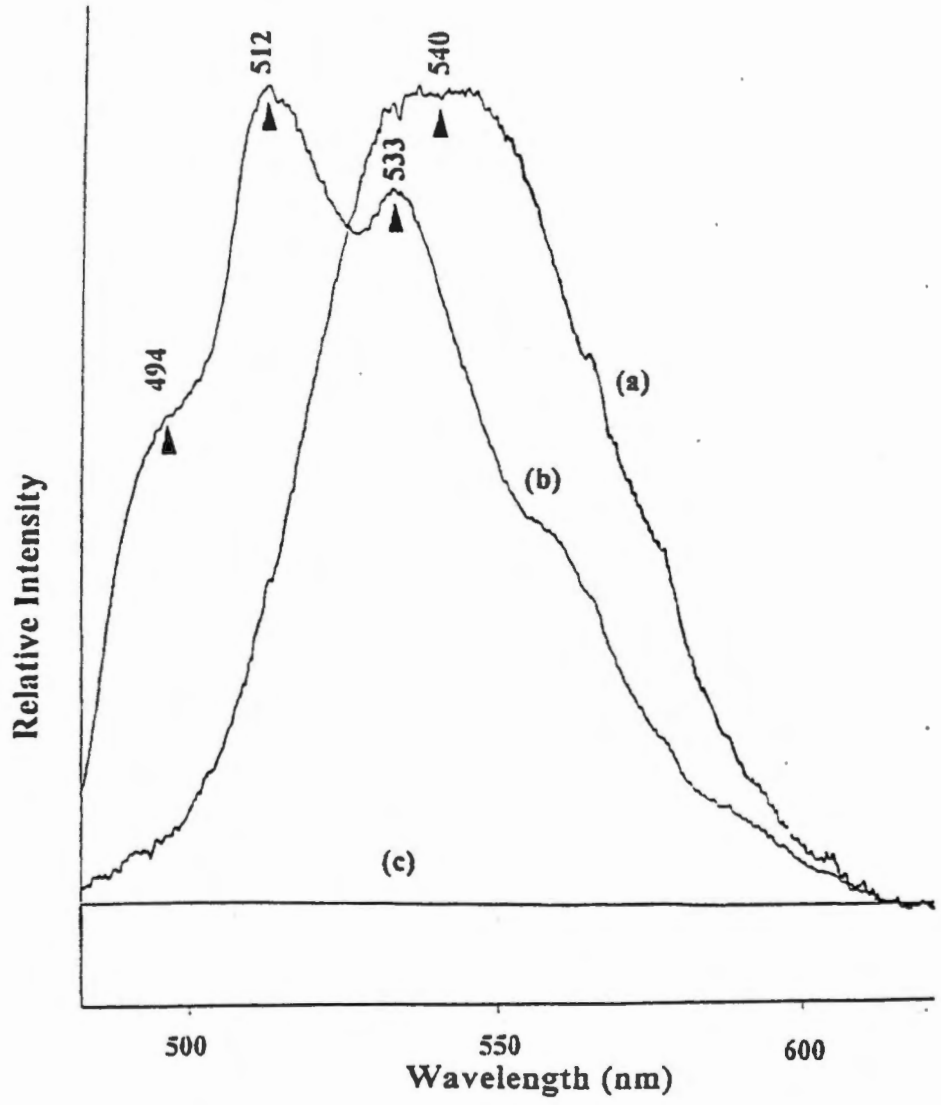


Figure 7. Comparison of uranyl fluorescence spectra of (a) uranyl nitrate, (b) uranyl carbonate, and (c) U precipitated or adsorbed on Fe^0 and in iron precipitates

neutral, and alkaline solutions (Matheson and Tratnyek, 1994). When the column was opened after the dechlorination experiments, Fe^0 filings and sand filters on the top of the columns were covered by crystalline and amorphous iron hydroxide. During reductive dechlorination, most of the chlorine is released as a chloride ion or combines with ferrous iron to precipitate out as amorphous iron hydroxides (Fig. 8a) and green rust $[Fe_3^{II}Fe^{III}(OH)][Cl \cdot 2H_2O]$ (Fig. 8b). It has been postulated that iron oxidation is one of the main mechanisms of reductive dechlorination of TCE. However, the role of the iron (hydr)oxide surface film formed by the hydrolysis of the oxidized iron on the TCE dechlorination rate is not very well understood. There is an uncertainty over how to incorporate the kinetics of the oxide film growth on the metal surface with the kinetics of dechlorination. Precipitates within reactive material could, over time, fill the pore spaces, thereby reducing permeability. Precipitates may also adhere to the iron surfaces, blocking reaction sites and thus reducing the reactivity of the Fe^0. The effect of the iron hydroxide formation on iron reactor performance is described in Part 4.

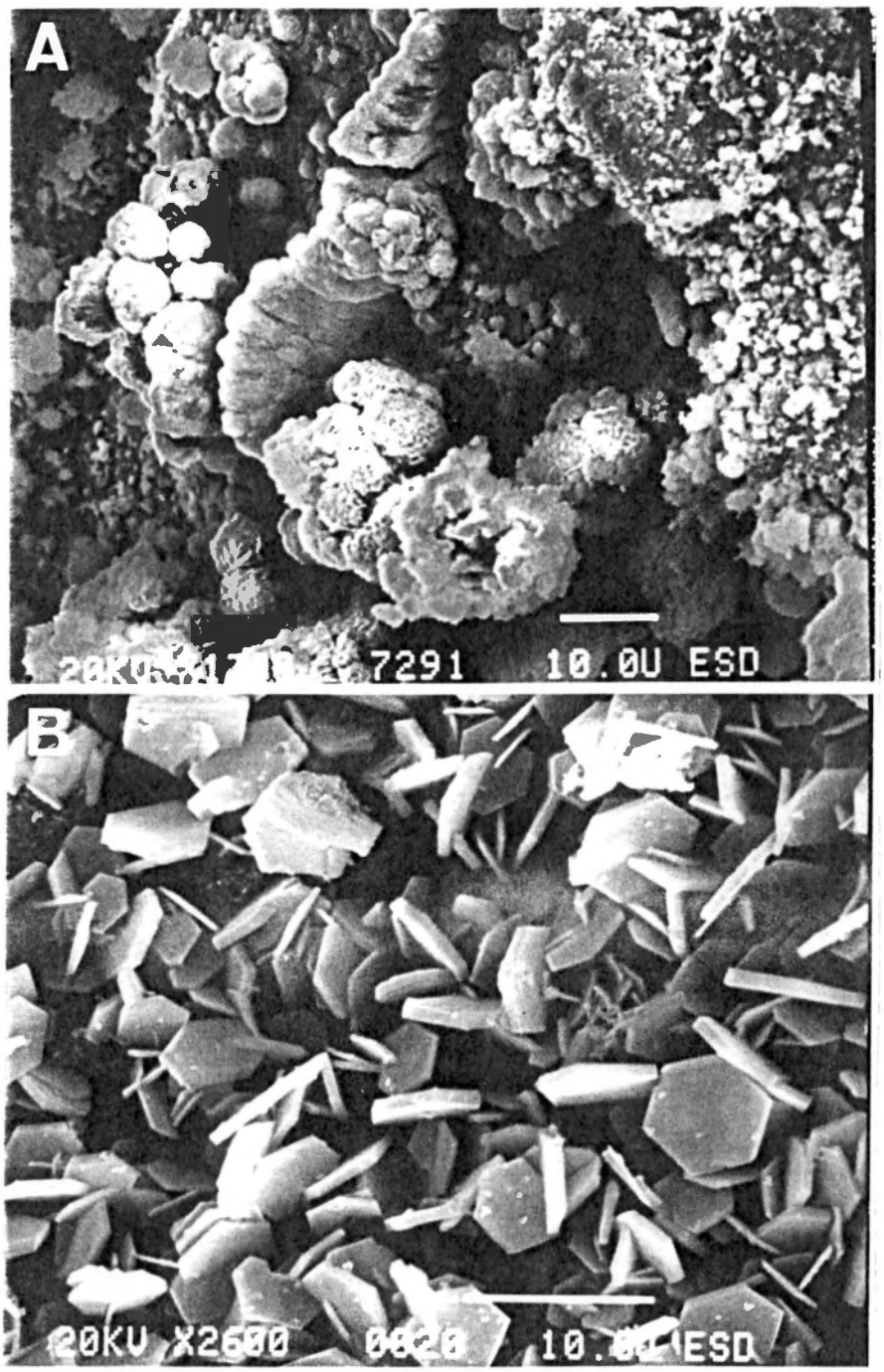


Figure 8. Scanning electron micrograph of (a) spherical amorphous iron hydroxide and (b) the precipitate displaying platy, hexagonal shaped pyroaurite-type mineral, green rust

5. CONCLUSIONS

The bench-scale column tests confirmed that the application of direct current with Fe^0 is highly effective in enhancing the rate of TCE dechlorination and radionuclide immobilization. Bench-scale studies revealed that the effectiveness of the process is controlled by several factors, such as: (a) voltage and current; (b) influent concentration; and (c) distance between anode and cathode. Reduction of U^{6+} to U^{4+} and Tc^{7+} to Tc^{4+} and coprecipitation of radionuclides as iron hydroxide appear to be the preferred removal mechanism by supplying electrons and corroded iron substrates. The dechlorination mechanism appears to be reductive, with the electrons supplied by the iron oxidation and external DC power supply serving as the source of the electrons.

Because the electro-enhanced treatment is based on reductive precipitation and degradation rather than the addition of chemical reductants, the technology has a potential to simplify the decontamination process for treating groundwater that is contaminated with radionuclides, heavy metals, and COCs. In addition, this process produces only a minimal, stable, secondary waste in the form of a iron precipitate. This precipitate can be easily removed from the treated waters through the use of a conventional filtering setup, and the clean water can then be discharged to streams. In summary, this technology would *(a)* reduce U(VI) to U(IV), and Tc(VII) to Tc(IV) in one step; *(b)* be kinetically fast enough for flow-through systems; (*c*) provide substrate for the coprecipitation and adsorption of the reduced species; *(d)* control solution pH and other environmental parameters without chemical additions; *(e)* produce only a minimal amount of waste which

will be in the form of a sparingly soluble mineral; *(f)* discharge treated water directly; and *(g)* be economical and environmentally safe.

Further studies of the consequences of the reactions and means of controlling these consequences are anticipated to determine the long-term impact of the growing surface coating on reductive dechlorination of TCE, immobilization of radionuclide, and the capacity of the medium for in situ application.

REFERENCES

Baes, C. F., and R. E. Mesmer. 1976. The hydrolysis of cations. John Wiley & Sons. New York.

Borovec, Z. 1981. The adsorption of uranyl species by fine clay. Chemical Geol. 32:45-58

Cantrell, K. J., D. I. Kaplan, and T. W. Wietsma. 1995. Zero-valent iron for the in situ remediation of selected metals in groundwater. J. Hazard. Mat. 42:201-212

Chung, F-W., R. A. Larsen, and M. S. Wessman. 1995. Zero-valent iron promoted dechlorination of polychlorinated biphenols. Environ. Sci. Technol. 29(9):2460-2463

Cutshall, N. H., and I. L. Larsen. 1980. BGSUB and BGFIX: Fortran programs to correct Ge(Li) gamma-ray spectra for photopeaks from radionuclides in background. ORNL/TM-7051, Oak Ridge National Laboratory, Oak Ridge, Tennessee

Dai, S., G. D. Del Cul, D. Metcalf, and L. M. Toth. 1994. Modification of cary 14th spectrometer into a fiberoptic absorption spectrometer. Spect. Let. 27(5):687-690

Dai, S., L. M. Toth, G. D. Del Cul, and D. H. Metcalf. 1996a. Solubilities of uranium(VI) dioxide in magnesium chloride, calcium chloride, and aluminum chloride melts: A comparative study. J. Phys. Chem. 100:220-223.

Dai, S., W. Xu. D. H. Metcalf, and L. M. Toth. 1996b. Energy transfer between UO_2^{2+} and Eu^{3+} in sol-gel glasses:a spectroscopic investigation. Chem. Phy. Lett. 262:315-320

Dai, S., Y. S. Shin, L. M. Toth, and C. F. Barnes. 1997. Spectroscopic probing of adsorption of uranyl to uranyl-imprinted silica sol-gel glass via steady-state and time-resolved fluorescence measurement. J. Phys. Chem. 101:5521-5524

Del Cul, G. D., and W. D. Bostick. 1995. Simple method for technetium removal from aqueous solutions. Nucl. Technol. 109:161-162

Environmental Protection Agency. 1988. U. S. EPA methods for the determination of organic compounds in drinking water:Method 502.2, Revision 2.0, EPA-600/4-88/039, U. S. Environmental Protection Agency, Cincinnati, Ohio

Gotpagar, J., E. Grulke, T. Tsang, and D. Bhattacharyya. 1997. Reductive dehalogenation of trichloroethene using zero-valent iron. Environ. Prog. 16:137-143

Ho, C. H., and N. H. Miller. 1985. Effect of humic acid on uranium uptake by hematite particles. J. Colloid Interface Sci. 106:281-288

Hsi, C. K. D., and D. Langmuir. 1985. Adsorption of uranyl onto ferric oxyhydroxides: Application of the surface complexation site-binding model. Geochim. Cosmochim. Acta 49:1931-1941

Langmuir, D. 1978. Uranium solution-mineral equilibria at low temperatures with applications to sedimentary ore deposits. Geochim. Cosmochim. Acta. 42:547-569.

Lee, S. Y. and E. A. Bondietti. 1983a. Technetium behavior in sulfide and ferrous iron solutions. Mat. Res. Soc. Symp. Proc. 15:315-322.

Lee, S. Y. and E. A. Bondietti. 1983b. Removing uranium from drinking water by metal hydroxide and anion exchange resin. Am. Water Works Assoc. 75:537-540

Liang, L., B. Gu, and X. Yin. 1996. Removal of technetium-99 from contaminated groundwater with sorbents and reductive materials. Sep. Technol. 6:111-122

Liang, L., O. R. West, N. E. Korte, J. D. Goodlaxson, D. A. Pickering, J. L. Zutman, F. A. Anderson, C. W. Welch, M. J. Pelfrey, and M. J. Dickery. 1997. The X-625 groundwater treatment facility:A field-scale test of trichloroethene dechlorination using iron filing for the X-120/X-749 groundwater plume. ORNL/TM-13410. Oak Ridge National Laboratory. Oak Ridge, Tennessee.

Matheson, L. J., and P. G. Tratnyek. 1994. Reductive dehalogenation of chlorinated methanes by iron metal. Environ. Sci. Technol. 28:2045-2053.

Olsen, C. R., P. D. Lowry, S. Y. Lee, I. L. Larsen, and N. H. Cutshall. 1986. Geochemical and environmental process affecting radionuclide migration from a formerly used seepage trench. Geochim. Cosmochim. Acta. 50:593-607.

Pourbaix, M. 1966. Atlas of electrochemical equibria, Pergamon Press, Oxford.

Pourbaix, M. 1973. Lectures on electrochemical corrosion. Plenum Press, New York.

Powell, R. M., R. W. Puls, S. K, Hightower, and D. A. Sabatini. 1995. Coupled iron corrosion and chromate reduction: Mechanisms for subsurface remediation. Environ. Sci. Technol. 29:1913-1922.

Roberts, A. L., L. A. Totten, W. A. Arnold, D. R. Burris, and T. J. Campbell. 1996. Reductive elimination of chlorinated ethylenes by zero-valent metals. Environ. Sci. Technol. 30(8):2654-2659

Roh, Y., S. Y. Lee, and M. P. Elless. Electroremediation of uranium and technetium contaminated waters. Extended Abstract. Annual Meeting of the Chemical Society, I&EC Division, Emerging Technologies in Hazardous Waste Management VIII, Sept., 9-12, 1996. Birmingham, Alabama. 582-585.

SAIC. 1996. Field characterization report on Phase I of the Bear Creek Valley treatability study, Oak Ridge Y-12 Plant, Oak Ridge, TN, Y/ER-286

SAIC. 1998. Phase II report on the Bear Creek Valley treatability study, Oak Ridge Y-12 Plant, Oak Ridge, Tennessee. BJC/OR-3. Bechtel Jacobs Company.

Siegel, F. R. 1974. Applied Geochemistry. John Wiley and Sons, Inc., New York, London, Sydney and Toronto. 353 p.

Tsunashima, A., G. W. Brindley, and M. Bastovanov. 1981. Adsorption of uranium from solutions by montmorillonite: Compositions and properties of uranyl montmorillonites. Clays Clay Min. 29:10-16

Vogel, T. M., C. S. Criddle, and P. L. McCarthy. 1987. Transformations of halogenated aliphatic compounds. Environ. Sci. Technol. 21:722-736.

PART 3

ELECTROCHEMICAL DECHLORINATION OF TCE

BY PALLADIZED, IRON OXIDE MINERALS *

* Information in this part of research should be handled as a confidential material because the host research institution, Oak Ridge National Laboratory, is evaluating a potential for United States patent application

1. ABSTRACT

Recently, researchers have successfully applied palladium (Pd)-coated zero-valent iron (Fe^0) for rapid dechlorination of organic contaminants to overcome the slow reaction rate of the Fe^0. However, a prolonged exposure of the palladized Fe^0 surface to groundwater contaminated with trichloroethene (TCE) results in the growth of palladium sulfide (PdS) and iron sulfide (FeS) films that deactivate the palladized Fe^0 surface. Formation of the PdS minerals resulted from microbial-mediated reduction of sulfate to sulfide in the groundwater. The objective of this study is to develop electrochemically-enhanced dechlorination of TCE using palladized, multiphasic oxide minerals (mainly magnetite and wüstite®) for in situ and ex situ remediation of contaminated groundwaters. The Pd was electrochemically deposited on the multiphasic oxide minerals using direct current (DC). A 2-cm-diameter and 35-cm-long flow through column packed with the palladized iron oxide medium with an iridium-coated cathode and anode at each end was prepared for bench-scale flow through column tests. Contaminated groundwaters with about 16 mg/L TCE from the Portsmouth Gaseous Diffusion Plant in Portsmouth, Ohio were passed from the cathode side to the anode side of the column while the system was supplied with DC (30 V and 0.5 A) from a rectifier. Analytical results of the treated effluent water indicated that all of the TCE in the groundwater was dechlorinated even after 3000 mL were passed through 27-mL column volume (52% pore volume) with 0.62 mL/min flow rate. Furthermore, intermediate reaction products, such as dichloroethene (DCE) isomers and vinyl chloride (VC), commonly derived during reductive

dechlorination processes, were not detected in the treated groundwater. Theoretical and mechanistic interpretations of the observed results are impossible at this time. However, three methods of dechlorination in a developed system are: (a) direct electroreduction on the surface of semiconductive medium by external electron supply, (b) catalytic hydrogenation with electrodeposited metallic palladium microspheres, and (c) destabilization C:Cl covalent bonds with electrons generated through oxidation of ferrous to ferric iron in the medium. This interpretation is based on the fact that such a high dechlorination efficiency was obtained only when the operating system had all three components (i.e., external source of electrons, electrodeposited Pd surfaces, and iron oxide medium). The multiphasic iron oxide has great advantages over the metallic iron, including effectiveness and longevity as a reactive medium for TCE dechlorination.

2. INTRODUCTION

Many U.S. Department of Energy (DOE) facilities, Department of Defense (DoD) bases, and Environmental Protection Agency (EPA) Superfund sites have problems associated with contaminated groundwater plumes that contain unacceptable levels of chlorinated organic compounds (COCs), such as trichloroethene (TCE), and tetrachloroethylene (PCE). As an alternative remediation technology to a pump-and-treat system, an in situ reactive barrier and funnel-and-gate system that use Fe^0 as a reactive medium have been installed in the path of flowing groundwater to passively remove dissolved organic contaminants (Matheson and Tratnyek, 1994; Cantrell et al., 1995; Del Cul and Bostick, 1995; Liang et al., 1997). The Fe^0 is an effective dechlorination medium through hydrogenolysis (Matheson and Tratnyek, 1994), but the rate of dechlorination is too slow at a high-flow-rate source of contaminated water. A slow reaction rate would require a prohibitively thick barrier or a large reactor vessel to extend the contaminant's residence time in the system.

Recent studies indicated that the addition of a trace amount of a heavy metal (e.g., Pd, Ni, Zn, or Cu) added into the Fe^0 improved the dechlorination rate to varying degrees (Grittini et al., 1995; Cheng et al., 1997; Liang et al., 1997). Furthermore, Schreier and Reinhard (1995) found that the addition of hydrogen gas (H_2) to the system enhanced the dechlorination rate of PCE and vinyl chloride (VC) with metallic Pd, as expressed in the following reaction:

$$H_2 + R\text{-}Cl \Rightarrow R\text{-}H + H^+ + Cl^- \quad (1)$$

Palladium has the unique property for promoting dechlorination of organic compounds because Pd has the ability to adsorb hydrogen into its lattice and to maintain a high surface concentration of hydrogen until transfer to the COCs (Lawson et al., 1991). The bimetals (Pd/Fe), prepared by Pd doping or iron reduction in a $PdCl_2$ solution, showed a significant increase in the dechlorination rate relative to Fe^0 alone (Liang et al., 1997; Nic Korte, 1997). However, the catalytic activity of Pd could be hindered in the presence of certain compounds. Some potential catalyst inhibitors or poisons include molecules containing (1) elements such as N, P, As, Sb, S, Se, and Te; (2) compounds of toxic metals such as Hg, Pb, Bi, Sn, Zn, Cd, and Cu; and (3) multiple bonds such as CO, cyanogen compounds, and strongly adsorbing organic molecules (Hughes, 1984). However, Schreider and Reinhard (1995) reported that catalytic hydrodehalogenation of COCs occurred on the Pd surface (with H_2 gas addition) even in the presence of oxygen, nitrite, nitrate, sulfate, and chloride, but not in the presence of bisulfide.

The long-term effectiveness of the Pd deposited on an iron surface depends on the characteristics of the surface, because prolonged exposure of the Pd/Fe surface to an aqueous TCE solution results in the growth of an iron hydroxide film that may deactivate the catalytic process of the surface. Liang et al., (1997) reported that the reactivity of palladized iron after an extended application to TCE-contaminated groundwaters decreased as a result of the poisoning of the Pd surface by sulfides produced from the microbial reduction of sulfates in the groundwater.

The objective of this study is to develop electrochemically enhanced dechlorination of TCE in the contaminated groundwater from Portsmouth, Ohio, using palladized, multiphasic iron oxides as the reactive medium. The expected benefits of the new treatment system over the conventional Fe^0 medium approaches are (1) a faster reaction rate and higher treatment capacity by supplying an external source of electrons, which means the possibility of downsizing the reactor or barrier while maintaining an equivalent enhanced performance; (2) moderation of the corrosion rate, which means a reduction in the clogging potential of the reactive medium; and (3) freedom to control transient chemical processes of the system and thus extend the effective performance period.

3. MATERIALS AND METHODS

3.1 Materials

A sponge-like multiphasic iron oxide (Fe oxide foam®, Cercona of America, Inc., Dayton, Ohio) was used for this study. Multiphasic Fe oxides have the following characteristics: (a) 92% FeO and Fe_3O_4, balanced with aluminosilicate; (b) 0.9-g/cc bulk density, and (c) a 0.5 to 1 m^2/g estimated specific surface area. The material obtained from Cercona of America, Inc., was originally considered to consist predominantly of magnetite. However, mineralogical characterization results showed that the material has three crystalline oxide mineral phases, including magnetite (Fe_3O_4), wüstite (FeO), and hercynite ($FeAl_2O_4$) (Fig. 1a,b). Palladium was deposited on the multi-phasic iron oxides with an electroplating process using a constant current (1 mA and 30 V) until the characteristic pale orange color of the $PdCl_2$ solution disappeared and a pale yellow color occurred after the redox reaction (equation 2).

$$PdCl_2 + 2e^- + (Fe^{2+}Fe^{3+})_xO_y \Rightarrow Pd^0 + 2Cl^- + Fe_xO_y \qquad (2)$$

$$2H_2O + 2e^- \Rightarrow H_2(\uparrow) + 2OH^- \qquad (3)$$

This process took approximately 4 hours. During this time, hydrogen evolution was visually observed from the cathodically contacted multiphasic iron oxide surface (equation 3). Palladized multiphasic Fe oxides were then removed from the electrolysis solution, washed with deionized water, and dried in a 90°C oven overnight. Scanning electron

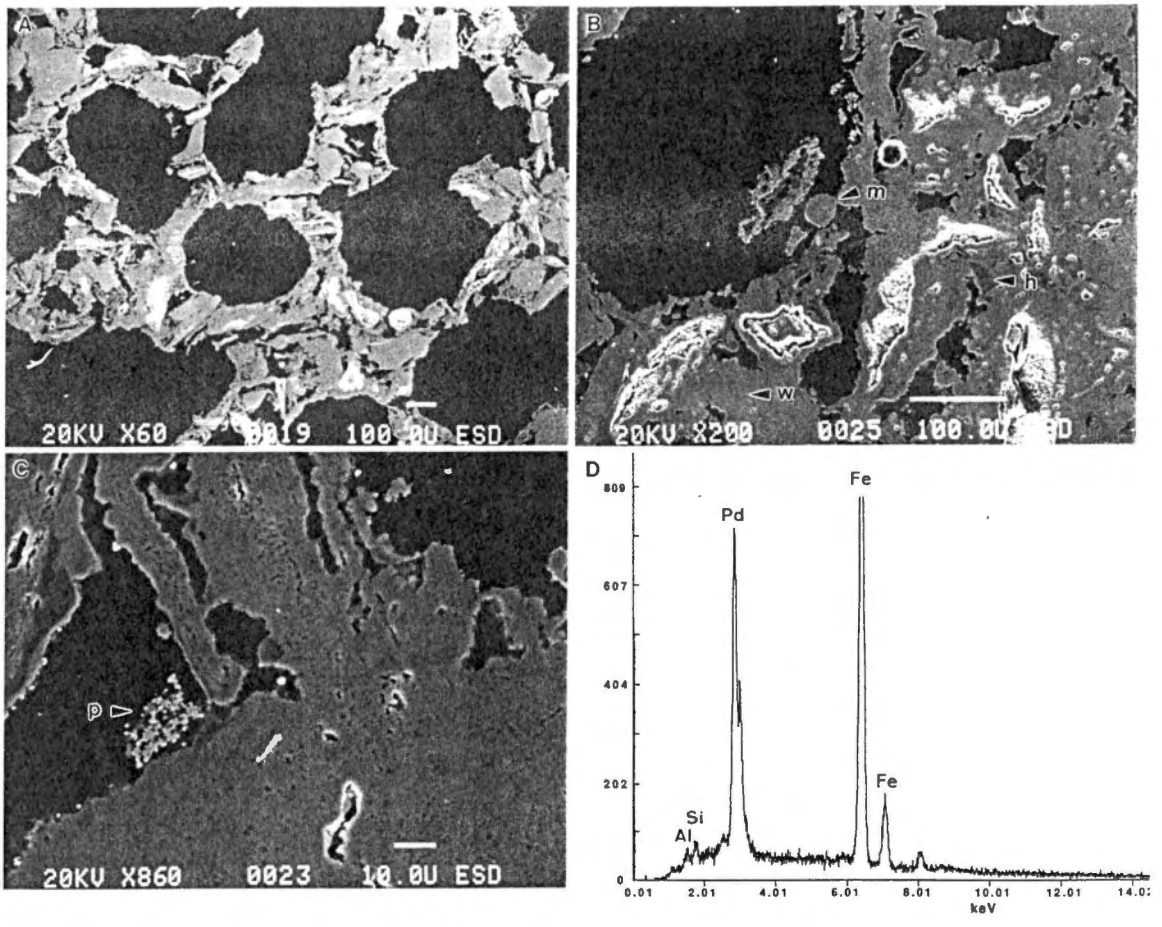


Figure 1. Scanning electron migraph of the palladized multiphasic Fe oxide foam (a, b, c) consisted of magnetite (m), wüestite (w), hercynite (h), and palladium (p) and EDX spectra (d)

micrographs of a polished section of the reactive medium show that multiphasic iron oxides are partially covered by numerous, submicron Pd particles (Fig. 1c). Energy-dispersive X-ray spectrometry confirmed the presence of Pd particles on the surface of the multiphasic oxide minerals (Fig. 1d).

3.2 Methods

The columns used for these experiments were 2-cm-diameter and 35-cm-long borosilicate glass columns with internally threaded ends (i.e., inlet and outlet ports). The columns had two side ports at 8 and 29 cm from the inlet for electrode placement. Both the cathode and anode were metal rods about 1-mm in diameter. The cathode had a 9-cm packed column length with a mass of 35 g, and the anode was placed in the carbon pad (12 cm length, 4 g mass) stacked on top of the oxides (Fig. 2). The rest of the column was packed with Ottawa sand. The contaminated groundwater (Table 1) from the Portsmouth X-701B site used in this study had a TCE concentration ranging from 13.7 to 16.7 mg/L and a cis-DCE concentration ranging from 2.1 to 2.2 mg/L. The chemical properties of the groundwater, particularly its seasonal variation in composition, are summarized in Table 1. During the column experiments, the contaminated groundwater was held in a 10-L collapsible Tedlar sample bag to minimize losses from volatilization as the source water was consumed. The groundwater in the collapsible bag was pumped to the column with a MasterFlex Digi-Staltic pump (Cole-Parmer, Vernon Hills, Illinois) at a flow rate 0.63

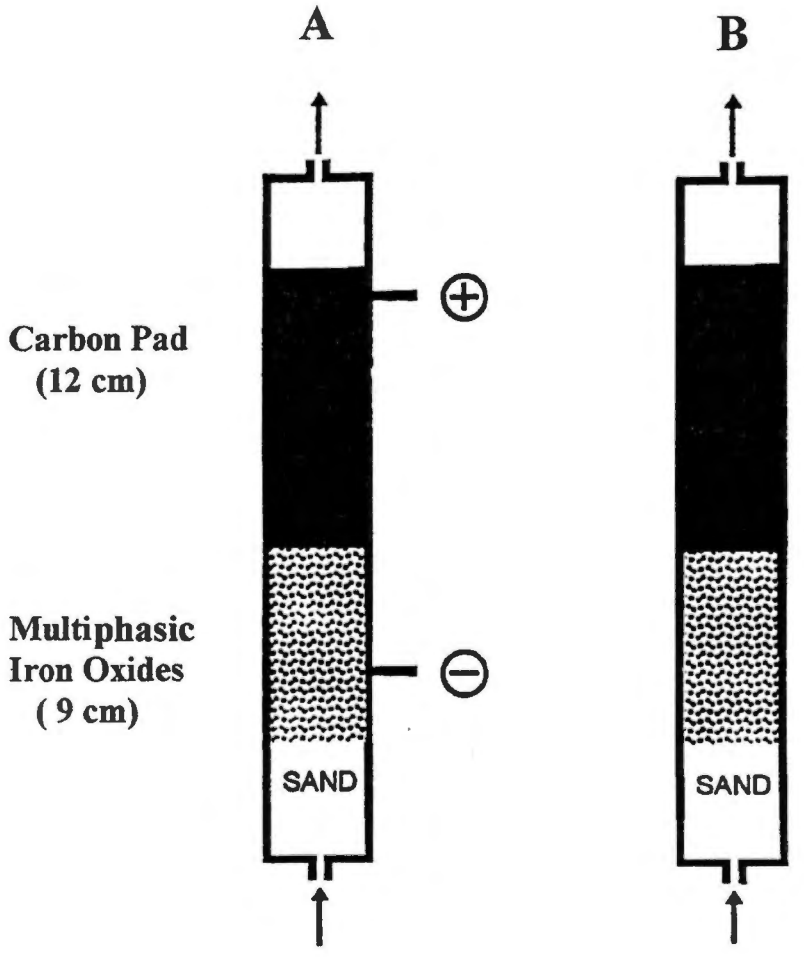


Figure 2. Schematic diagram showing experimental setup of the electroremediation using multiphasic Fe oxides

Table 1. Composition of Portsmouth X-701B water[†]

Parameter	No. of samples analyzed	Minimum	Mean	Maximum
		Field Measurements		
Conductivity (µs/cm)	92	144	637	1 811
DO[‡] (mg/L)	88	0.3	1.8	5.5
Tenperature (°C)	92	6.2	14	20.6
pH	92	4.3	5.7	7.5
		Anions (mg/L)		
Alkalinity	85	6	65.6	332
Chloride	92	2.6	49.8	214
Sulfate	92	3.3	175	702
		Dissolved metals (µg/L)		
Cadmium	10	2.2	2.9	3.6
Calcium	92	6 740	45 113	260 000
Chromium	16	3.5	14.9	45.1
Iron (total)	62	7.3	573	8 070
Lead	8	18.6	23.7	28
Magnesium	92	5 050	26 196	114 000
Manganese	4	691	871	1 080
Nickel	26	7.8	37.5	81.8
Potassium	92	750	2 459	6 680
Sodium	92	8 360	46 060	91 200
		Total Radiochemistry (pCi/L)		
Alpha activity	10	4	8	19
Beta activity	43	7	51.6	178
Technetium	28	21	93.1	266

[†] Annual Report for 1997 Groundwater Monitoring Quarterly Sampling Results from Portsmouth Gaseous Diffusion Plant, Ohio

[‡] Dissolved oxygen

mL/min, which was determined by measuring the discharge rate. Viton tubing was used only for the pump roller assembly, but Teflon tubing was used for all other delivery systems to minimize TCE loss. Four columns were constructed to investigate the effects of direct current application on dechlorination of TCE in the multiphasic Fe oxides and palladized multiphasic Fe oxides. The first column was packed with multi-phasic Fe oxides with a carbon pad (Fig. 2b). The second column was packed with multiphasic Fe oxides with a cathode and an anode electrically connected carbon pads (Fig. 2a). The third column was packed with palladized, multiphasic Fe oxides without electrodes (Fig. 2b), and the fourth column (Fig. 2b) was similar to the second, but packed with palladized multiphasic Fe oxides with electrodes (Fig. 2a).

One control column, containing only sand, was used to determine any loss caused by volatilization of TCE during the column experiments. The control column containing only sand gave a TCE breakthrough curve typical of a nonreactive solute in a nonreactive medium, (i.e., the solute concentration in the effluent was approximately 0.5 after one pore volume had passed through the column, and by two pore volumes, the influent and effluent concentration were approximately equal).

3.3 Sampling and Analyses

Samples for TCE and by-product analyses were collected from the influent and effluent lines with a 5.0-mL glass syringe. The samples were injected into a purge-and-trap concentrator (Teker 3000, Tekmar, Cincinnati, Ohio) and then analyzed for reaction by a gas chromatographer (GC) (HP-5890 Series II, Hewlett Packard, Wilmington,

Delaware) equipped with a flame ionization detector (FID) and a 0.53-mm capillary column (DB624, J&W Scientific, Folsom, California) The following GC retention times were measured: TCE, 9.654 minutes; cis-1,2-DCE, 6.476 minutes; trans-DCE, 4.782 minutes; 1,1-DCE, 3.657 minutes; VC, 2.156 minutes; and ethene and ethane, 1.668 minutes. It was not possible to distinguish ethene from ethane with the analyses used. The method detection limits (MDL) for COC's, as determined by the U.S. EPA method (EPA, 1988), were 0.005 mg/L for TCE; 0.005 mg/L for 1,1-DCE; 0.02 mg/L for cis-1,2-DCE; and 0.005 mg/L for VC. The Eh measurements were made immediately after effluent sample collection using a expandable ion analyzer (Orion Research, Beverly, Massachusetts) with a platinum microelectrode (Microelectrodes, Inc., Londonerry, N.H.). The same type of analyzer using a combined pH electrode was used for pH measurements, standardized with pH buffer 7 and an appropriate buffer of either pH 4 or pH 10.

4. RESULTS

4.1 Dechlorination of TCE Using Multiphasic Iron Oxides

The results obtained using multiphasic iron oxides and carbon pads without current (Fig. 2b) and multiphasic iron oxides with a cathode and an anode electrically connected carbon pad (Fig. 2a) are shown in Fig. 3. The initial TCE concentration in the groundwater used for these experiments was 13.8 mg/L. The column experiment using multiphasic iron oxides without current showed that TCE in the effluent rapidly increased ($C/C_0 = 0.55$) until 16 pore volumes and then remained at $C/C_0 = 0.7$ until 60 pore volumes passed through the column (Fig. 3a). Adsorption and reactive dechlorination on the surface of the multiphasic iron oxides in the column are attributed to the observed reduction of TCE and transformation to intermediate by-products. Concentration of the by-products, including VC and cis-DCE, in the effluent after 16 pore volumes are given in Table 2. The results of the multiphasic iron oxides with current showed that the current application did not significantly improve the dechlorination rate of TCE (Fig. 3b). Concentrations of by-products remained high in the effluent even after 140 pore volumes passed through the column (Table 2). Trans-1,2-DCE was not detected in the effluent.

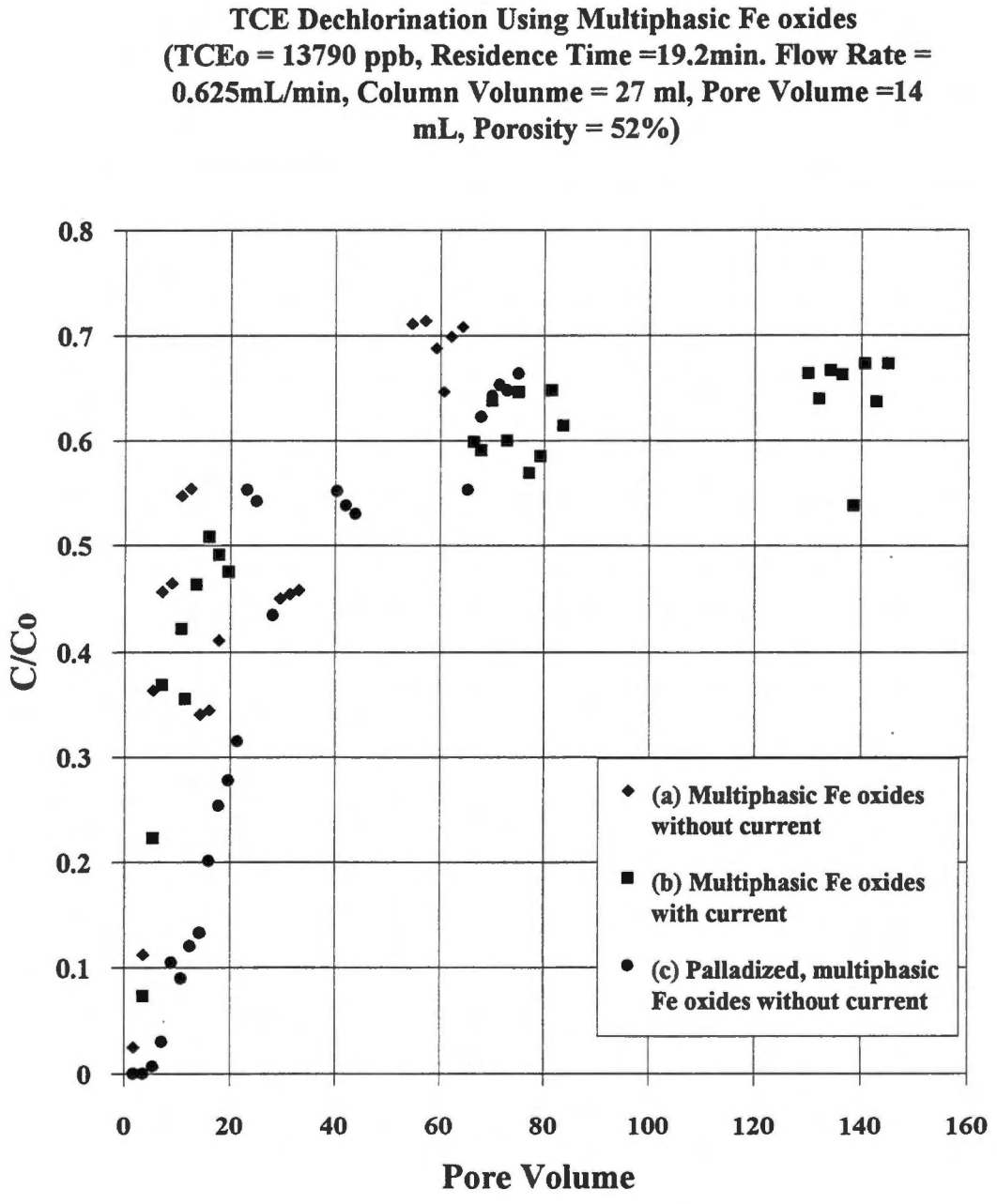


Figure 3. TCE dechlorination using (a) multiphasic Fe oxides without current, (b) multiphasic Fe oxides with current, and (c) palladized, multiphasic Fe oxides without current

Table 2. Summary of the TCE dechlorination experiments using multiphasic Fe oxides

Experimental conditions‡	Current/ Voltage	TCE in Influent (μg/L)	By-products in Effluent (μg/L)			
			COCs	16 Pore Volume	60 Pore Volume	140 Pore Volume
Multiphasic iron oxides	NA†	13790±20	cis-DCE	822	2198	
			VC	76	51	
			C_2¶	3037	110	
Pd-coated multiphasic iron oxides	NA	13790±20	cis-DCE	494	1442	
			VC	38	23	
			C_2	3364	682	
Multiphasic iron oxides	30V, 0.08A	13790±20	cis-DCE	1687	1838	1984
			VC	28	19	10
			C_2	134	134	64
Pd-coated multiphasic iron oxides	30V, 0.5A	16750±30	cis-DCE			
			VC			
			C_2	1680	51010	53560
	10V, 0.02A	16750±30	cis-DCE			
			VC	221	117	205
			C_2	2210	6430	7258

† Not applied direct current

‡ All of the experiment used the following experimental conditions:

¶ Ethene and ethane

40 g of multiphasic Fe oxides used; flow rate = 0.625 ml/min; residence time = 19.2 min; pore volume = 14 mL; column volume with multiphasic iron oxides = 27 mL

4.2 Dechlorination of TCE Using Palladized, Multiphasic Fe Oxides

The results of palladized, multiphasic iron oxides and carbon pad without DC application indicated that the palladization of the medium slightly improved dechlorination efficiency over the non-palladized systems described in Section 4.1 (Fig. 3). In the palladized medium system, the initial breakthrough started after passing through 6 pore volumes and 50% of initial concentration after passing through 30 pore volumes of the groundwater. However, as shown in the non-palladized medium system, the effluents of the palladized medium system also had a level that was of concern of VC and cis-DCE by-products transformed from TCE during the treatment. The observed improvement may be significant in a scaleup treatment system, but it was not considered a breakthrough in a technology development point of view.

When the contaminated groundwater passed through the cathodic, palladized, multiphasic iron oxides column, the TCE in the groundwater disappeared in the effluent solution even after a 210-pore-volume treatment (Fig. 5). The dechlorination process was so complete when the system operated at 30 V and 0.5 A, that there were no detectable amounts of intermediate by-products except ethane and/or ethene as end products of the dechlorination (Figure 4, Table 2). However, when the operational conditions of the same column were changed to 10 V and 0.02 A, a trace amount of VC was detected in the effluents after passing through 150 pore volumes of the contaminated groundwater. The results indicate that the processes involved in the system may be complex, but dechlorination coupled with hydrogenation should be the major route in view of the dependancy on the potential and

current of the reaction.

When the groundwater passed through the column, the pH increased from 6.6 to 7.3, and the redox potential (Eh) decreased from 90 mV to - 40 mV during the operation. These pH/Eh changes are attributed to electrolysis of water on the surface of the reactive medium in the column. Ferrous iron concentration was increased from < 0.1 mg/L to 0.4 – 0.5 mg/L as a result of electrochemical dissolution of the iron oxides (wüstite, magnetite). Dissolved oxygen (DO) decreased from 1 – 5 mg/L in the influent to 10 – 100 µg/L in the effluent. Low DO in effluent is attributed to consumption of DO by the processes involved, which means the highly reducing conditions were created in the electrochemical column.

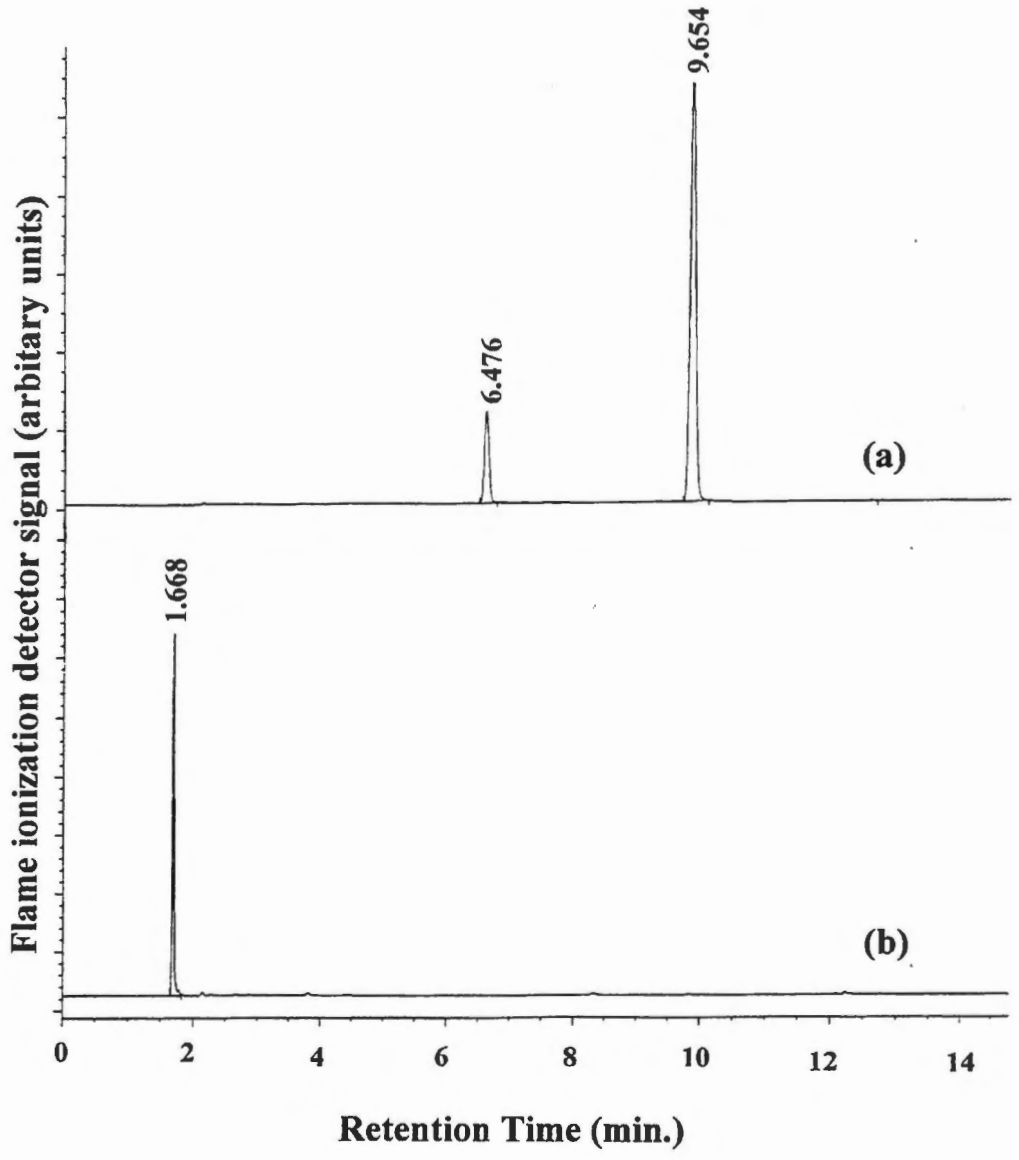


Figure 4. Gas chromatographic analyses of the Portsmouth X-701B TCE-contaminated water (a) before treatment and (b) after treatment with palladized, multiphasic Fe oxides with current.

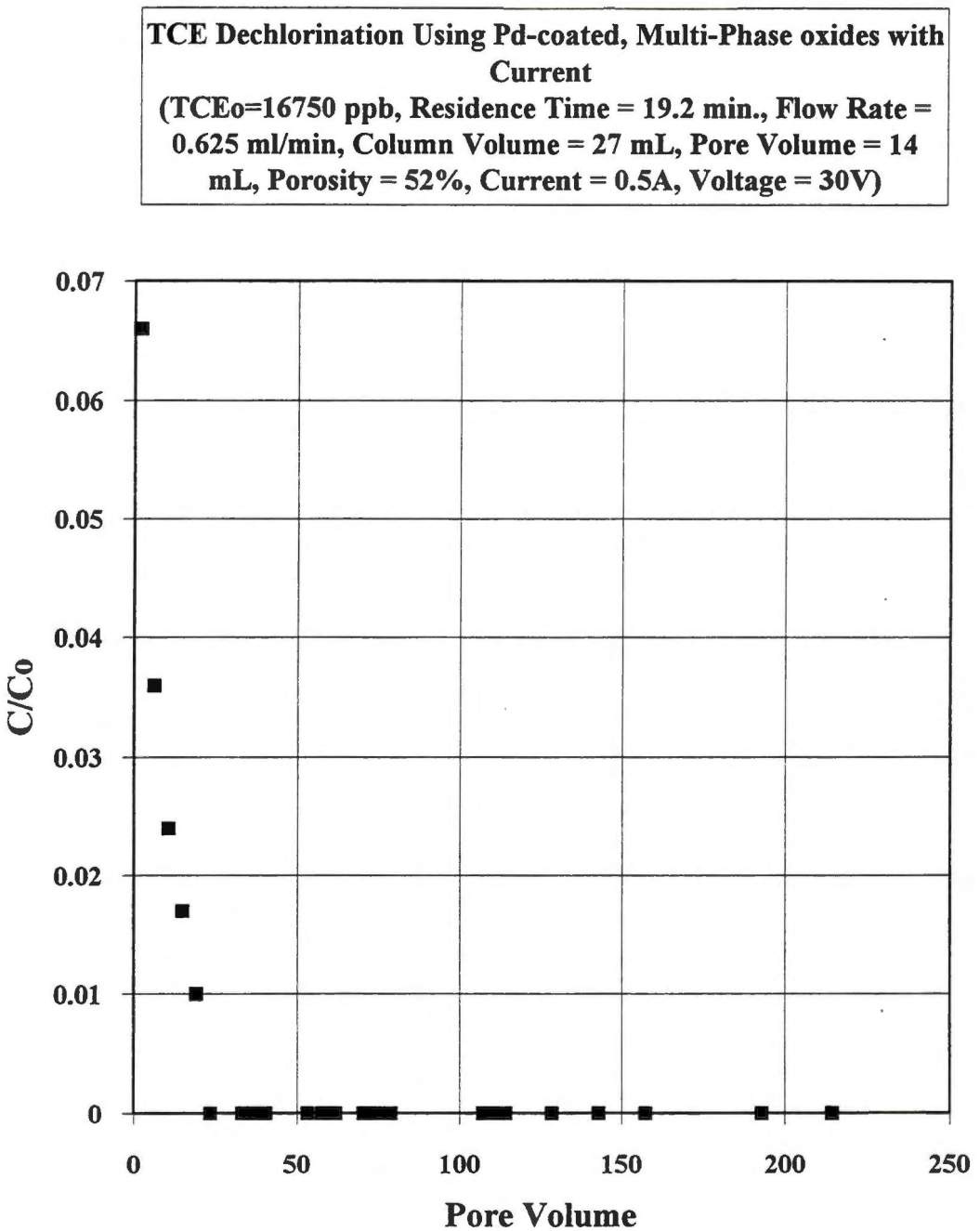


Figure 5. TCE dechlorination using palladized, multiphasic Fe oxides with current (30 V, 0.5 A)

5. DISCUSSION

The results of the column experiment with two different medium with and without DC applications indicated that the palladium on the semiconductive material enhanced the dechlorination of TCE, but that the impact was not significant without DC application. An acceleration of dechlorination of TCE in contaminated groundwater by palladization of metal surfaces has been reported (Grittini et al., 1995; Liang et al., 1997). Such an enhancement of dechlorination was also observed from the electrochemical system having metallic iron without palladization as discussed in Part 2. Another systematic long-term testing is required to compare the two different medium (i.e., palladized metallic iron and multiphasic iron oxide) with DC application.

The detailed pathways and mechanisms for the dechlorination reactions of TCE in the metallic iron and palladized metallic iron treatments have been investigated by many researchers (Grittini et al., 1995; Schreier et al., 1995; Cheng et al., 1997). However, this study represents the first investigation using the electro-enhanced palladized multiphasic iron oxide treatment system. Therefore, interpretation of the results is speculative at the best. There are three possible methods for dechlorination in the electro-enhanced, palladized, multiphasic Fe oxides system: (a) direct electroreduction at the cathodic medium surface by electrons supplied through external current flow, (b) catalytic dechlorination and hydrodehalogenation on Pd islands developed during electro-deposition (Muftikian el., 1996; Grittini et al., 1995), and (c) dechlorination at the interface of the multimedium metallic Pd-magnetite-wüstite with external electrons (Cheng et al., 1997).

The reductive dechlorination could occur on the metallic Pd surface because the strong attraction of chlorine by Pd could destabilize the Cl:C bonds of TCE (Bodnariuk et al., 1989). Hydrogen gas generated at the cathode by electrolysis also participates in the rapid, reductive hydrodehologenation of TCE (Schreier and Reinhard, 1995).

Palladized multiphasic Fe oxide systems have several advantages over palladized Fe^0: (a) the high hydrogen and oxygen potentials allow the multiphasic Fe oxide electrode to be operated at high polarization with only minimal electrolysis; (b) the oxides are less susceptible to passivation by Fe hydroxide than Fe^0; (c) the oxides are more stable, meaning a longer operation life than a metallic iron substrate for in situ and ex situ application; and (d) less secondary waste and ferrous iron discharge are anticipated from the oxide mineral system.

The electro-enhanced dechlorination system has the following three synergistic unique features: (1) matrix material; (2) Pd phase; and (3) DC application. The matrix material has three crystalline mineral phases, including wüstite, magnetite, and hercynite. Among them, wüstite (with stoichiometrically excess iron) may be one of the key components of the dechlorination process although it has not been previously known. Catalytic dechlorination of TCE by Pd on metallic iron has been reported, but the synergistic role of electrochemically deposited Pd on Fe oxide minerals has not been previously reported. The dechlorination system does not entirely depend on oxidation of the medium for reductive dechlorination because application of DC current provides external electrons to maintain the system under reduced conditions.

6. CONCLUSIONS

Palladium was electrochemically deposited on the multiphasic Fe oxides that consisted of wüstite, magnetite, and hercynite. The application of direct current to the palladized, multiphasic Fe oxides was very effective in promoting the dechlorination of TCE in contaminated groundwater from Portsmouth, Ohio. Application of direct current provided external electrons to the system so that the system did not depend entirely on the oxidation of the medium for the reductive dechlorination. The enhancement of dechlorination by the system developed and tested in this investigation can be attributed to the following reactions: (1) the evolution of hydrogen gas by the electrolysis of water at the cathode; (2) the adsorption of the evolved hydrogen gas by Pd^0, and the formation of the powerful reducing species, $Pd \bullet H_2$, and destabilization of C:Cl bond; and (3) the electroreduction of the compound by external electrons on the Pd/Fe-oxide surfaces.

The electrochemical dechlorination of TCE using palladized, multiphasic Fe oxides is a complex process, therefore further laboratory studies are required to provide a fundamental understanding of the reaction mechanisms before full-scale engineering development as a treatment technology.

REFERENCES

Bodnariuk, P., B, Coq, G. Ferrat, and F. Figueras. 1989. Carbon-chlorine hydrogenolysis over PdRh and PdSn bimetallic catalysts. J. Catalysis. 116:459-466

Cheng, I. F., Q. Fernando, and N. Korte. 1997. Electrochemical dechlorination of 4-chlorophenol to phenol. Environ. Sci. Technol. 31(4):1074-1078

Environmental Protection Agency. 1988. U. S. EPA methods for the determination of organic compounds in drinking water:Method 502.2, Revision 2.0, EPA-600/4-88/039, U. S. Environmental Protection Agency, Cincinnati, Ohio

Grittini, C., M. Malcomson, Q. Fernando, and N. Korte. 1995. Rapid dechlorination of polychlorinated biphenyls on the surface of a Pd/Fe bimetallic system. Environ. Sci. Technol. 29(11):2898-2900

Hughes, R. 1984. Deactivation of catalysts. Academic Press, London.

Lawson, D. R., M. J. Tierney, I. F. Cheng, and L. S. Van Dyke. 1991. Use of a coulometric assay technique to study the variables affecting deuterium loading levels within palladium electrodes. Electrochim. Acta. 36(9):1515-1522

Liang, L., N. Korte, J. D. Goodlaxson, J. Clausen, Q. Fernando, and R. Muftikian. 1997. Byproduct formation during the reduction of TCE by zero-valent iron and palladized iron. Ground Water Monitoring and Remediation. Winter:122-127

Mallat, T., and Zs. Bondar, and J. Petro. 1991. Reduction by dissolving metals. Tetrahedron 47(3):441-446

Marques, C. A., M. Selva, and P. Tundo. 1993. Facile hydrodehalogenation with hydrogen and Pd/C catalyst under multiphase conditions. J. Org. Chem. 58:5256-5260

Marques, C. A., M. Selva, and P. Tundo. 1994. Facile hydrodehalogenation with hydrogen and Pd/C catalyst under multiphase conditions. 2. Selectivity and Kinetics. J. Org. Chem. 59:3830-3837

Muftikian, R., Q. Fernando, and N. Korte. 1995. A method for the rapid dechlorination of low molecular weight chlorinated hydrocarbons in water. Wat. Res. 29(10):2434-2439

Muftikian, R., K. Nebesny, Q. Fernando, and N. Korte. 1996. X-ray photoelectron spectra of the palladium-iron bimetallic surface used for the rapid dechlorination of chlorinated organic environmental contaminants. Environ. Sci. Technol. 30(12):3593-3596

Schreier, C. G., and M. Reinhard. 1995. Catalytic dehydrohalogenation of chlorinated ethylenes using palladium and hydrogen for the treatment of contaminated water. Chemosphere 31(6):3475-3487

PART 4

IRON HYDROXIDE FORMATION FROM ZERO-VALENT IRON (Fe^0) DURING CONTAMINATED GROUNDWATER TREATMENT AND ITS EFFECTS ON REACTIVE WALL PERFORMANCE

1. ABSTRACT

In recent years, zero-valent iron (Fe^0) filings have been used for reductive dechlorination of chlorinated solvents and precipitation of heavy metals and radionuclides in contaminated groundwater. Formation of iron hydroxide and carbonate during the treatment with passive reactive wall applications is an important issue regarding the performance of the technology because by-products of the process will decrease the reactivity and permeability of the iron bed. The objective of this study is to conduct geochemical and mineralogical characterization of the reactive Fe^0 barrier during contaminated groundwater treatment under varying conditions.

Geochemical characteristics such as redox potential (Eh), pH, alkalinity, dissolved oxygen (DO), sulfate and ferrous iron (Fe^{2+}) concentration were monitored. The reactive medium, precipitated materials, corrosion products, and contaminant phases are characterized using scanning electron microscopy (SEM) with energy-dispersive X-ray (EDX) analyses and X-ray diffraction analyses (XRD). The principal corrosion products of Fe in reactive iron medium are magnetite, intermediate products (green rusts), and hydrated forms of ferric oxides such as akaganeite (β-FeOOH), goethite (α-FeOOH), or lepidocrocite (γ-FeOOH), depending on the degree of oxidation. Other minerals including calcite, aragonite, siderite, mackinawite, and sulfur (S) are also precipitated on the surface of reactive medium depending on the groundwater chemistry. Many factors contribute to mineralogy of the precipitates including (a) contaminants and chemical composition of groundwater and (b) occurrence of sulfate-reducing bacteria (SRB). The mineral

assemblage observed after treatments reflects the influence of the geochemical environment at the sites. The surface-coating materials formed during the treatment reduce the effectiveness of the Fe^0 medium. Detailed mineralogical characterization is, therefore, imperative to predict the long-term performance of the Fe-based passive reactive wall.

2. INTRODUCTION

Using barriers filled with reactive medium such as zero-valent metals to clean contaminant plumes is an emerging technology for in situ and ex situ remediation of contaminated groundwaters (Matheson and Tratnyek, 1994). Reactive medium degrades, sorbs, precipitates, or removes chlorinated solvents, metals, radionuclides, and other pollutants as the contaminant plume flows through the treatment wall. Zero-valent iron is the leading treatment medium to dechlorinate halogenated hydrocarbons (Gillham and O'Hanneisin, 1994; Orth and Gillham, 1996: Liang et al., 1997), and to precipitate heavy metals (Powell et al., 1995) and radionuclides (Cantrell et al., 1995; Roh et al., 1996). Other medium that can be used in treatment walls include zeolites and activated carbon, which grab and entrap contaminants on the barrier surface, and limestone, which neutralizes acidic, lead-contaminated groundwater and traps lead in the barrier (Morrison and Spangler, 1993; Haggerty and Bowman, 1994; EPA, 1996).

Because the solubility of uranium (U), technetium (Tc), chromium (Cr), and chlorinated organic compounds (COCs) are redox sensitive, they are easily susceptible to reduction and coprecipitation through oxidation of Fe^0 as shown in the following reactions (Roh et al., 1996; Powell et al., 1995; Matheson and Tratnyek, 1994):

$$2Fe^0 + 1.5UO_2^{2+} + 10H^+ + TcO_4^- = 2Fe^{3+} + 1.5U^{4+} + TcO_2 + 5H_2O \quad (1)$$

$$Fe^0 + CrO_4^{2-} + 4H_2O = Fe(OH)_3 + Cr(OH)_3 + 2OH^- \quad (2)$$

$$3Fe^0 + C_2HCl_3 + 3H^+ = 3Fe^{2+} + C_2H_4 + 3Cl^- \quad (3)$$

Contaminated water passing through a reactive barrier of Fe^0 undergoes geochemical changes, such as Eh/pH, carbonate alkalinity, DO, sulfate and Fe^{2+} concentration. These geochemical changes can result in precipitation on the reactant surfaces, potentially reducing reactivity and permeability of the reactive zone over time. Waters high in carbonates might result in significant buildup of calcite ($CaCO_3$) or siderite ($FeCO_3$) (Blengino et al., 1995). In addition, Fe hydroxides and Fe sulfide can also be expected to precipitate as a result of geochemical changes and occurrence of SRB in iron-water system (Blengino et al., 1995; Badan et al., 1991; Hao et al., 1996). Green rusts, pyroaurite-type minerals, form as corrosion products of steel, especially microbially-induced corrosion, and as a mineral in poorly-drained redoximorphic horizons (Trolard et al., 1997; Genin et al., 1998).

The geochemical changes in reactive medium, depending upon the inorganic characteristics of the water, could result in the formation of other solid phases. Precipitates formed within the reactive medium could, over time, fill the pore spaces, thereby reducing the permeability. Precipitates also adhere to the Fe^0 surfaces, blocking the reaction sites and thus reducing the reactivity of the Fe^0. Further studies of the inorganic consequences of the reactions and means of controlling these consequences are needed. Therefore, the objectives of this study are (a) mineralogical characterization of the precipitates formed during contaminated groundwater treatment using Fe^0 under

varying conditions such as groundwater chemistry, and types and concentration of contaminants and (b) to evaluate the effect of precipitation on iron wall performance.

3. MATERIALS AND METHODS

3.1 Materials Used as a Reactive Medium

For the laboratory study, two experimental setups were used: (1) a 2.54-cm-diameter and 26-cm-long borosilicate glass column with Cercona Fe^0 foam and (2) a 2.0-cm-diameter and 35-cm-long borosilicate glass column with Master Builder and Peerless Fe^0 filings. Both experimental setups with current application were used to treat groundwater contaminated with radionuclides and TCE. Application of direct current to both experimental setups was also employed to precipitate radionuclides and to dechlorinate TCE in groundwater. Detailed description of the laboratory study with direct current was described in Part 3.

For field study, the X-625 groundwater treatment facility was constructed to evaluate reactive barrier technology for remediating TCE-contaminated groundwater at the Portsmouth Gaseous Diffusion Plant (Portsmouth, Ohio) (Liang et al., 1997). The Bear Creek Valley Treatability Study at Y-12 site (Oak Ridge, Tennessee) was designed to remediate radionuclide-contaminated groundwater using a reactive wall (SAIC, 1998).

The reactive Fe^0 barrier medium used for the treatment wall is summarized in Table 1. The reactive barrier media tested are (1) fine-grade Fe^0 filings (Master Builder Fe^0 filing) purchased from Master Builders, Inc. (Streetsbros, Ohio), (2) stock Fe^0 filings (Peerless Fe^0 filing) purchased from Peerless Metal Powders and Abrasive, Inc.(Detroit, Michigan), and (3) Cercona Fe^0 foam (Cercona of America, Inc., Dayton, Ohio).

Table 1. Reactive Fe^0 medium used for treatment of contaminated waters

Reactive Fe^0 Medium	Size	Characteristics	Mineralogy
Master Builder Fe^0 Filing	40 mesh	~95% Fe^0 and carbon, and 5% other metals and silicon	Zero-valent iron (Fe^0), Magnetite (Fe_3O_4)
Peerless Fe^0 filing	+8 to 50 mesh	~86% Fe^0, 3-4% carbon, 3% silicon, and other metals	Zero-valent iron (Fe^0), Magnetite (Fe_3O_4)
Cercona Fe^0 Foam	+2 to 8 mesh	92 to 94% Fe^0 balanced with aluminosilicate (Al_2O_3:$2SiO_2$)	Zero-valent iron (Fe^0), Magnetite (Fe_3O_4), Hercynite ($FeAl_2O_4$)

3.2 Geochemical Characterization

Periodic water sampling of influent and effluent was conducted to measure the following chemical parameters over time: pH, DO, Fe^{2+}, alkalinity, and sulfate concentration for both laboratory and field observations. Effluent from both Fe^0 filing and Fe^0 foam columns was collected promptly to prevent oxidation of dissolved iron in the treated water. Dissolved ferrous iron (Fe^{2+}) was measured by colorimetric techniques using test kits from Hach (Loveland, Colorado). Dissolved oxygen was measured by using self-filling ampoules for colorimetric analysis from CHEMets® (CHEMetrics, Inc., Calverton, Verginia). Alkalinity was determined by titration. The pH measurements were conducted using a combination of pH electrode and a ORION EA™ 920 expandable ion analyzer (Orion Research, Beverly, Massachusetts), standardized with the pH buffer 7 and appropriate buffer of either pH 4 or pH 10.

3.3 Mineralogical Characterization of Precipitates

Columns and canisters used for groundwater treatment were opened and sampled at varying columns positions (i.e., top, middle and bottom) for morphological and mineralogical characterization. Portions of sample used for treatment were embedded in epoxy resin to prepare polished cross section specimens. The polished specimens were used to measure pore, iron hydroxide, and residual metal volumes. Pore space was determined by point counting of used Fe^0 filing from the Portsmouth site using optical microscopy more than 200 points on a polished cross section surface. Other portions of the column materials were used for the characterization of precipitated materials, corrosion products, and contaminants phases. Precipitates as corrosion products in the treated water were collected from treated water before and after aging by filtration with 0.45-μm millipore filters. Precipitates on Fe^0 were isolated sonification (about 30 minutes) in acetone, filtered using millipore filter (< 0.45-μm), and used for mineralogical characterization. Mineralogical characterization of the precipitates was performed using (a) XRD using Scintag XDS 2000 diffractometer at 45 kV, 40 mA (Sunnyvale, California) and (b) JEOL-JSM35CF SEM with EDX analyzer (Tokyo, Japan) .

4. RESULTS AND DISCUSSION

4.1 Geochemical Changes in Reactive Iron Barrier

The chemical parameters of the influent water for field study are summarized in Table 2. The major aqueous components of radionuclide-contaminated water from the Y-12 site are bicarbonate, nitrate, sulfate, calcium (Ca), and magnesium (Mg) which reflect inputs from the underlying carbonate geology and contaminated site (S-3 pond). The chemical parameters of the Portsmouth X-625 influent water have shown consistent pH values of 6.1 to 6.2. The alkalinity measurements are between 83 to 85 mg/L. The DO varied from 0.2 to 5 mg/L and Fe^{2+} ranged from 0.3 to 0.6 mg/L. The dechlorination of TCE by Fe^0 was conducted using simulated groundwater that has a composition similar to that of the Portsmouth Gaseous Diffusion Plant (Table 2). The immobilization of radionuclides by Fe^0 was conducted using uranyl carbonate and pertechnetate solutions that were diluted with tap water (Table 3).

Important geochemical processes in reactive iron medium include Fe dissolution, precipitation kinetics, sorption to Fe^0 surfaces, and chemical behavior of contaminants (i.e., radionuclides, heavy metals, and chlorinated organic carbons) and major elements such as carbon, Fe, Ca, and sulfate. Zero-valent iron is inherently unstable under ambient geochemical conditions so that corrosion will contribute both electrons and dissolved iron to the aqueous environment (Pourbaix, 1973). Potential redox reactions include reduction of coexisting aqueous species, consumption of DO, and the precipitation of Fe hydroxide

Table 2. Chemical composition in influent and effluent streams of the reactive barrier used in the field

Parameter	X625 water, Portsmouth Gaseous Diffusion Plant, Ohio		GW-837, Y-12 sute, Oak Ridge, Tennessee	
	Influent[1]	Effluent[2]	Influent[3]	Effluent[4]
DO (mg/L)	0.2 - 5	< 0.1	ND[†]	ND
Turbidity (NTU)	1	ND	ND	ND
pH	6.1 – 6.2	6.9 – 7.3	5.6 – 5.7	6.9 – 7.5
Eh (mV)	400	-200 – -400	420	0 – -200
		Anions (mg/L)		
Alkalinity	83 – 85	50 – 270	300 – 500	50 – 100
Chloride	38	ND	167	ND
Sulfate	400	150	461	461
Nitrite as Nitrogen	ND	ND	5.6	5.6
Nitrate as Nitrogen	ND	ND	650	650
		Dissolved metals (mg/L)		
Calcium	21.3	ND	1681	ND
Ferrous iron	0.3 – 0.6	2 – 120	14.3	17 – 250
Magnesium	13.3	ND	158	ND
Manganese	ND	ND	159	ND
Potassium	1.7	ND	42	ND
Sodium	18.7	ND	705	ND
		Contaminants		
Uranium (pCi/L)	ND	ND	2.1 – 2.9	0.002 – 0.1
TCE (µg/L)	150 – 200	< 2	ND	ND

[1] Annual Report for 1997 Groundwater Monitoring Quarterly Sampling Results from Portsmouth Gaseous Diffusion Plant, Ohio

[2] Linag et al. (1997)

[3] Field characterization report on phase 1 of the Bear Creek Valley treatability study, Oak Ridge Y-12 plant, Oak Ridge, TN, Y/ER-286

[4] SAIC (1998) [†]Not determined

phases. Metal corrosion is an electrochemical process in which oxidation of Fe^0 to Fe^{2+} is the anodic half reaction. The associated cathodic reaction may vary with the reactivity of available electron acceptors. In anoxic aqueous media, the acceptors include H^+ and H_2O, the reduction of which yields OH^- and H_2. Thus, the overall process of corrosion in anaerobic Fe^0-H_2O systems is described by the following reactions:

$$Fe^0 + 2H_2O = Fe^{2+} + H_2 + 2OH^- \qquad (4)$$

Organic oxidants also react with Fe^0, as illustrated by the dechlorination of chlorinated hydrocarbons, R-Cl:

$$Fe^0 + R\text{-}Cl + H^+ = Fe^{2+} + R\text{-}H + Cl^- \qquad (5)$$

This reaction can contribute significantly to the net dissolution of iron, even in predominantly aqueous systems (Matheson and Tratnyek, 1994). Therefore, effluent pH following reactive wall treatment rising to above 9 and Eh lowering to minus several hundred millivolts are due to electrolysis of water by the Fe-water reaction (Table 2,3). Electrolysis of water produces large quantities of hydroxyl ions and hydrogen gas. When solution pH increases to 9 and Eh decreases significantly, precipitates of Fe hydroxide and Ca/Fe carbonates may occur and cause clogging. Dissolved oxygen decreased from 1 – 5 mg/L in the influent to 10 –100 µg/L in effluent (Table 2). Low DO in the effluent is

Table 3. Chemical composition in influent and effluent streams of the reactive barrier used in laboratory

Parameter	Simulated ^{235}U-and ^{95m}Tc-contaminated water[1]		Simulated TCE contaminated water[2]	
DO (mg/L)	4 – 5	< 0.01	4 – 5	< 0.01
pH	5.2	7.5 – 9.0	6.2	7.0 – 8.7
Eh (mV)	400	-50 – -400	430	0 – -200
		Anions (mg/L)		
Alkalinity	ND†	ND	ND	ND
Chloride	ND	ND	37	ND
Sulfate	ND	ND	46	ND
Nitrite as Nitrogen	ND	ND	115	ND
Nitrate as Nitrogen	ND	ND	ND	ND
		Dissolved metals (mg/L)		
Calcium	34	ND	25	ND
Iron (total)	<0.01	ND	< 0.01	ND
Magnesium	9	ND	10	ND
Potassium	1.58	ND	3.5	ND
Sodium	5.35	ND	50	ND
		Contaminants		
Technetium (pCi/L)	2.92E-9	BD		
Uranium (mg/L)	7 – 2500	< 25		
TCE (μg/L)			150 – 3200	<2 – 750

[1] Simulated water using tap water
[2] Simulated Portsmouth Water
† Not determined

attributed to consumption of DO by redox reactions in aqueous environments, thereby creating highly reducing conditions. The alkalinity decrease with residence time in the Y-12 site water suggests the precipitation of ferrous carbonate (siderite) and Ca-carbonate (aragonite and calcite) (Table 2). However, the cause of the alkalinity increase in Fe^0 medium at the Portsmouth site is unknown (Table 2). We postulate that sulfides and titratable organic compounds that are produced by SRB may have contributed to the alkalinity. The increase in sulfate concentration at Portsmouth site may be attributed to microbial activity of the SRB (Table 2).

Ferrous iron is produced from reductive dechlorination and aerobic reaction between Fe^0 and water (Table 2). In short-term column experiments (< 60 pore volumes passed), Fe^{2+} release increased with time in the column (Fig. 1) during TCE dechlorination and radionuclide immobilization. Considerable concentration of Fe^{2+} by Fe^0 corrosion (Fe^{2+} =140 mg/L) occurred when radionuclide-contaminated water from Y-12 site was treated with a column without current in the laboratory. Systems containing carbonate species in the Y-12 water may act as electron acceptors to oxidize Fe^0 and promote Fe^0 corrosion (Wiekowski et al., 1983a,b). The presence of dissolved Fe^{2+} in the effluent may cause possible effects on water quality and on the hydraulic conductivity of the soil downgradient of the treatment system.

Iron corrosion rate with an application of direct current is lower than the column experiment without current (Fig. 1) testing TCE dechlorination and radionuclide immobilization. This is attributed to the cathodic Fe protection by the impressed current (Pourbaix, 1973) because Fe^0 in the column is in direct contact with cathode. The direct

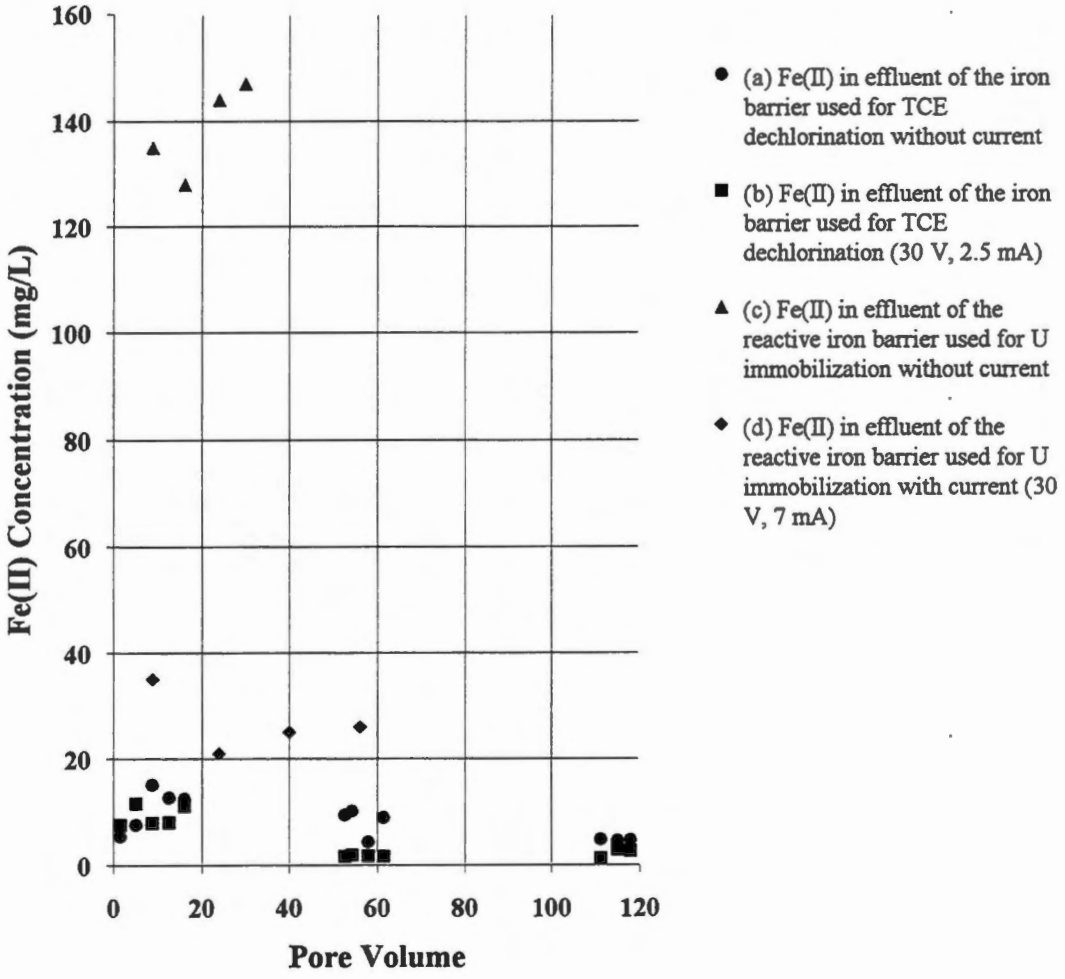


Figure 1. Dissolved Fe^{2+} concentration in effluent of the reactive Fe^0 medium in the laboratory experiment

current application is one way to reduce dissolved iron discharge, if regulatory limits are placed on the discharge of soluble Fe from a permeable reactive barrier (SAIC, 1998).

In long-term reactive barrier experiments for TCE dechlorination in the field (more than 900 pore volumes passed), Fe^{2+} release slowed with time as a result of the passivation of the surfaces by increasing thicknesses of oxide surface layers (Liang et al., 1997). Decrease $[Fe^{2+}]$ in effluent is associated with iron hydroxide formation and adsorption because the Fe^0 surface must become $Fe^{2+/3+}$-enriched with continued reaction, and will gradually convert to iron hydroxides. Because of the pH and $[Fe^{2+}]$ increase, precipitation of solid phases, depending upon the inorganic chemistry of the natural groundwater, can be anticipated.

4.2 Mineralogical Characterization of the Precipitates

Iron hydroxide precipitation: The stability field of Fe^0 lies below the water redox line, indicating that Fe^0 should oxidize in the presence of water and will dissolve with evolution of hydrogen gas in acid, neutral, and alkaline solutions (Matheson and Tratnyek, 1994). Oxidation of Fe^0 can proceed along several reaction pathways (Schwertmann and Cornell, 1991). Continued corrosion of Fe leads to saturation and precipitation of $Fe(OH)_2$. The Eh-pH diagram indicated that the Fe metal will be passivated by green rusts such as $[Fe_4(OH)_8Cl \bullet nH_2O]$, $[Fe_6(OH)_{12}][CO_3 \bullet nH_2O]$, and $[Fe_7(OH)_{18}SO_4 \bullet nH_2O]$ in moderately neutral solution ($6.5 < pH < 8.0$), and passivated by Fe hydroxide (FeOOH) in the presence of alkaline solution ($pH > 8.0$) (Olowe and Genin, 1991; Drissi et al., 1995; Genin et al., 1996; Refait et al., 1997; Simon et al., 1997). In the reduced environment

and at low temperature, $Fe(OH)_2$ is stable, but is predicted thermodynamically to convert to either magnetite, intermediate products (green rusts) or hydrated forms of ferrous/ferric iron oxides as shown in the following reactions:

$$Fe^0 = Fe^{2+} + 2e^- \text{ (iron oxidation)} \quad (6)$$

$$Fe^0 + 2H_2O = Fe(OH)_2 + 2H^+ + 2e^- \text{ (precipitation of Fe hydroxide)} \quad (7)$$

$$3Fe(OH)_2(s) = Fe_3O_4(s) + H_2(g) + 2H_2O + 2e^- \text{ (transformation into magnetite)} \quad (8)$$

$$4Fe(OH)_2(s) + Cl^- = Fe_3^{II}Fe^{III}(OH)_8Cl + e^- \text{ (transformation into green rust I)} \quad (9)$$

$$6Fe(OH)_2(s) + CO_3^- + 2H_2O$$
$$= [Fe_4^{II}Fe_2^{III}(OH)_{12}][CO_2 \cdot 2H_2O] + 2e^- \text{ (transformation into green rust I)} \quad (10)$$

$$6Fe(OH)_2(s) + SO_4^{2-} + 2H_2O$$
$$= [Fe_4^{II}Fe_2^{III}(OH)_{12}][SO_4 \cdot 2H_2O] + 2e^- \text{ (transformation into green rust II)} \quad (11)$$

$$Fe(OH)_2(s) = FeO(OH) + H^+ + e^- \text{ (transformation into iron hydroxides)} \quad (12)$$

When the treatment column or reactor was opened after the dechlorination of TCE and immobilization of radionuclide experiments in the lab and field, Fe^0 filings and sand

filters on the top of the columns were covered by crystalline and amorphous Fe hydroxide. The SEM micrograph of Peerless and Master Builder Fe^0 filings used for dechlorination at the Portsmouth site revealed that the Fe^0 was covered with amorphous Fe (hydr)oxides (Fig. 2a,b). The SEM micrograph of the Master Builder Fe^0 used for immobilization of radionuclides at the Y-12 site revealed that the Fe^0 was covered with amorphous Fe oxides (Fig. 2c) with precipitation of uranium (Fig. 2d).

The SEM micrograph of the Master Builder Fe^0 filing used at Portsmouth revealed that the Fe hydroxide had a green rust mineral morphology (Fig. 3a), but XRD analyses did not confirm the presence of this mineral as a result of a undectable amount of the mineral. Precipitates collected from filtered effluent of TCE dechlorination experiments using Peerless Fe^0 in the laboratory showed a platy, pseudo hexagonal form as the Fe corrosion products (Fig. 3b). During reductive dechlorination, most of the chlorine is released as the chloride ion or combined with Fe^{2+} to precipitate out as amorphous Fe hydroxides [$Fe_4(OH)_8Cl$] and green rust I [$Fe_3^{(II)}Fe^{(III)}(OH)$][$Cl{\cdot}2H_2O$]. The TCE dechlorination columns with or without current showed that green rusts precipitated on sand filters in the top of the both columns. Scanning electron microscopy, however, shows that more green rusts are formed on sand filters in the column under current application than under the same condition used in the column without current. The SEM micrograph of Master Builder Fe^0 filing used at the Y-12 site also showed the presence of a green rust mineral morphology (Fig. 3c), and XRD analyses confirmed the presence of the hydrated sulfate form of green rust II (Table 4).

Table 4. Summary of the reactive iron barrier experiments in the field and laboratory

Contaminated Waters	Operation Period	Reactive Fe^0 Medium	Flow Rate	Mineralogy
Field Study				
X-625 water, Portsmouth site, Portsmouth, Ohio	6 months	Peerless Fe^0 filing Master Builder Fe^0 filing	11.34 mL/min	Amorphous Fe (hydr)oxides, Goethite, Magnetite, Akageneite, Lepidocrocite, Green rust I (chloride form), Iron sulfide, Sulfur
GW-837 water, Y-12 site, Oak Ridge, Tennessee	2 months	Master Builder Fe^0 filing	2 mL/min	Amorphous Fe (hydr)oxides, Goethite, Lepidocrocite, Magnetite, Akageneite, Aragonite, Calcite, Siderite
Laboratory Study				
Simulated Portsmouth TCE-contaminated water	3 days	Peerless Fe^0 filing Master Builder Fe^0 filing	4 mL/min	Amorphous Fe (hydr)oxides, Green rust I (chloride form)
U- and Tc-contaminated water simulated with tap water	8 hours	Cercona Fe^0 foam	6.2 mL/min	Amorphous Fe (hydr)oxides
GW-837 water, Y-12 site, Oak Ridge, TN	3 days	Peerless Fe^0 filing	2 mL/min	Amorphous Fe (hydr)oxides, Calcite, Siderite
Laboratory Study with Direct Current				
TCE-contaminated water simulated with tab water	3 days	Peerless Fe^0 filing	4 mL/min	Amorphous Fe (hydr)oxides, Green rust I (chloride form)
U- and Tc-contaminated water simulated with tap water	8 hours	Cercona Fe^0 foam	6.2 mL/min	Amorphous Fe (hydr)oxides, Green rust I (carbonate form)
GW-837 water, Y-12 site, Oak Ridge, Tennessee	3 days	Peerless Fe^0 filing	2 mL/min	Amorphous Fe (hydr)oxides, Green rust II (sulfate form)

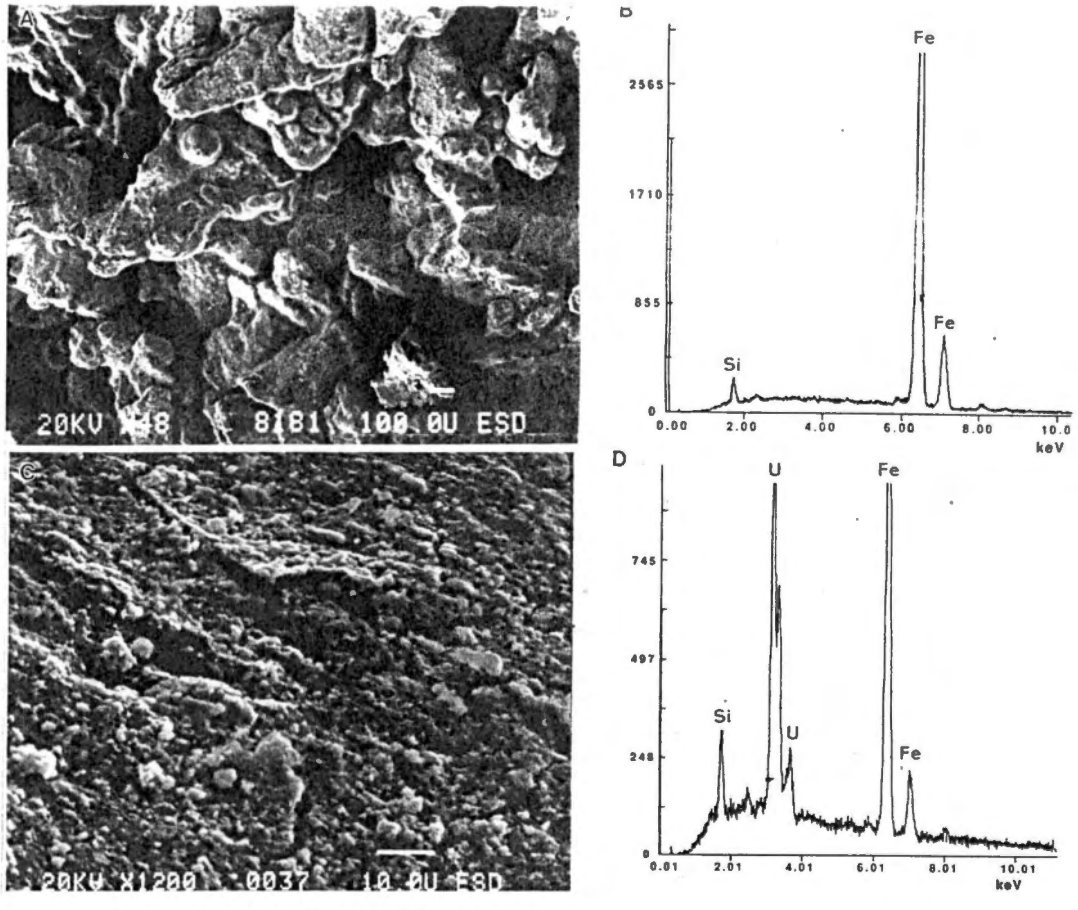


Figure 2. SEM and EDX spectra of the reactive Fe^0 barrier used at the Portsmouth site (a,b) and at the Y-12 site (c,d)

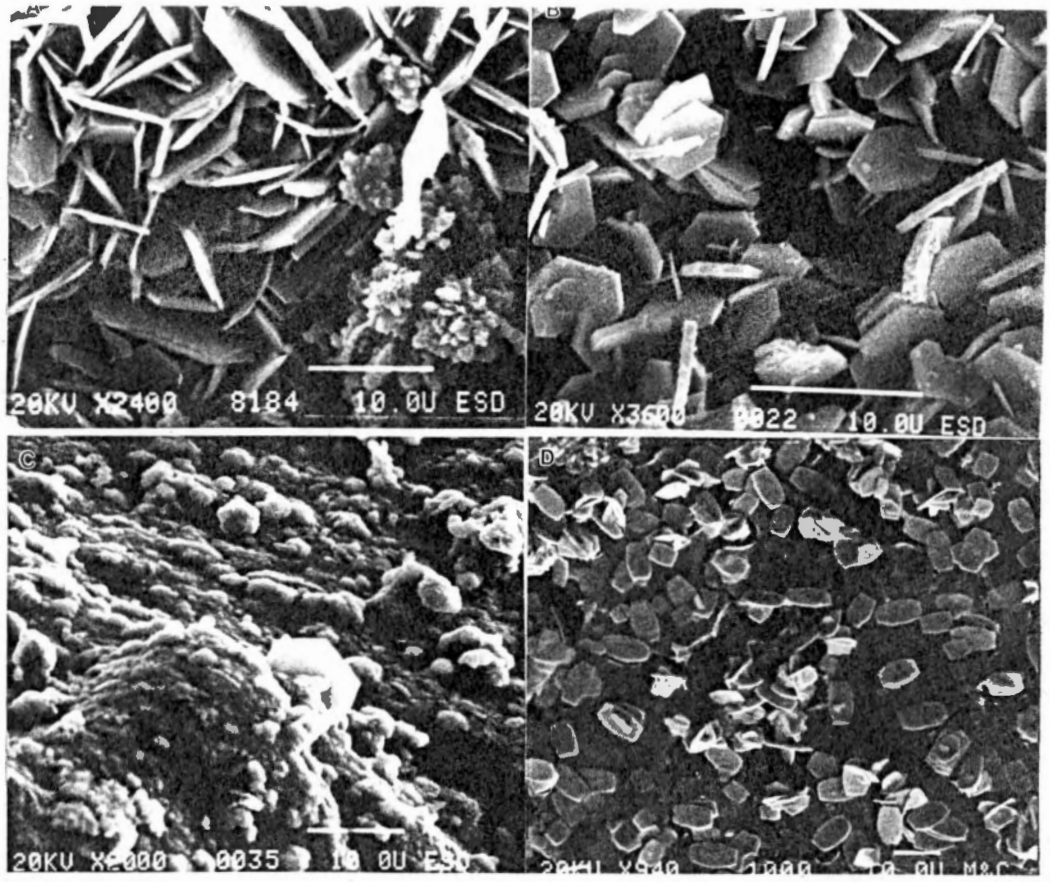


Figure 3. Scanning electron micrograph:(a) green rust formed from Peerless Fe^0 filing used at the Portsmouth site, (b) green rust formed from Peerless Fe^0 filing during electrochemical dechlorination of TCE, (c) green rust formed from Master Builder Fe^0 filing used at the Y-12 site, and (d) green rust formed from Cercona Fe^0 foam during electrochemical immobilization of radionuclides

Precipitates collected from filtered effluent of radionuclide immobilization experiments using Peerless Fe^0 in the laboratory showed that the pseudo hexagonal form of green rust as the Fe corrosion product (Fig. 3d). X-ray diffraction analysis confirmed the identification of green rust in the carbonate form (Table 4). Pyroaurite-type minerals (green rusts) were synthesized by coprecipitation of reduced U with Fe eroded from a sponge-like Fe^0 foam under direct current (DC) during the remediation of the radionuclides, $^{235,238}U$ and ^{99}Tc, from contaminated waters (Roh et al., 1996) (Table 4). Further research is required to assess the effect of electric current on coprecipitation and crystallization of Fe (hydr)oxides.

The pseudo hexagonal Fe mineral, green rust, and magnetite contain both Fe^{2+} and Fe^{3+} in the structure while other Fe (hydr)oxides have only Fe^{3+}. Green rusts often form as an intermediate product during the hydrolytic oxidation of Fe^{2+} solutions to FeOOH (Schwertmann and Cornell, 1991). Green rusts convert to goethite (α-FeOOH), lepidocrocite (γ-FeOOH), maghemite (Fe_2O_3), or magnetite (Fe_3O_4), depending on the rate of oxidation and dehydration (Hansen et al., 1994). The freshly-precipitated ferrihydrite reacts with excess Fe^{2+} in the system and induces the hydrolysis of Fe^{2+}, which leads to the formation of green rusts (Schwertmann and Cornell, 1991). Green rust is a reductant capable of TCE dechlorination and reduction of heavy metals and radionuclides (Myneni et al., 1997). A synthetic and natural material of similar crystal structure is likely able to reduce nitrate and heavy metals under abiotic conditions, although these reactions are generally quite slow (Hansen et al., 1996).

The SEM micrograph and XRD analysis of the Peerless and Master Builder Fe^0

filing used at the Portsmouth site revealed the presence of lepidocrosite (γ-FeOOH) (Fig. 4c) and goethite (α-FeOOH) with irregular platy or spherical amorphous iron hydroxide (Fig. 4b,c). It is not obvious when the Fe minerals were transformed from the amorphous Fe hydroxides; however, the presence of pores inside the crust and the out-going growth pattern suggest that the crystallization may have proceeded during the Fe column operation. Dome-shaped Fe (hydr)oxide crusts were commonly observed on the Master Builder Fe^0 filing samples used at Portsmouth site (Fig. 4a,b). In some areas, the surface of the crust was fairly smooth, and in other areas, the surface was porous because of crystallization of Fe (hydr)oxide minerals (Fig. 4b). The minerals precipitated on Master Builder Fe^0 filing used at the Y-12 site were also dominantly lepidocrosite and goethite. X-ray diffraction analyses confirmed that the presence of iron hydroxide such as goethite at the Portsmouth and Y-12 site (Table 4).

The surface coating materials formed during the treatment reduced the effectiveness of Fe^0 medium because Fe^0 is passivated by coated amorphous Fe oxides, intermediate Fe oxides, and Fe hydroxides. The surface coating also limits access of the contaminants to the Fe^0 surface for reductive dechlorination and coprecipitation. The precipitates had also blocked the pore spaces between some Fe particles. This may result in the appearance of daughter products of incomplete dechlorination and unreacted radionuclides appearing in the effluent after reaction period of the treatment.

Calcium and iron carbonate precipitation: Corrosion produces OH^- ions that increase pH (Table 2, 3) and react with dissolved carbonic acid and bicarbonate species in the

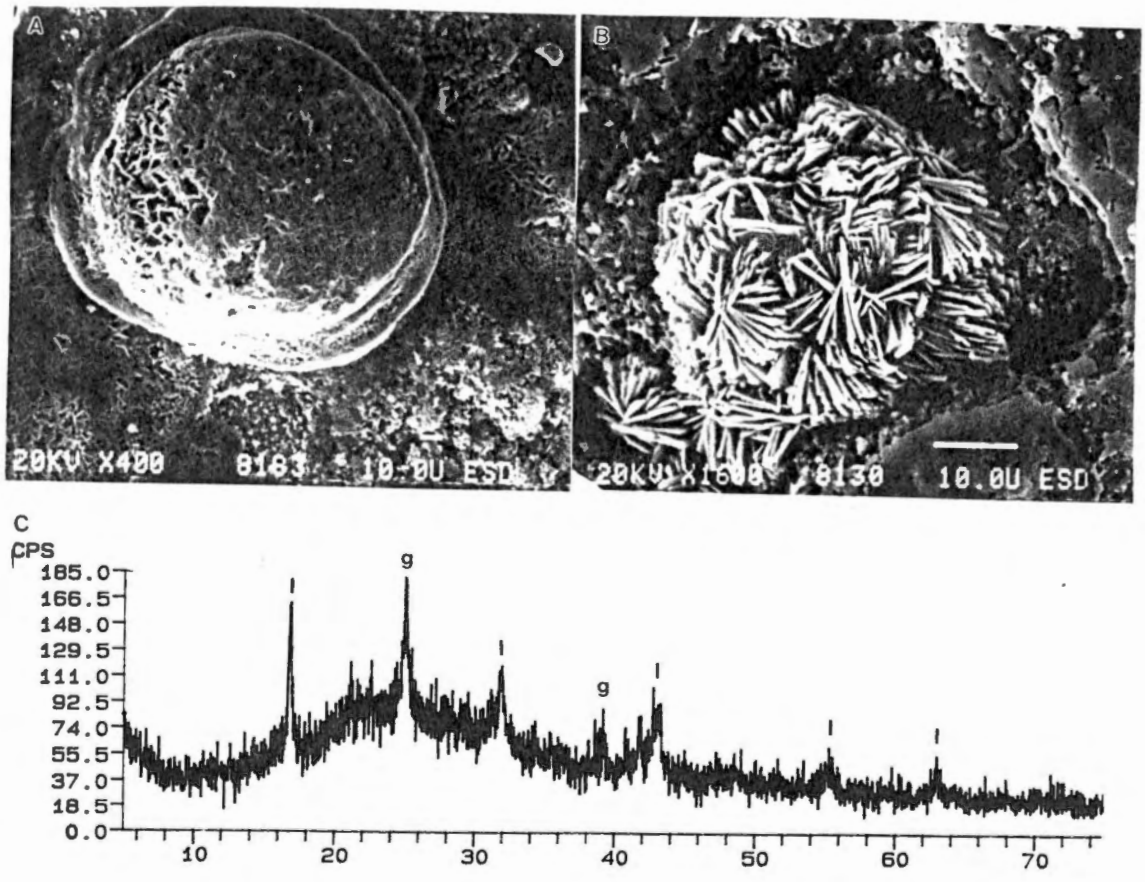


Figure 4. Scanning electron micrograph of (a) iron hydroxide formation from dome-shaped iron (hydr)oxides, (b) goethite formation with micropore, and (c) XRD analysis of lepidocrocite (l) and goethite (g) formed from Fe^0 filing used at the Portsmouth site.

groundwater to produce carbonate ions:

$$H_2CO_3^0 + 2OH^- = CO_3^{2-} + 2H_2O(l) \quad (13)$$

$$HCO_3^- + OH^- = CO_3^{2-} + H_2O(l) \quad (14)$$

Buildup of carbonate ions eventually results in the precipitation of carbonate solid species:

$$Ca^{2+}(aq) + CO_3^{2-} = CaCO_3(s) \quad (15)$$

$$Ca^{2+}(aq) + HCO_3^-(aq) = CaCO_3(s) + H^+ \quad (16)$$

$$Fe^{2+}(aq) + CO_3^{2-} = FeCO_3(s) \quad (17)$$

$$Fe^{2+}(aq) + HCO_3^-(aq) = FeCO_3(s) + H^+ \quad (18)$$

Therefore, waters high in carbonate like the Y-12 site might result in a significant buildup of calcite ($CaCO_3$) and siderite ($FeCO_3$) (Fig 5a,c). Depending on the chemical composition of the groundwater, such minerals including aragonite have been precipitated (Fig. 5b, Table 4). The presence of sulfate and Mg in the treated water at the Y-12 site (Table 2) may promote the formation of aragonite rather than calcite (Berner, 1975). The carbonate coatings on reactive Fe^0 surface could prevent adsorption and precipitation of the reducible radionuclides from the contaminated water, especially in limestone aquifers such as the Y-12 site (SAIC, 1996). In general, the chemical composition of the contaminated groundwater would control the mineralogy of the precipitates in the reactive

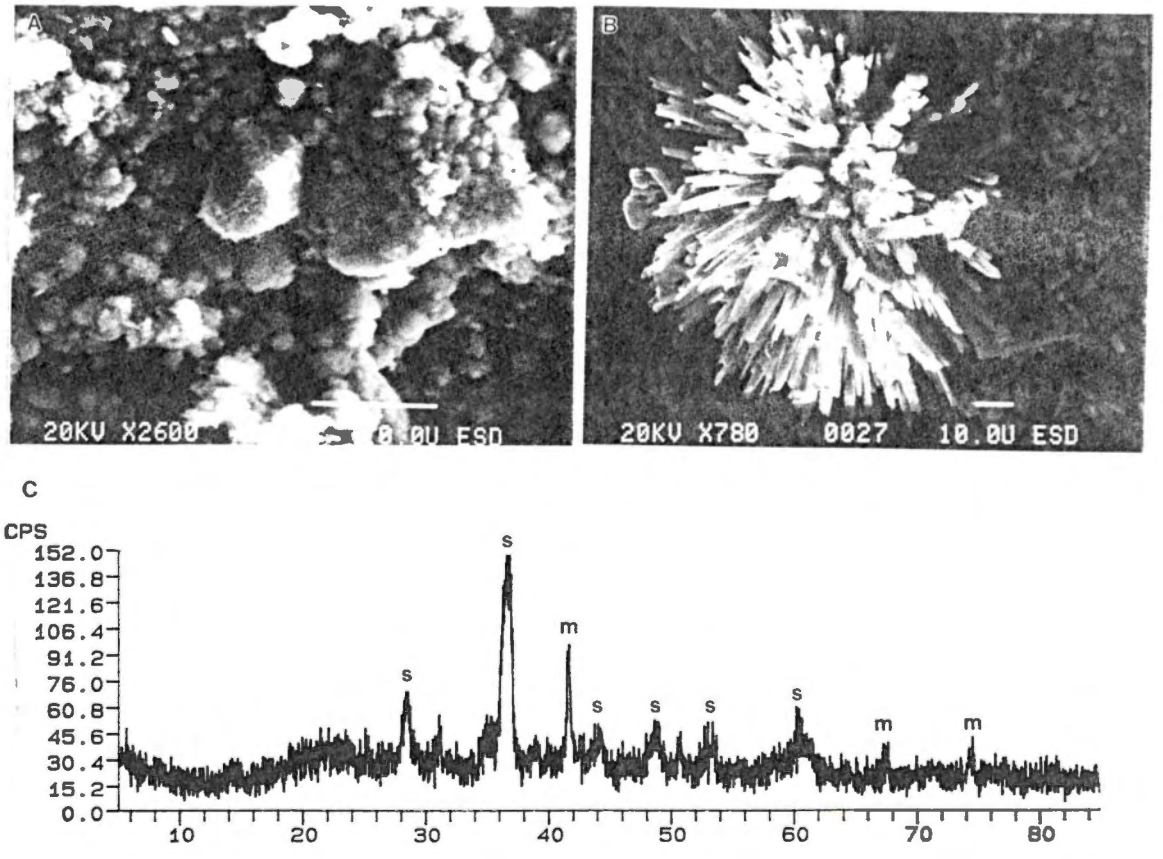


Figure 5. Scanning electron micrograph of (a) calcite and (b) aragonite formed on Fe^0 filing used at the Y-12 site, and (c) XRD analysis of siderite (s) and magnetite (m) formed from Fe^0 filing used at the Y-12 site



iron barrier.

Iron sulfide precipitation: Pure cultures of SRB have demonstrated the ability to use cathodic hydrogen as an energy source for growth in short-term batch experiments (Rajagopal and Legall, 1989). Anaerobic bacteria can catalyze the reductive dechlorination of chlorinated organic carbons (COCs) because reductive dechlorination can be supported using cathodic hydrogen produced by anaerobic corrosion of the added Fe^0 (Weathers et al., 1997). Zero-valent iron can also support the growth of anaerobic bacteria, which are commonly associated with metal corrosion (Hamilton, 1985; Lee et al., 1993a,b). Iron sulfides are precipitated by the occurrence of SRB and Fe oxidation (Hamilton, 1985). The SRB normally influence the corrosion of metals:

$$SO_4^{2-} + 8H^+ + 8e- = S^{2-} + 4H_2O \text{ (cathodic depolarization reaction by SRB)} \quad (19)$$

$$4Fe^0 + SO_4^{2-} + 4H_2O = FeS + 3Fe(OH)_2 + 2OH^- \text{ (Fe sulfide precipitation)} \quad (20)$$

For abiotic systems, the simultaneous presence of oxygen and hydrogen sulfide further accelerates the corrosion process of Fe^0 and prevalent corrosion product is ferrous sulfide, FeS (Lewandowski et al., 1997). Oxidation of iron sulfides results in the generation of highly corrosive products such as elemental sulfur according to the reaction (Lewandowski et al., 1997):

$$6H_2O + 4FeS + O_2 + 8e- = 4S^0 + 4FeO(OH) + 8\ H^+ \quad (21)$$

Both Fe^0 filings used at Portsmouth site were dark in color and did not have the metallic sheen of unused materials. X-ray diffraction analyses of the coated precipitates on Fe filings separated by sonification showed that iron sulfide (mackinawite, FeS_{1-x}) precipitated in the Fe^0 filing during the TCE-contaminated groundwater treatment. The occurrence of SRB can thereby affect the mineralogy of the precipitates in the reactive iron barrier. Sulfate-reducing bacteria were detected in the water samples collected from the treatment trains and in the iron filing used from the canisters at the Portsmouth (Liang et al., 1997). Therefore, the Fe sulfide (mackinawite) may be precipitated via the occurrence of SRB and Fe oxidation (Fig. 6a,c) (McNeil and Little, 1990). Pyramidal sulfur crystals were formed through sulfate reduction by the action of sulfur-forming bacteria as reported by Hurlbut and Klein (1985) (Fig. 6b). Microbial, Fe^0 treatment systems may offer advantages over abiotic Fe^0 schemes because reductive dechlorination was apparently supported using cathodic hydrogen produced by anaerobic corrosion of the added Fe^0 (Weathers et al., 1997). Potential negative consequence of bacteria is biofouling, because the proliferation in an improperly designed reactive barrier could reduce the hydraulic conductivity of the barrier, thereby hindering the flow of groundwater through it (Weathers et al., 1997). The surface-coated materials formed during the treatment also reduce the effectiveness of Fe^0 media because Fe^0 is passivated by coated Fe sulfide and sulfur.

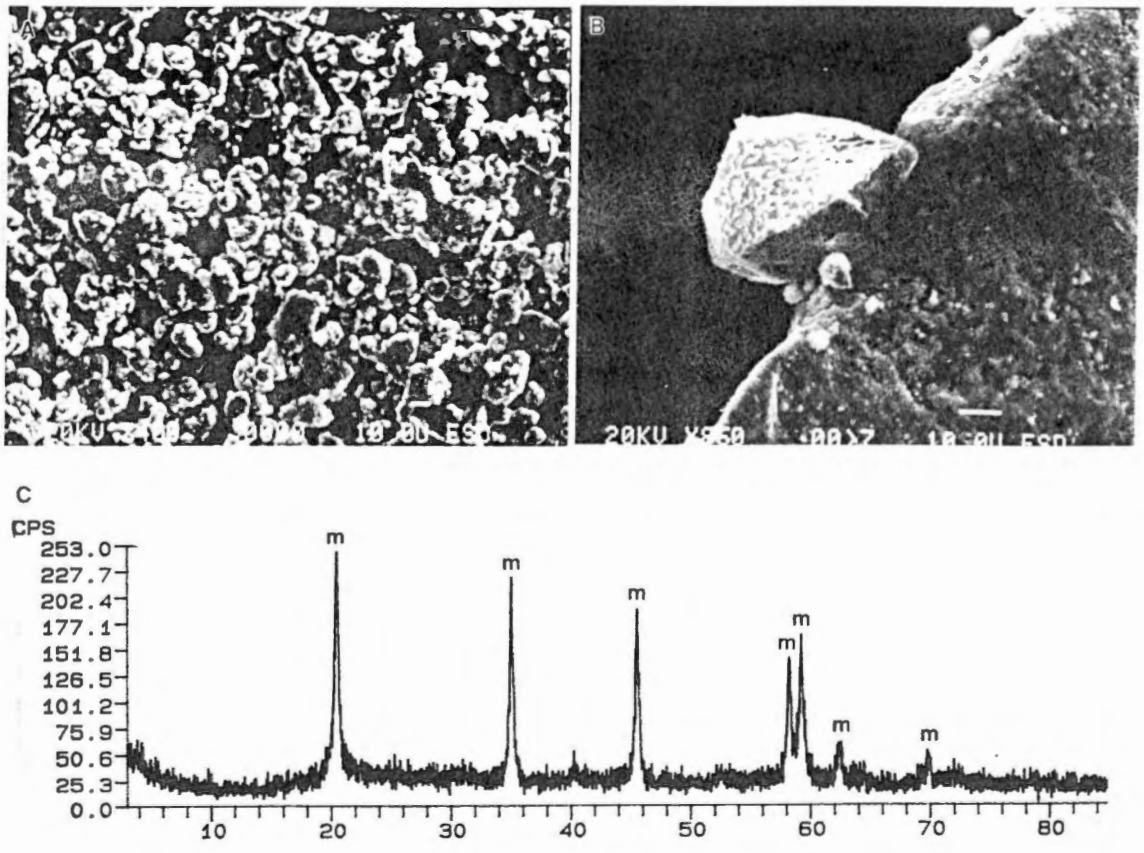


Figure 6. Scanning electron micrograph of (a) mackinawite and (b) sulfur formed on Fe^0 filing used at the Portsmouth site, and (c) XRD analysis of mackinawite (m) formed from Fe^0 filing used at the Portsmouth site



4.3 Effect of Precipitates on Iron Wall Performance

It has been postulated that Fe oxidation is one of the main mechanisms of reductive dechlorination of TCE and immobilization of reducible toxic metals and radionuclides. However, the role of the Fe hydroxide surface film formed by the hydrolysis of the oxidized Fe on the dechlorination rate of TCE and coprecipitation rate of the heavy metals and radionuclides are not very well understood. There is uncertainty over how to incorporate the kinetics of the oxide film growth on the metal surface with the kinetics of dechlorination, adsorption, and coprecipitation. The long-term performance is still an issue because Fe^{2+} release will be slowed with time as a result of the passivation of the surfaces by increasing thickness of inorganic surface layers.

Porosity: The original pore volume of both Master Builder and Peerless Fe^0 filings used in Portsmouth site was about 60%. Microscopic examination revealed that the Peerless Fe^0 samples consist of varying sizes, typically less than 4-mm in length, of elongated irregular particles (Fig. 7a,b). The particle size of the Master Builder Fe^0 filing samples were generally less than 1-mm length and relatively smaller than Peerless Fe^0 filing samples (Fig. 7c,d). A polished cross section of the Peerless Fe^0 filing used at the Portsmouth site shows a uneven thickness of hydroxide coating (darker gray) on the surface of Fe^0 (lighter gray) (Fig. 7a,b). The thickness of the coating varied from 10 to 100 μm. A greater thickness was observed at the rough concave-surface of the particles and/or surfaces between two particles which were packed closely together (Fig. 7b). The point counting data of the used Peerless Fe^0 filing showed that about one half of the initial pores was

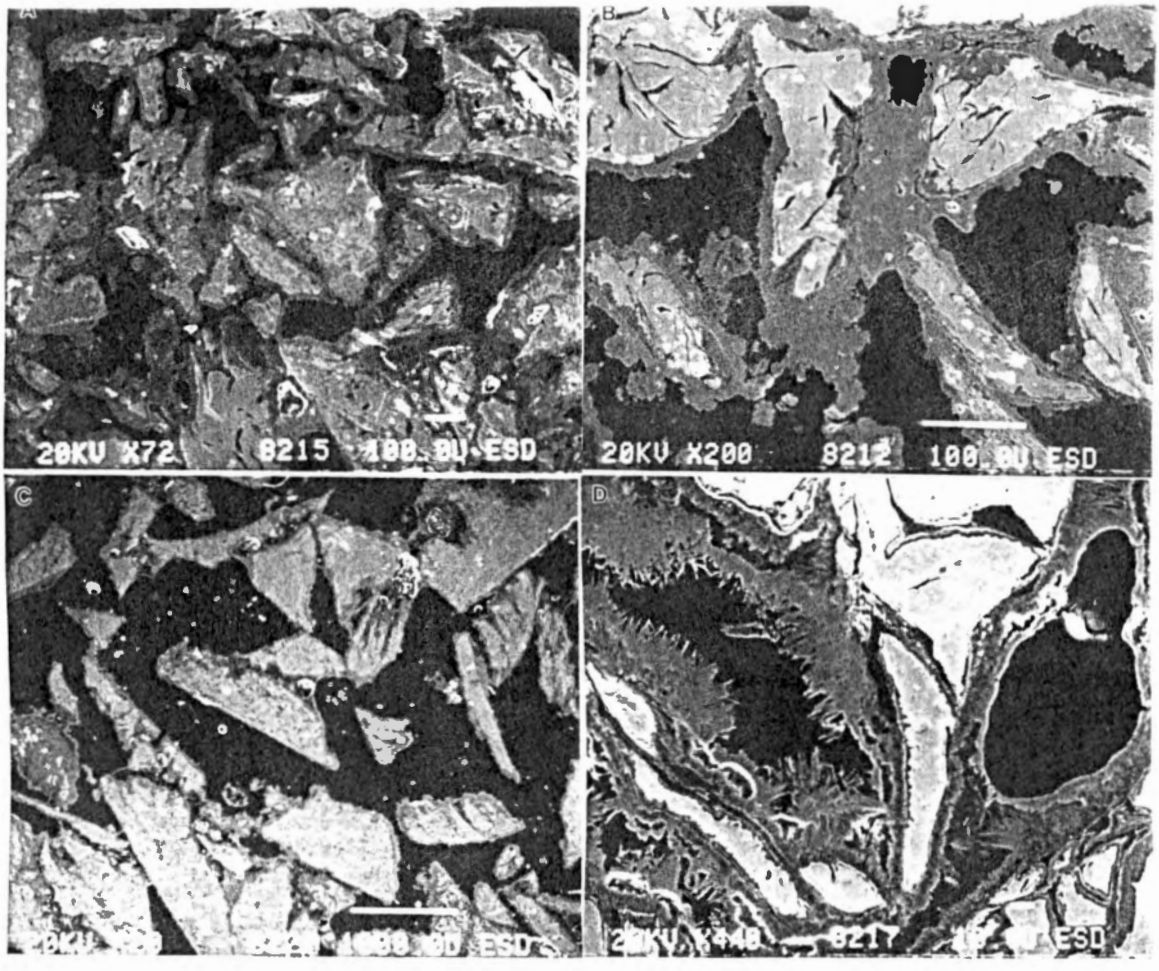
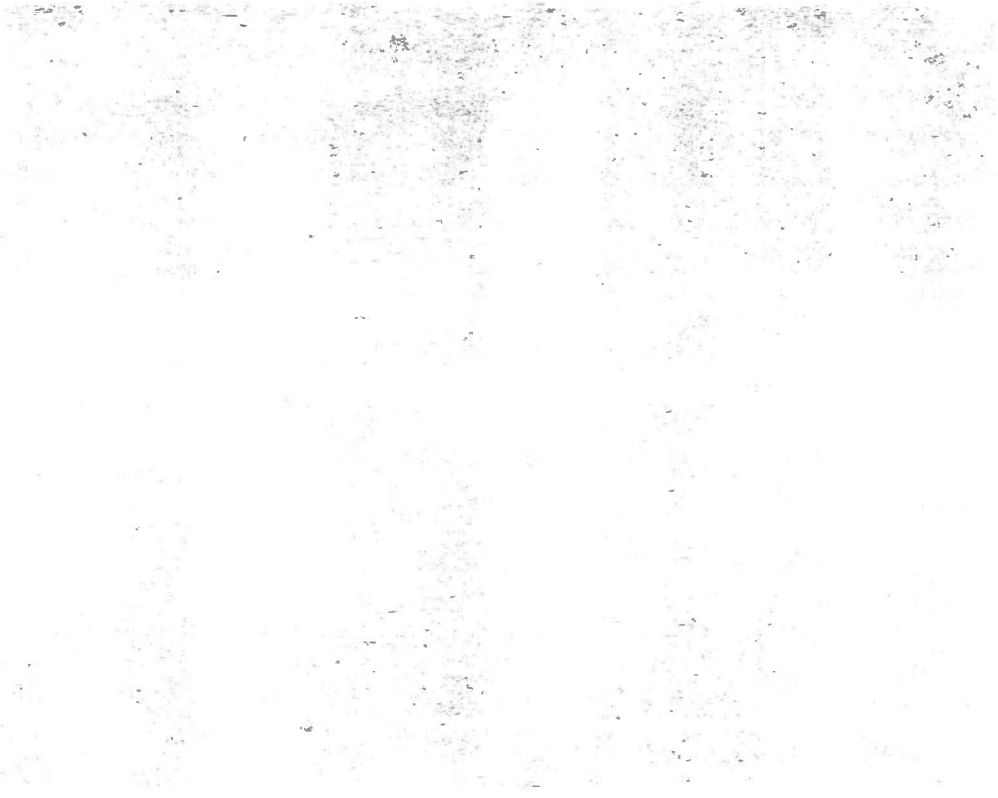


Figure 7. Scanning electron micrograph of polished cross section:(a,b) Peerless Fe^0 filing and (c,d) Master Builder Fe^0 filing used at the Portsmouth site



replaced by Fe (hydr)oxides (Table 5). The Fe particles of used Master Builder Fe^0 were covered extensively by crystalline and amorphous Fe (hydr)oxide and cemented together by the coated materials, thereby changing their individual particle shape.

Table 5. Porosity analyses using point counting of pore space, metallic iron and iron hydroxide phases

Material used as reactive barrier	Fe^0	Iron hydroxide	Pore
	---------- % ----------		
Peerless #1	38.3	31.3	30.4
Peerless #2	41.2	25.5	33.3
Peerless #3	39.5	26.3	34.2
Average	39.7	27.7	32.6
Master Builder #1	26.4	48.8	28.8
Master Builder #2	34.9	46.1	19.0
Average	30.6	47.4	23.4

The point counting data of the used Master Builder Fe^0 filing showed that a noticeable volume of large pores ranged from 19 to 28% so that the finer Fe samples were easily corroded because of their increased surface areas. Therefore, precipitates on Fe^0 medium could (a) decrease porosity and (b) minimize the amount of time water is held in the barrier and keep it from being treated effectively.

The observed morphology of the reactor bed fragments indicates that the reduction of flow rate was caused by the buildup of Fe (hydr)oxide coatings. As the flow rate was

reduced, the growth rate of coating might be increased due to increases in Fe concentration in the pore water and subsequent precipitation on the existing coating surfaces.

Flow rate and kinetics (half-life): Flow rates were stable in short-term lab studies (< 200 pore volumes of water passed) and small-scale ex situ operation (< 2-month operation) at the Y-12 site, but there were gas buildups in both columns. Flow through during the start-up phase at the Portsmouth site was not stable due to gas build-up in the canister (Liang et al., 1997). This gas contained 22.3% H_2, 4.2% O_2, 0.05% CO_2, and 0.01% methane (Liang et al., 1997). To maintain a constant flow rate in the treatment train, venting is required. Flow through the reactive Fe^0 barrier was relatively stable during the first month (3 gpm), but flow through the Master Builder Fe^0 filing train started to decrease from <1 gpm to 0.3 gpm after approximately 2 months operation (Liang et al., 1997). Flow through the Peerless Fe^0 treatment train was relatively stable in comparison with that in the Master Builder Fe^0 treatment train because there appears to be a decreasing trend in flow through after approximately 5 months operation (Liang et al., 1997). The apparent decrease in flow rate is attributed to the precipitation of Fe (hydr)oxides, sulfides and carbonates, thereby reducing pore spaces available for water flow (Table 4,5).

At the system start-up phase with both Fe^0 barriers at the Portsmouth site, TCE removal was rapid: the half-life of TCE dechlorination has less than 19 minutes for Peerless Fe^0 filing and 10 minutes for Master Builder Fe^0 filing until approximately 45 pore

volumes of water were treated (Liang et al., 1997). Half-life of TCE in Peerless Fe^0 filing trains almost doubled (43.4 minutes) when 144 to 562 pore volumes of water treated. Half-life of TCE in Master Builder Fe^0 filing increased to 43.5 minutes after 326 pore volumes of water were treated. Therefore, the selection of reactive medium is important for long-term operation. The changes in degradation characteristics with time resulted from (1) reduction in Fe surface reactivity due to passivation of Fe^0 by precipitates including Fe (hydr)oxides, calcium carbonates, and Fe sulfides (Table 4), and (2) alternation of flow paths through Fe filings as a result of precipitation and cementation (Fig. 7).

At this time, the effect of these precipitates in reactive barrier over the lifetime of an in situ field installation is not fully understood, but column clogging in an ex situ field operation and lab studies has been observed. Monitoring of flow rates and system back-pressure is needed to evaluate potential clogging problem.

5. CONCLUSIONS

The principal corrosion products of Fe in reactive Fe^0 medium are magnetite (maghemite), intermediate products (green rusts), and hydrated forms of ferric oxides such as akaganeite (β-FeOOH), goethite (α-FeOOH), lepidocrocite (γ-FeOOH), depending on the degree of oxidation. Other minerals such as calcite, aragonite, siderite, mackinawite, and elemental sulfur also precipitated on the surface of reactive medium depending on the groundwater chemistry. Many factors contribute to the mineralogy of the precipitates including (a) contaminants in the treated groundwater; (b) chemical composition of groundwater; and (c) occurrence of SRB. The observed morphology of the reactor bed fragments indicates that the reduction of flow rate and reactivity was caused by the buildup of precipitates on Fe^0 surfaces, especially in the space where the Fe^0 particles were in contact. The presence of carbonate forming species in the water leads to an inert layer of metal carbonate-forming on the metal surface. This layer may greatly reduce the overall reaction rate.

Potential negative consequences of SRB in the reactive Fe^0 barrier are biofouling and precipitation of Fe sulfides and sulfur that could reduce the hydraulic conductivity and effectiveness of the barrier, thereby degrading overall performance.

Thus, successful application of this reactive barrier requires a detailed characterization of the contaminants, groundwater chemistry, ground-water flux, and subsurface geology. In addition to periodic sampling of the influent and effluent for the contaminants of interests, monitoring of flow rates and system back-pressure would also

be needed evaluate maintaining the system in operation. Further studies for means of controlling Fe corrosion and precipitation are needed because the discharge of soluble Fe from permeable reactive barrier may affect the hydraulic conductivity of the soil and sediment downgradient of the treatment system. Iron corrosion control can also extend the life of the reactive barrier.

REFERENCES

Badan, B., M. Magrini, and E. Ramous. 1991. A study of the microbiological-corrosion products of steel and cast iron pipes in fresh water. J. Material Sci. 26:1951-1954

Berner, R. A. 1975. The role of magnesium in the crystal growth of calcite and aragonite from sea water. Geochim. Cosmochim. Acta. 38:489-504

Blengno, J, M., M. Keddam, J. P. Labbe, and L. Lobbiola. 1995. Physico-chemical characterization of corrosion layers formed on iron in a sodium carbonate-bicarbonate containing environments. Corrosion Sci. 37(4):621-643

Cantrell, K. J., D. I. Kaplan, and T. W. Wiestsma. 1995. Zero-valent iron for the in-situ remediation of selected metals in groundwater. J. Hazardous Materials. 42(2):201-212

Drissi, S. H., Ph. Refait, M. Abdelmoula, and J. M. R. Genin. 1995. The preparation and thermodynamic properties of Fe(II)-Fe(III) hydroxide-carbonate (green rust 1); Pourbaix diagram of iron in carbonate-containing aqueous media. Corrosion Sci. 37(12):2025-2041

Environmental Protection Agency. 1996. A citizen's guide to treatment walls. United States Environmental Protection Agency. EPA 542-F-96-001

Genin, J. M. R., A. A. Olowe, and Ph. Refait. 1996. On the stoichiometry and Pourbaix diagram of Fe(II)-Fe(III) hydroxy-sulfate or sulfate containing green rust 2:An electrochemical and Mössbauer spectroscopy study. Corrosion Sci. 38:1751-1762

Genin, J. M. R., G. Bourrie, F. Trolard, M. Abdelmoula, A. Jaffrezic, P. Refait, V. Maitre, B. Humbert, and A. Herbillon. 1998. Thermodynamic equilibria in aqueous suspensions of synthetic and natural Fe(II)-Fe(III) green rusts: Occurrences of the mineral in hydromorphic soils. Environ. Sci. Technol. 32:1058-1068

Gillham, R. W., and S. F. O'Hanneisin. 1994. Enhanced degradation of halogenated aliphatics by zero-valent iron. Ground Water. 32(6):958-967

Haggerty, G. M., and R. S, Bowman. 1994. Sorption of chromate and other inorganic anions by organo-zeolite. Environ. Sci. Technol. 28(3):452-458

Hamilton, W. A. 1985. Sulfate-reducing bacteria and anaerobic corrosion. Ann. Rev. Microbiol. 39:195-217

Hansen, H. C. B., O. K. Borggaard, and J. Sorensen. 1994. Evaluation of the free energy of formation of Fe(II)-Fe(III) hydroxide-sulfate (green rust) and its reduction of nitrite.

Geochim. Cosmochim. Acta. 58:2599-2608

Hansen, H. C. B., C. B. Koch, H. Nancke-Krogh, O. K. Borggaard, and J. Sorensen. 1996. Abiotic nitrate reduction to ammonium:Key role of green rust. Environ. Sci. Technol. 30:2053

Hao, O. J., J. M. Chen, and L. Huang. 1996. Sulfate reducing bacteria. Critical Reviews in Environ. Sci. Technol. 26(2):155-187

Hurlbut, C. S. Jr., and C. Klein 1985. Manual of Mineralogy. 20th ed. New York. Wiley

Lee, W., Z. Lewandowski, S, Okabe, W. G, Characklis, and R. Avci. 1993a. Corrosion of mild-steel underneath aerobic biofilms containing sulfate reducing bacteria. Part I: At low dissolved oxygen concentration. Biofouling. 7:197-216

Lee, W., Z. Lewandowski, S, Okabe, W. G, Characklis, and R. Avci. 1993b. Corrosion of mild-steel underneath aerobic biofilms containing sulfate reducing bacteria. Part II: At high dissolved oxygen concentration. Biofouling. 7:217-239

Lewandowski, Z., W. Dickinson, and W. Lee. 1997. Electrochemical interactions of biofilms with metal surfaces. Wat. Sci. Tech. 36(1):295-302

Liang, L., O. R. West, N. E. Korte, J. D. Goodlaxson, D. A. Pickering, J. L. Zutman, F. A. Anderson, C. W. Welch, M. J. Pelfrey, and M. J. Dickery. 1997. The X-625 groundwater treatment facility:A field-scale test of trichloroethene dechlorination using iron filing for the X-120/X-749 groundwater plume. ORNL/TM-13410. Oak Ridge National Laboratory. Oak Ridge, Tennessee

Matheson, L. J., and P. G. Tratnyek. 1994. Reductive dehalogenation of chlorinated methanes by iron metal. Environ. Sci. Technol. 28(12):2045-2053

McNeil, M. B., and B. J. Little. 1990. Mackinawite formation during microbial corrosion. 46:599-600

Morrison, S. J., and Spangler, R. R. 1993. Chemical barriers for controlling groundwater contamination. Environ. Prog. 12(3):175-181

Myneni, S. C. B., T. K. Tokunaga, and G. E. Brown. 1997. Abiotic selenium redox transformation in the presence of Fe(II,III) oxides. Science. 278(5340):1106-1109

Olowe, A. A., and J. M. R. Genin. 1991. The mechanism of oxidation of ferrous hydroxide in sulfated aqueous media:Importance of the initial ratio of the reactants. Corrosion Sci. 32(9):965-984

Orth, W. S., and R. W. Gillham. 1996. Dechlorination of trichlorothene in aqueous solution using Fe^0. Environ. Sci. Technol. 30(1):66-71

Pourbaix, M. 1973. Lectures on electrochemical corrosion. Plenum Press, New York.

Powell, R. M., R. W. Puls, S. K. Hightower, and D. A. Sabatini. 1995. Coupled iron corrosion and chromate reduction:Mechanisms for subsurface remediation. Environ. Sci. Technol. 29(8):1913-1922

Rajagopal, B. S., and S. LeGall. 1989. Utilization of cathodic hydrogen by hydrogen-oxidizing bacteria. J. Appl. Microbiol. Biotechnol. 31:406-412

Refait, Ph., S. H. Drissi, and J. Pytkiewicz. 1997. The anionic species competition in iron aqueous corrosion:Role of various green rust compounds. Corrosion Sci. 39:1699-1710

Roh, Y., S. Y. Lee, and M. P. Elless. Electroremediation of uranium and technetium contaminated waters. Extended Abstract. Annual Meeting of the Chemical Society, I&EC Division, Emerging Technologies in Hazardous Waste Management VIII, Sept., 9-12, 1996. Birmingham, Alabama. 582-585.

SAIC. 1996. Field characterization report on Phase I of the Bear Creek Valley treatability study, Oak Ridge Y-12 Plant, Oak Ridge, TN, Y/ER-286

SAIC. 1998. Phase II report on the Bear Creek Valley treatability study, Oak Ridge Y-12 Plant, Oak Ridge, Tennessee. BJC/OR-3. Bechtel Jacobs Company.

Schwertmann, U., and R. M. Cornell. 1991. Iron oxides in the laboratory. VCH Publishers, Inc., New York.

Simon, L., J. M. R. Genin, and Ph. Refait. 1997. Stand free enthalpy of formation of Fe(II)-Fe(III) hydroxysulphite green rust one and its oxidation into hydroxysulfate green rust two. Corrosion Sci. 39:1673-1685

Trolard. F., J. M. R. Genin, M. Abdelmoula, G. Bourrie, B. Humbert, and A. Herbillon. 1997. Identification of a green rust mineral in a reductomorphic soil by Mössbaur and Raman spectroscopies. Geochim. Cosmochim. Acta. 61:1107-1111

Wieckowski, A., E. Gahli, M. Szlarczyk, and J. Sobkowski. 1983a. The behavior of iron electrode in CO_2-saturated neutral electrolyte-I. Electrochemical study. Electrochim. Acta. 28:1619-1626

Wieckowski, A., E. Gahli, M. Szlarczyk, and J. Sobkowski. 1983b. The behavior of iron

electrode in CO_2-saturated neutral electrolyte-II. Radiotracer study and corrosion considerations. Electrochim. Acta. 28:1627-1633

Weathers, L. J., G. F. Parkin, and P. J. Alvarez. 1997. Utilization of cathodic hydrogen as electron donor for chloroform cometabolism by a mixed methanogenic culture. Environ. Sci. Technol. 31:880-885

PART 5

ELECTROCHEMICAL SYNTHESIS OF PYROAURITE-TYPE MINERALS

1. ABSTRACT

During electrochemical remediation of radionuclide ($^{235,238}U$ and ^{99}Tc)-contaminated waters, pyroaurite-type minerals, ideally $[M^{II}M^{III}(OH)_{16}CO_3 \bullet 4H_2O]$, were synthesized following coprecipitation with eroded iron (Fe) from metallic iron (Fe^0) anode. The effect of radionuclides and electric current on the transformation of initially amorphous precipitate into crystalline pyroaurite-type minerals was investigated using X-ray diffraction (XRD), scanning electron microscopy (SEM) with energy dispersive X-ray (EDX) analysis, Fourier transform infrared (FTIR) spectroscopy, and fluorescence spectroscopy. All the synthetic iron carbonate hydroxide minerals had 0.7-nm and 0.35-nm XRD peaks, and the FTIR spectrum represented a brucite-like layer structure with carbonate occupying the interlayer and Fe^{2+}, eroded from the electrode, within the octahedral hydroxide layers. The carbonate anions in the interlayer neutralize the positive charges generated through isomorphous substitution of the $Fe^{2+/3+}$ by reduced uranium (U^{4+}) and technetium (Tc^{4+}). Pyroaurite-type, U- and Tc-bearing Fe carbonate hydroxide synthesis through this electrochemical process represents an effective approach for removing U and Tc from contaminated waters than traditional technologies.

2. INTRODUCTION

There are many ways to treat heavy metals and radionuclides in contaminated waters (Sorg, 1990; Smith, 1996). One of the conventional treatment methods is coprecipitation of radionuclides in water with Fe(II) by addition of Fe(II) salts (Lee et al., 1982; Lee and Bondietti, 1983a,b). An electrochemical process has been applied to coprecipitate and adsorb metals and radionuclides and to dechlorinate volatile organics from contaminated waters (Brewster and Passmore, 1994; Roh et al., 1996). Previous studies showed that the electrochemical process has advantages including (1) no chemical addition is required, (2) reaction rates can be controlled by applied current, and (3) no secondary waste treatment is required (Brewster and Passmore, 1994; Roh et al., 1996). During the electrochemical process, amorphous iron hydroxide containing contaminants, including heavy metals and radionuclides, was precipitated and transformed into a crystalline pyroaurite-type mineral upon aging in the treated water for 2 to 14 days (Roh et al., 1996). Minerals of the pyroaurite group can be synthesized through chemical mixing of aluminum (Al), magnesium (Mg), and Fe compounds. To date, the influence of temperature, pH, various organic acids, silicate, and common anions (CO_3^{2-}, Cl^-, NO_3^-, and SO_4^{2-}) and the presence of Al^{3+}, $Mn^{2+ \text{ or } 3+}$, Cu^{2+}, Zn^{2+}, Ni^{2+}, Co^{2+}, and Ti^{4+} have been investigated (Gastuche et al., 1967; Brown and Gastuche, 1967; Miyata, 1975; Bish, 1977; Miyata and Okada, 1977; Brindley and Kikkawa, 1979). Pyroaurite-type minerals, green rusts, form when Fe corrodes in the presence of O_2; when Fe^{2+}, $FeOH^+$, or $Fe(OH)_2$ is oxidized by O_2 in aqueous solution around pH 7; or when Fe(III) oxide-hydroxides, like

ferrihydrite or lepidocrocite (γ-FeOOH), are reductively dissolved through reaction with Fe^{2+} or $FeOH^{+}$ at pH values above 6.5 (McGill et al., 1976; Taylor, 1980; Hansen, 1989). A pyroaurite-type mineral often forms as an intermediate product during the hydrolytic oxidation of Fe^{2+} solutions to FeOOH (Schwertmann and Cornell, 1991). A pyroaurite-type mineral converts to goethite (α-FeOOH), lepidocrocite (γ-FeOOH), maghemite (Fe_2O_3), or magnetite (Fe_3O_4) depending on the rate of oxidation and dehydration (Hansen et al., 1994). The freshly precipitated ferrihydrite reacts with excess Fe^{2+} in the system and induces the hydrolysis of Fe^{2+}, which leads to the formation of pyroaurite-type minerals (Schwertmann and Cornell, 1991).

A common structural scheme of phyllosilicates consists of tetrahedral and octahedral sheets as principal layers bearing a negative charge with positively charged, interlayer cations. In contrast, pyroaurite group minerals are composed of positively charged principal layers interleaved with interlayer sheets of anions and water molecules. The principal layer has a brucite-like trioctahedral arrangement. Replacement of some of the divalent cations in the brucite-like layer by trivalent cations gives rise to a positive charge that is counterbalanced by an interlayer sheet of anions (in natural materials mostly carbonate), which lie parallel to the brucite-like layer (Brown, 1980). Structural studies of hydroxy-carbonates in pyroaurite have been carried out by Ingram and Taylor (1967) and Bish (1977).

Pyroaurite-type mineral precipitation under reducing conditions may act as a sink for certain heavy metals and phosphate through their incorporation into the hydroxide layers and interlayers, respectively (Tamaura, 1985; Dutta and Puri, 1989; Myneni et al.,

1997). In anoxic soils and sediments, a pyroaurite-type minerals may also lead nitrite or nitrate reduction to ammonium, at rates of similar magnitude or even higher than microbial reduction rates (Hansen et al., 1994; Hansen et al., 1996). Hence pyroaurite-type minerals should be considered a possible important reductant for nitrate and heavy metals in subsoils, sediments, or aquifers where microbially mediated reduction rates are slow.

The objectives of this study are (a) to conduct a mineralogical characterization of the electrochemically synthesized pyroaurite-type minerals for understanding the mechanisms of the chemical processes involved and (b) to understand the effect of water chemistry on the initial precipitation and subsequent phase transformation of the precipitate. This paper will describe the synthesis of a pyroaurite-type mineral as the waste product and its implications for electrochemical remediation of U- and Tc-contaminated waters.

3. MATERIALS AND METHODS

3.1 Material Synthesis

The following four solutions were prepared to precipitate iron-bearing minerals by the electrochemical process: (1) uranyl carbonate [$UO_2(CO_3)_2^{2-}$], 5 mL uranyl nitrate [$UO_2(NO_3)_2^{2-}$] solution added to 9 mL of 0.5 *M* sodium carbonate, and pertechnetate (TcO_4^-) solution diluted with tap water (200 mL); (2) cobaltic carbonate, oxidation of a cobaltous salt (2 m*M* $CoCl_2 \cdot 6H_2O$) in the presence of sodium bicarbonate (2 m*M* $NaHCO_3$); (3) 2 m*M* $Mg_5(CO_3)_4(OH)_2 \cdot 4H_2O$ solution; and (4) 2 m*M* Na_2CO_3. In addition, a uranyl nitrate [$UO_2(NO_3)_2^{2-}$] solution was used to test anion effects on precipitation of an iron-bearing minerals by an electrochemical process. Solution samples containing ^{235}U and ^{95m}Tc were analyzed using high purity intrinsic germanium gamma-ray detector equipped with a Nuclear Data Model 6700 microprocessor programmed in 4096 channels (Cutshall and Larsen, 1980). The counting error (2δ) was kept < 2% in the analysis of all solutions. For the pertechnetate anion, sodium pertechnetate ($^{95m}TcO_4^-$, half life = 61 days) purchased from Du Pont Nen Products was used in these experiments because the fission product ^{99}Tc constitutes a potential long-term environmental hazard because of its long half-life (2.13×10^5 years).

These four solutions were provided individually to the electrochemical column to coprecipitate radionuclides and heavy metals. The electrochemical column (2.54-cm-diameter and 26-cm-long) had two iridium-coated-titanium oxide electrodes (anode and cathode), and the anode was contacted with Fe^0 foam (9 g). Cercona Fe^0 foam (Cercona

of America, Inc., Dayton, Ohio) was used as the electrode material. The Fe^0 foam has the following characteristics: (a) 92 % Fe^0 balanced with aluminosilicate (Al_2O_3:$2SiO_2$); (b) 0.9 g/cc bulk density; and (c) 0.5-1 $m^2 g^{-1}$ estimated specific surface area. Mineralogy of the Fe^0 is metallic iron (Fe^0), fayalite (Fe_2SiO_4), and hercynite ($FeAl_2O_4$). Both electrodes were connected to an external power supply (Fig. 1). Solutions were pumped from the container to the column using a MasterFlex Digi-Staltic pump (Cole-Parmer, Vernon Hills, Illinois) at a flow rates of 3.24 mL/min that were determined by measuring the discharge rate. A direct current (DC) power supply (30 V/11 mA) was used to accelerate dissolution of the Fe^0 foam. Oxidation of the Fe^0 (i.e., corrosion) at the electrodes caused reduction of the target contaminants, thereby converting these contaminants to less soluble forms. These metals then coprecipitated with dissolved Fe out of solution. The precipitate was left to age in the treated solution at room temperature (~25 °C). A small portion of each precipitate was taken periodically throughout the first month of aging for analysis. Each sample was collected on a 0.45-μm millipore filter and washed three times with deionized water prior to mineralogical characterization.

3.2 Mineralogical Analysis

All coprecipitated phases were examined by XRD, SEM with EDX, FTIR spectroscopy, and fluorescence spectroscopy to determine their mineralogical and morphological characteristics as well as the association of contaminants in the structure. Well-crystallized minerals were solvated with glycerol at room temperature for 12 hours and 180°C for 2 hours for XRD examination (Koch and Hansen, 1996). X-ray diffraction

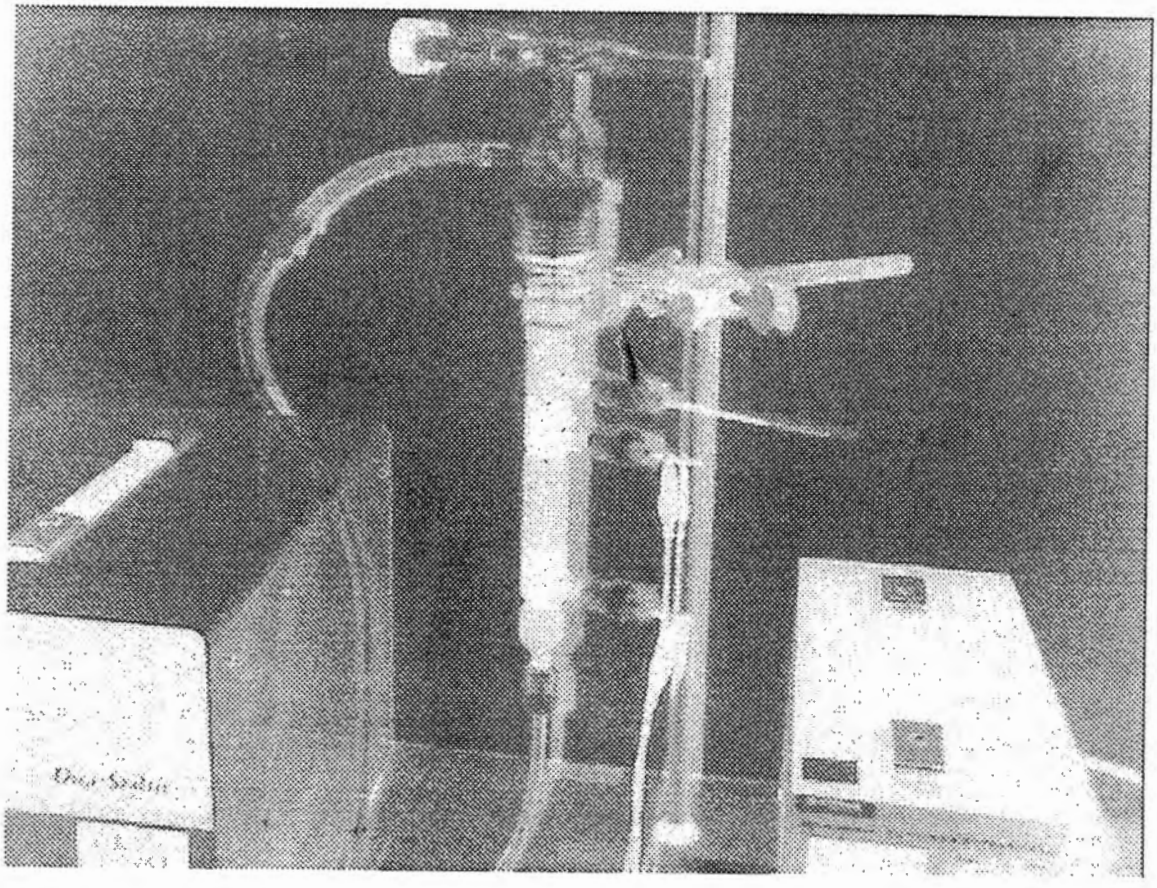


Figure 1. Photograph showing an electrochemical synthesis system (26-cm-long by 2.54-cm-intenal diameter glass column) with external DC power and contaminated water supply

analyses were performed using a Scintag XDS2000 diffractometer (Sunnyvale, California) equipped with CoKα radiation (45 kV, 40 mA). All scans were run at 2° 2θ/min. A JEOL JSM-35CF (Tokyo, Japan) SEM (20 kV) was used to discern the morphology of the coprecipitated forms. EDX analysis was also utilized to determine the elemental composition of the precipitate.

Gamma activity of the ^{235}U and ^{95m}Tc isotopes in the influent and filtered solutions were determined using a high purity intrinsic germanium gamma-ray detector equipped with a Nuclear Data Model 6700 microprocessor programmed in 4096 channels (Cutshall and Larsen, 1980). Infrared spectra of synthesized minerals were obtained with a Nicolet FTIR using a NaCl prism with a spectral range from 4000 to 400 cm^{-1}. The pressed pellet technique was used to prepare samples for infrared examination (Farmer, 1974). The synthesized mineral (2 mg) was mixed with 200 mg of potassium bromide (KBr) using an agate mortar to prepare a 12-mm diameter KBr pressed disk.

A fluorescence technique was used to probe the oxidation state of U in the synthesized mineral. Steady-state luminescence spectra were measured by means of a fiber-optic probe directly inserted in the uranyl nitrate, and uranyl carbonate solutions and in the crystalline mineral (Dai et al., 1994). The 337-nm line of a pulsed nitrogen laser (pulse = 5 ns) was used as the excitation source in this study. A fiber-optic superhead probe (Dillor) was used for both the excitation and collection of the signal from the samples. The emission was collected at 180° with respect to the excitation direction and dispersed with a Spex 500M monochromator with a 150-nm groove/mm grating blaze at 655 nm. The dispersed radiation was detected using a CCD detector (Spex System One)

with an entrance slit width of less than 0.8 nm and a resolution of 0.2 nm. The first major peak of the fluorescence spectrum was expected at 499.6 nm for the uranyl nitrate complex (Dai et al., 1996b). No fluorescence signal is expected for the reduced U(IV) species (Dai et al., 1996b).

4. RESULTS

Iron minerals formed through the electrochemical process had the following characteristics:

Fe-(U,Tc)-CO_3 system: The solution containing U-carbonate and pertechnetate as contaminants generated coprecipitates of the U and Tc with the eroded $Fe^{2+/3+}$ from Fe^0. The precipitates were originally X-ray amorphous, but the amorphous precipitates transformed into a 0.7-nm crystalline mineral within a 2-week aging period while left in the treated water, as identified by XRD (Fig. 2a). Scanning electron microscopy with EDX chemical analysis has shown that the crystalline mineral containing U and Tc displays a keg- or barrel-shaped morphology and shows a pronounced platy habit (Fig. 3a). These particles contain significant quantities of uranium and iron, as identified by EDX spectra (Fig. 3b). Technetium is also believed to be incorporated in the mineral but in undetectable concentrations. X-ray diffraction analysis of an oriented sample of the precipitates shows sharp and intense reflections, attesting to the highly crystalline nature of the precipitate (Fig. 2a). The platy crystal habit and parallel orientation of the basal planes enhanced the intensities of the 00*l* reflections. During aging, the activity of radionuclides adsorbed or coprecipitated did not changed, which suggests that a solid-phase transformation occurs without solubilization of the amorphous phases. During the electrochemical process, the influent solution pH 5.8 increased to pH 8.5 – pH 9.8 in the effluent. Redox potential decreased from +400 mV in the influent to -200 – -400 mV in the effluent.

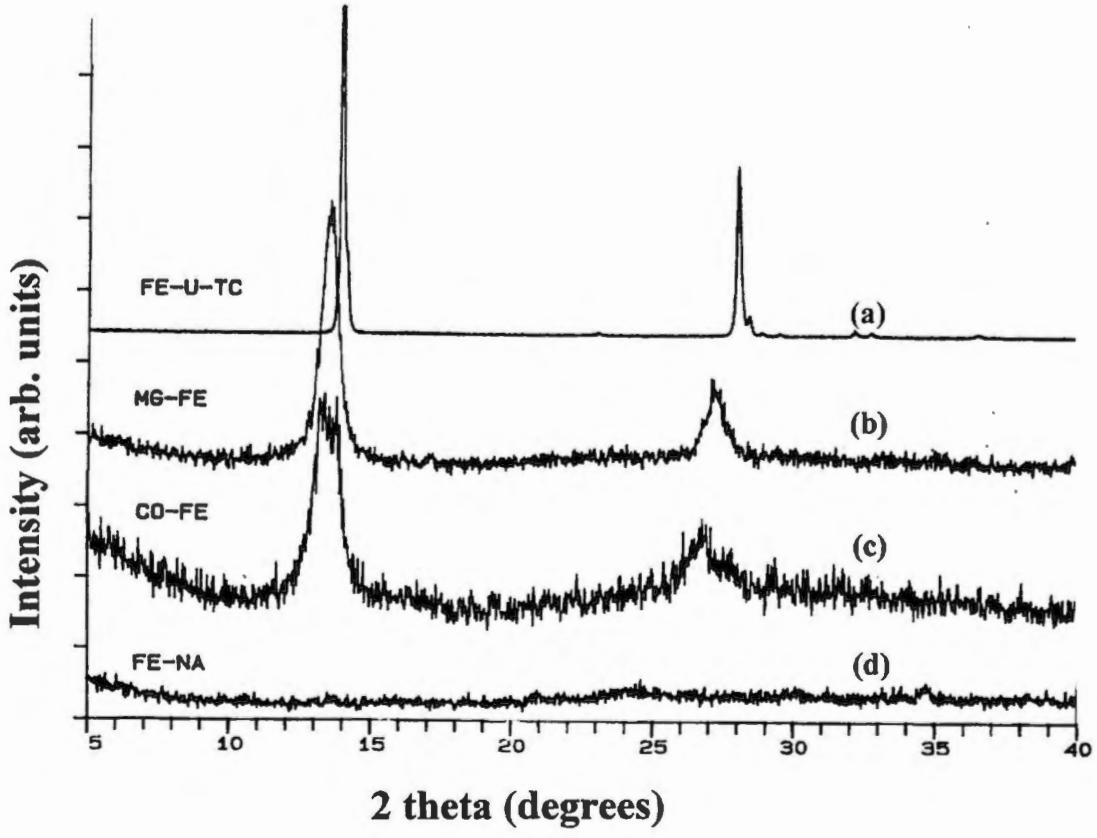


Figure 2. X-ray diffraction analyses of the crystalline precipitates: (a) U-Tc-Fe carbonates (b) Mg-Fe carbonates, (c) Co-Fe-carbonates, and (d) Na-Fe-carbonates.

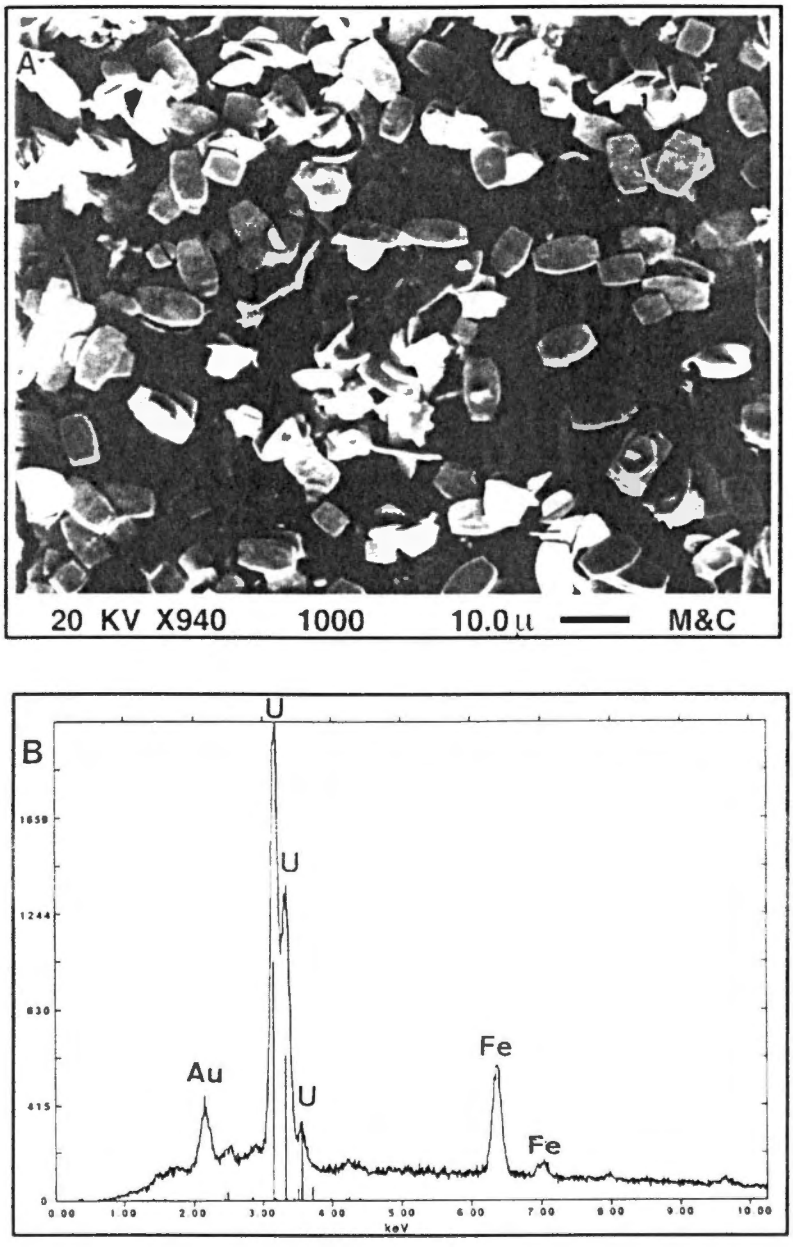


Figure 3. (a) Scanning electron micrograph of the coprecipitates displaying barrel- or keg-shaped morphology and (b) energy-dispersive X-ray spectra showing the chemical composition of the precipitate is mainly iron and uranium

Fe-Mg-CO_3 system: When the solution containing dissolved Mg-carbonate passed through the electrochemical column, the dissolved Mg was coprecipitated with the eroded Fe. The initially amorphous precipitates transformed into a 0.7-nm crystalline mineral within a 7-day aging period (Fig. 2b). The crystalline mineral consists of Mg and Fe and has a pseudo-hexagonal morphology and platy habit. SEM revealed that these crystalline minerals containing Mg are microcrystalline (< 1-μm).

Fe-Co-CO_3 system: In the same manner, the dissolved Co was also coprecipitated with the eroded Fe and crystallized into a 0.7-nm mineral within a 7-day aging period (Fig. 2c) The chemical composition of the crystalline mineral is mainly Fe and Co and has a pseudo-hexagonal morphology and a pronounced platy crystal habit. Scanning electron microscopy revealed that the crystalline minerals containing Co are microcrystalline (< 1-μm).

Fe-Na-CO_3 system: On the contrary, the solution containing Na-carbonate generated only Fe hydroxide precipitate which remained X-ray amorphous even after 2 weeks aging (Fig. 2d).

X-ray diffraction analyses of the precipitates that formed in the three different systems (except for Fe-Na-CO_3 system), revealed that the crystalline mineral is similar to pyroaurite-type mineral or green rust I (Table 1). The two main XRD peaks for the pyroaurite-type mineral, Fe(II)Fe(III) hydroxy carbonate, are 0.750 and 0.376-nm (green rust 1) (Schwertmann and Cornell, 1991). For the U- and Tc- bearing minerals, hot glycerol treatment (180°C) replaced interlayer anions and water molecules and expanded the 0.73-nm peak to 0.9-nm (Table 1) because this mineral has a layer structure (Koch and

Table 1. X-ray diffraction data of the precipitates formed from 4 systems

	XRD peaks (nm) of the oriented samples	XRD peaks (nm) after hot glycerol treatment at 180°C
Fe-(U,Tc)-CO_3 system	0.730 0.363	0.902 0.448
Fe-Mg-CO_3 system	0.775 0.339	0.922 0.455
Fe-Co-CO_3 system	0.760 0.382	0.912 0.454
Fe-Na-CO_3 system	Amorphous	Amorphous
Mg-Fe(III) hydroxy carbonate[†]	0.78	1.170

[†] Phyroaurite-type mineral formed by chemical mixing (Koch and Hansen, 1996)

Hansen, 1996). The crystalline precipitate containing Mg and Co had the same pattern of expansion after hot glycerol treatment (Table 1). Fourier transform infrared spectra showed that the crystalline mineral with U, Tc, Co, and Mg contain carbonate ions in the mineral structure. The presence of the carbonate anion showed an absorption at 1392 cm^{-1} for the U- and Tc-bearing mineral and 1385 cm^{-1} for Co-bearing mineral (Fig. 4), corresponding to carbonate-stretching vibrations similar to other carbonate minerals (Huang and Kerr, 1960). Hot-glycerol-solvated samples (1 mg) were mixed with 100 mg of KBr, a pressed KBr disk was prepared, and FTIR spectra were obtained. The spectra showed that these absorption bands disappeared after glycerol treatment because glycerol intercalated the carbonate anions.

Fluorescence spectroscopic techniques were used to identify the oxidation state of

U in the crystalline precipitate as well as in the contaminated waters, particularly the uranyl carbonate and uranyl nitrate solutions. Determination of the U oxidation state using fluorescence techniques is based on the fact that the oxidized U(VI) gives strong fluorescence, whereas the reduced U(IV) does not (Dai et al., 1994; Dai et al., 1996b; Dai et al., 1997). As expected, uranyl nitrate and uranyl carbonate showed strong fluorescence intensities (Fig. 5), but no fluorescence spectrum was observed for U in the crystalline mineral. This evidence indicates that the U in the crystalline precipitate is in a reduced state, U(IV), as predicted by the electrochemical reaction. In addition, uranyl nitrate passed the electrochemical column to confirm the effects of anion, nitrate, on the formation of these minerals by electrochemical process. Fluorescence spectra showed that soluble uranyl nitrate was reduced and coprecipitated with the eroded iron; however, the precipitates have remained amorphous throughout the aging period.

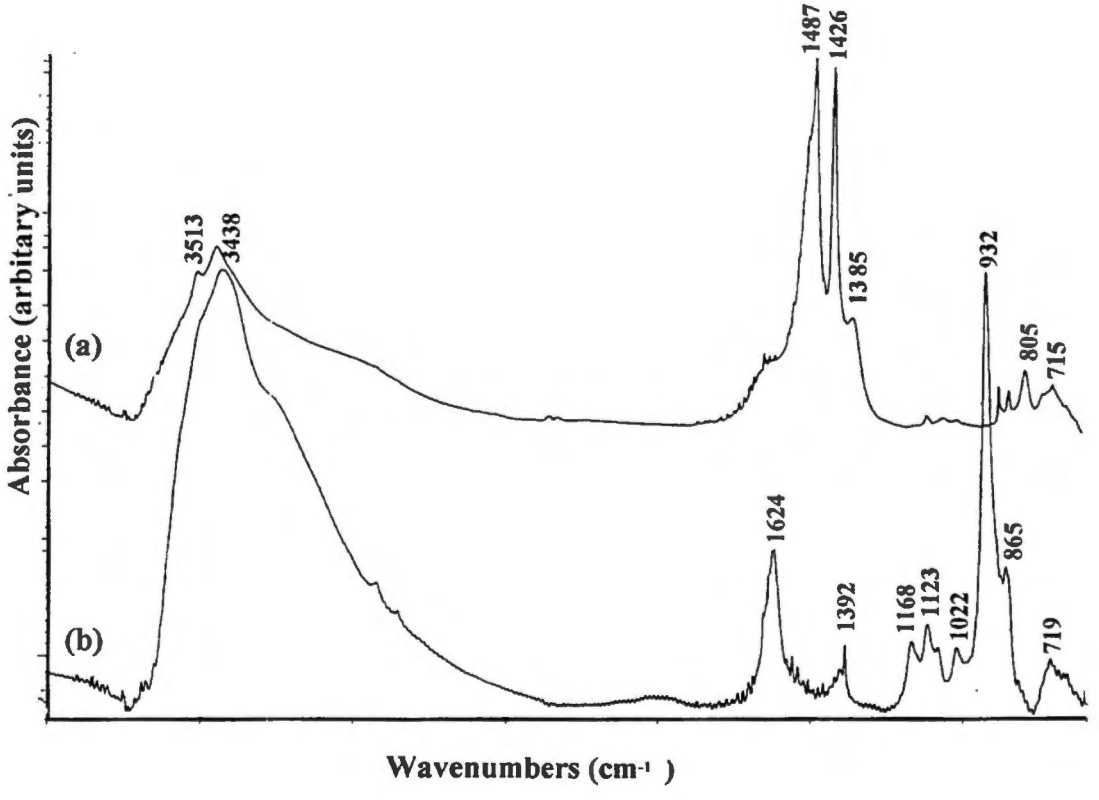


Figure 4. Fourier transformed infrared spectra of pyroaurite iron mineral: (a) Co-Fe-carbonates and (b) U-Tc-Fe carbonates

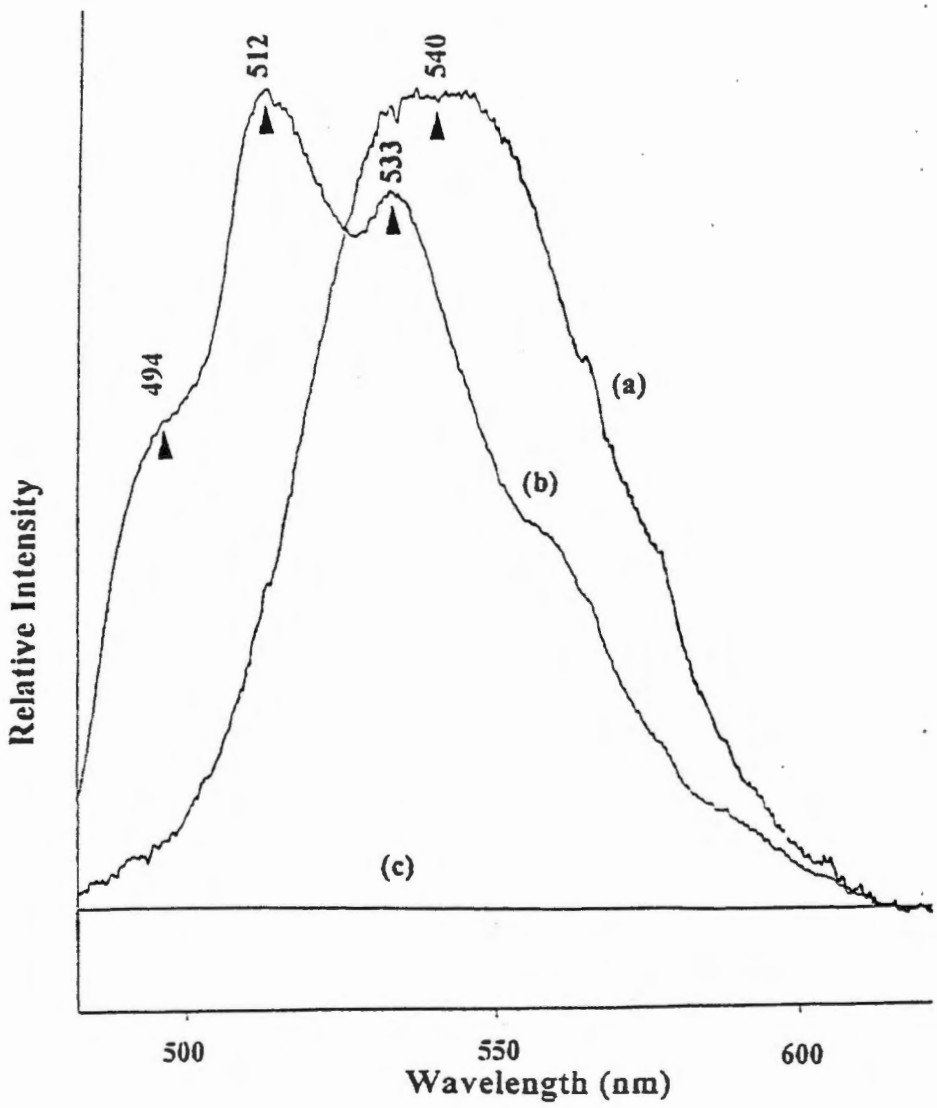


Figure 5. Comparison of fluorescence spectra of (a) uranyl nitrate, (b) uranyl carbonate, and (c) crystalline mineral.

5. DISCUSSION

During the preliminary development of the electrochemical process for groundwater treatment, formation of a crystalline pyroaurite-type mineral was obtained after a short aging period instead of amorphous U- and Tc-bearing Fe-(hydr)oxide. As expected, most of the U and Tc was removed from the solution as a coprecipitate of the Fe mineral (Roh et al., 1996). The other metals including Co and Mg are also coprecipitated with eroded iron from Fe^0 in the electrochemical column and crystallized into pyroaurite-type mineral. This electrochemical process has the potential for effective remediation of surface water and groundwater that are contaminated by radionuclides, heavy metals, and/or chlorinated organic compounds.

The precipitate was initially amorphous but became a crystalline mineral within a 2-week aging period at room temperature. The crystalline precipitates structurally resemble members of the pyroaurite group. Eroded $Fe^{2+ \text{ or } 3+}$ from corrosion of the electrode foams are base cations of the brucite-like hydroxide layer. Isomorphous substitution of the $Fe^{2+/3+}$ by U^{4+} and Tc^{4+} in the brucite-like layer generated positive charges, which were counterbalanced by the carbonate anion in the interlayer anions. Magnesium and Co coprecipitated with eroded Fe and crystallized into a pyroaurite-type mineral within a 2-week aging period. However, soluble uranyl nitrate was reduced and coprecipitated with eroded Fe, but its precipitates remained X-ray amorphous throughout the aging period. Therefore, carbonate is essential for generating a crystalline waste form such as pyroaurite-type minerals, via electrochemistry. Reductive coprecipitation of uranyl

carbonates by Fe oxides and Fe^0 is a thermodynamically favorable reaction (Langmuir, 1978; Cantrell et al., 1995), particularly as U(IV) readily forms oxyhydroxide precipitates from solution (Dai et al., 1996a). Because the chemical composition of the crystalline mineral is mainly U^{4+}, $Co^{2+ \text{ or } 3+}$, Mg^{2+}, $Fe^{2+ \text{ or } 3+}$, and the carbonate ion, it is concluded that the removal of radionuclides occurred via reductive coprecipitation with eroded iron which, in turn, is further crystallized into a carbonate mineral by electrochemistry.

A pyroaurite-type mineral, green rusts, often forms as an intermediate product during the hydrolytic oxidation of Fe^{2+} solutions to FeOOH (Schwertmann and Cornell, 1991). This pyroaurite-type Fe mineral converts goethite (α-FeOOH), lepidocrocite (γ-FeOOH), maghemite (γ-Fe_2O_3), or magnetite (Fe_3O_4), depending on the rate of oxidation and dehydration of pyroaurite (Hansen et al., 1994). A pyroaurite-type mineral is a possible inorganic reductant for nitrate and heavy metals in anoxic subsoil, sediments and aquifers where microbial reduction rates are limited by low carbon content (Hansen et al., 1996). The pyroaurite has considerable potential for application in environments such as water-purification processes, gas adsorbents, catalysis, and designed drug and pesticide delivery systems (Koch and Hansen, 1996).

6. CONCLUSIONS

Synthesis of Fe-carbonate minerals through this electrochemical process is an effective approach for remediating contaminated waters. This process generates waste may be more stable to leaching than conventional wastewater precipitation processes as a result of the crystallization. The formation of such a well-crystalline waste product is fortuitous because its solubility is expected to be much lower than that of an amorphous Fe oxide phase, thereby immobilizing the entrapped contaminants more effectively. Further research is required to assess remaining questions such as (a) the effect of electric current on coprecipitation and crystallization of the heavy metals and radionuclides with eroded iron, (b) the solubility of the electrochemically synthesized pyroaurite-type mineral as a waste form, and (c) the determination of the Fe-oxidation state in synthesized pyroaurite-type minerals.

REFERENCES

Bish, D. L. 1977. The occurrence and crystal chemistry of nickel in silicate and hydroxide minerals. Ph.D. Thesis, The Pennsylvania State University, University Park, Pennsylvania.

Brewster, M. D., And R. J. Passmore. 1994. Use of electrochemical iron generation for removing heavy metals from contaminated groundwater. Environ. Prog. 13(3):143-148

Brindley G. W., and Kikkawa. S. 1979. A crystal-chemical study of Mg, Al and Ni, Al hydroxy-perchlorates and hydroxy-carbonates. Am. Min. 64. 836-43

Brown G. 1980. Associated minerals. *In* The X-ray identification and crystal structures of clay minerals (G. Brown, Ed.), 2nd ed., Mineralogical Society, London.

Brown, G., and M. C. Gastuche. 1967. Mixed magnesium-aluminum hydroxides. II. Structural chemistry of synthetic hydroxy-carbonates and related minerals and compounds. Clay Min. 7:193-201

Cantrell, K. J., D. I. Kaplan, and T. W. Wietsma. 1995. Zero-valent iron for the in situ remediation of selected metals in groundwater. J. Hazard. Mat. 42:201-212

Cutshall, N. H., and I. L. Larsen. 1980. BGSUB and BGFIX: Fortran programs to correct Ge(Li) gamma-ray spectra for photopeaks from radionuclides in background. ORNL/TM-7051, Oak Ridge National Laboratory, Oak Ridge, Tennessee

Dai, S., G. D. Del Cul, D. Metcalf, and L. M. Toth. 1994. Modification of cary 14th spectrometer into a fiberoptic absorption spectrometer. Spect. Let. 27(5):687-690

Dai, S., L. M. Toth, G. D. Del Cul, and D. H. Metcalf. 1996a. Solubilities of uranium(VI) dioxide in magnesium chloride, calcium chloride, and aluminum chloride melts: A comparative study. J. Phys. Chem. 100:220-223

Dai, S., W. Xu. D. H. Metcalf, and L. M. Toth. 1996b. Energy transfer between UO_2^{2+} and Eu^{3+} in sol-gel glasses:a spectroscopic investigation. Chem. Phy. Lett. 262:315-320

Dai, S., Y. S. Shin, L. M. Toth, and C. F. Barnes. 1997. Spectroscopic probing of adsorption of uranyl to uranyl-imprinted silica sol-gel glass via steady-state and time-resolved fluorescence measurement. J. Phys. Chem. 101:5521-5524

Dutta, P. K., and M. Puri. 1989. Anion exchange in lithium aluminate hydroxides. J. Phys. Chem. 93:376-381

Farmer, V. C. 1974. The infrared spectra of minerals. Mineralogical Society. London.

Gastuche, M.C., G. Brown and M. M. Mortland. 1967. Mixed magnesium-aluminum hydroxides. I. Preparation and characterization of compounds formed in dialyzed systems. Clay Min. 7:177-92

Hansen, H. C. B. 1989. Composition, stabilization, and light absorption of Fe(II)Fe(III) hydroxy carbonate (green rust). Clay Mineral. 24:663-669

Hansen, H. C. B., O. K. Borggaard., and J. Sorensen. 1994. Evaluation of the free energy of formation of Fe(II)-Fe(III) hydroxide-sulfate (green rust) and its reduction of nitrite. Geochim. Cosmochim. Acta. 12:2599-2608

Hansen H. C. B., C. B. Koch, H. Nancke-Krogh, O. K. Borggaard, and J. Sorensen. 1996. Abiotic nitrate reduction to ammonium:Key role of green rust. Environ. Sci. Technol. 30:2053-2056

Huang, C. K., and P. F. Kerr. 1960. Infrared study of the carbonate minerals. Am Min. 45:311-324

Ingram, L., and H. F. W. Taylor. 1967. The crystal structures of sjögrenite and pyroaurite. Mineral. Mag. 36:465-479

Koch, C. B., and H. C. B. Hansen. 1996. On the reaction of pyroaurite with glycerol. Annual Meeting of the Clay Minerals Society, Jun 15-20, Gatlinberg, Tennessee. p. 96

Langmuir, D. 1978. Uranium solution-mineral equilibria at low temperatures with applications to sedimentary ore deposits. Geochim. Cosmochim. Acta. 42:547-569

Lee, S. Y., S. K. Hall, and E. A. Bondietti. 1982. Methods of removing uranium from drinking water:II. Present municipal water treatment and potential removal methods. Office of Drinking Water, U. S. EPA 570/9-82/003

Lee, S. Y., and E. A. Bondietti. 1983a. Technetium behavior in sulfide and ferrous iron solutions. Mat. Res. Soc. Symp. Proc. 15:315-322

Lee, S. Y., and E. A. Bondietti. 1983b. Removing uranium from drinking water by metal hydroxide and anion exchange resin. J. Am. Water Works Assoc. 75:537-540

McGill, I. R., B. McEnaney, and D. H. Smith. 1976. Crystal structure of green rust formed by corrosion of cast iron. Nature. 259:354-355

Myneni, S. C. B., T. K. Tokunaga, and G. E. Brown. 1997. Abiotic selenium redox

transformation in the presence of Fe(II,III) oxides. Science. 278(5340):1106-1109

Miyata, S. 1975. Synthesis of hydrotalcite-like compounds and their structures and physico-chemical properties I: The systems Mg^{2+}-Al^{3+}-NO_3^-, Mg^{2+}-Al^{3+}-ClO_4^-, Ni^{2+}-Al^{3+}-Cl^-, and Zn^{2+}-Al^{3+}-Cl^-. Clays Clay Min. 23:369-375

Miyata, S. And A. Okada. 1977. Synthesis of hydrotalcite-like compounds and their physico-chemical properties the systems Mg^{2+}-Al^{3+}-SO_4^{2-}, and Mg^{2+}-Al^{3+}-CrO_4^{2-}. Clays Clay Min. 25:14-18

Roh, Y., S. Y. Lee, and M. P. Elless. Electroremediation of uranium and technetium contaminated waters. Extended Abstract. Annual Meeting of the Chemical Society, I&EC Division, Emerging Technologies in Hazardous Waste Management VIII, Sept., 9-12, 1996. Birmingham, Alabama. 582-585

Schwertmann, U., and R. M. Cornell. 1991. Iron oxides in the laboratory. VCH Publishers, Inc., New York.

Smith, E. H. 1996. Uptake of heavy metals in batch systems by a recycled iron-bearing material. Water Res. 30(10):2424-2434

Sorg, T. J. 1990. Removal of uranium from drinking water by conventional treatment methods. *In* Cothern, C. R., and P. A. Revers (eds.). Radon, radium and uranium in drinking water. Lewis Publishers, Inc. Chelsea, Michigan.

Tamura, Y. 1985. Ferrite formation from the intermediate, GR II, in the transformation reaction of γ-FeO(OH) in aqueous suspension. Inorg. Chem. 24:4363-4366

Taylor, R. M. 1980. Formation and properties of Fe(II)Fe(III) hydroxycarbonate and its possible significance in soil formation. Clay Mineral. 15:369-382

VITA

The author grew up in Buan, Chonbuk, Republic of Korea. After graduating from Buan High School in 1983, he entered Chonbuk National University, Chonju, Republic of Korea. In 1987 he received a Bachelor of Science Degree in Earth Science Education, with concentration in geology. In 1987 he entered Yonsei University, Seoul, Republic of Korea as a Masters' candidate. He received M. S. Degree in geology in 1989, with a concentration in clay mineralogy. After completing the military service in Korea Army from 1989 to 1992, he worked as a graduate research assistant at Yonsei University from the fall of 1992 to summer of 1993.

In the fall of 1993 he entered The University of Tennessee, Knoxville as a Ph. D candidate. He received a Ph. D. in Plant and Soil Sciences with a concentration in soil mineralogy and groundwater chemistry in August of 1998. His research interests are in the areas of (1) electrochemical remediation of radionuclide- and TCE-contaminated waters using zero-valent iron and multiphasic Fe oxides, (2) mineralogical and morphological characterization of the precipitates in reactive iron barrier, and (3) mineralogical and physico-chemical characterization of uranium and mercury contaminated soils, and (4) iron oxides formation from zero-valent iron during contaminated groundwater treatment. He will begin his professional career by taking a Post Doc. position in the Environmental Sciences Division at Oak Ridge National Laboratory, Oak Ridge, Tennessee.

5339 1508 18
08-04-99 MRB